

POLITECNICO DI MILANO
SCHOOL OF ARCHITECTURE URBAN PLANNING
CONSTRUCTION ENGINEERING

MASTER OF SCIENCE IN BUILDING ENGINEERING



**Solar Energy in Low Temperature District Heating:
monitoring and simulation of an Innovative District in
Milan**

Supervisor: prof. **Rossano Scoccia**

Co-supervisor: **Alice Dénarié**

Master Dissertation of:

Dario Dall'Ara

Identification number:

919349

Academic Year 2019 / 2020

Solar Energy in Low Temperature District Heating: monitoring and simulation of an Innovative District
in Milan

“Man is the victim of an environment which refuses to understand his soul”

Charles Bukowski – Tales of Ordinary Madness (1972)

Solar Energy in Low Temperature District Heating: monitoring and simulation of an Innovative District
in Milan

Index

Sintesi	9
Abstract.....	11
1. Introduction and Aim of the Work	13
2. 4 th Generation District Heating: State of the art	16
2.1 The District Heating.....	16
2.2 Transition to the 4 th Generation DH	18
2.3 Decentralised Solar Thermal DH.....	20
2.4 Milan District Heating	21
3. Methodological Approach	23
3.1 Purpose of the Thesis	23
3.2 Used Tools	24
3.3 Validation of the Model.....	25
3.4 Implementation of the Model	26
4. Case Study: Merezzate Plus	27
4.1 Merezzate Plus Multi-Dwelling Units	27
4.2 Merezzate High Temperature Network	30
4.2.1 Multi-Dwelling Unit Substation.....	32
4.2.2 Innovative Flat Station	33
4.3 Merezzate Low Temperature Network.....	34
5. Merezzate Plus Pre-Sizing Data	36
5.1 BIN Method	38
5.2 Domestic Hot Water	42
5.3 UDC Space Heating & DHW Hourly Energy	44
6. TRNSYS Network System Modelling	47

6.1	TRNBuild Description.....	47
6.2	Apartments Simulation	48
6.2.1	Building Descriptions and Flat Parameters	48
6.2.2	Apartments TRNSYS Model.....	52
6.2.3	Flat n°25 Energy Needs & Energy Balance	54
6.2.4	Radiant Panels Modelling.....	56
6.2.5	Flat n°25 Radiant Panel Results	63
6.3	Merezzate District Heating Modelling	69
6.3.1	Work Introduction	69
6.3.2	Multi-dwelling unit Substation Modelling	71
6.3.3	Substation Heat Exchanger Sizing	72
6.3.4	Substation Data for Primary and Secondary Side	74
6.3.5	Merezzate Network TRNSYS Model.....	76
6.3.6	Pipes Thermal Losses	77
6.3.7	Merezzate District Heating Results	81
7.	Model Validation.....	83
7.1	Substation Results compared with the Monitoring Data	83
7.2	Model Validation	85
7.3	Validation of the Network Model.....	93
8.	Decentralised Solar Thermal Model.....	99
8.1	Solar Thermal DH and different Feed-in Connections	99
8.2	Solar Field Sizing.....	103
8.3	Decentralised Solar District HT Configuration	106
8.3.1	TRNSYS Model of Decentralised Solar System.....	107
8.3.2	Results of Decentralised Solar System HT	110
8.4	Decentralised Solar District LT Configuration.....	117

8.4.1	Results of Decentralised Solar System LT	118
8.4.2	Comparison between HT & LT Network	124
8.5	Economic and Environmental Analysis.....	125
8.6	Discussion of the Results	128
9.	Conclusions	129
	List of Figures.....	132
	List of Tables.....	134
	List of Graphs	136
	Nomenclature.....	138
	Bibliography	142
	Acknowledgments	147

Solar Energy in Low Temperature District Heating: monitoring and simulation of an Innovative District
in Milan

Sintesi

L'obiettivo di questo lavoro è l'analisi di una rete teleriscaldamento nel nuovo distretto di Merezzate, un quartiere di nuova costruzione della città di Milano, che alimenta diverse unità di condominio, composte da edifici di elevata classe energetica. L'impianto è innovativo nel suo genere in quanto gli appartamenti non possiedono scambiatori di calore per il riscaldamento né accumuli per la produzione di acqua calda sanitaria, grazie alle innovative stazioni satellite degli appartamenti che ricevono direttamente l'acqua di rete a 65 °C. Lo scopo principale di questo lavoro di tesi è la creazione di un modello energetico in regime dinamico in grado di simulare l'intero distretto di Merezzate al fine di valutare l'integrazione di energia solare distribuita sugli edifici e sulla rete. Il modello permette di analizzare tutte le grandezze significative di rete quali temperature di mandata e ritorno, portate ed energie utilizzate, in tutti i componenti della rete, simulandone l'andamento nel tempo, a seconda delle condizioni esterne imposte. La configurazione del modello del sistema di rete viene quindi validata utilizzando i dati reali di monitoraggio forniti dal gestore della rete, A2A Calore & Servizi. I risultati validati discostano dai dati reali con un errore medio del 2 %. Infine, viene valutata una soluzione innovativa di integrazione di energia solare termica. Il nuovo modello è integrato con un impianto solare termico decentralizzato che usa la rete di teleriscaldamento come accumulo per le unità di condominio. Il sistema di teleriscaldamento solare viene studiato con la configurazione odierna ad alte temperature (temperatura di mandata rete 100 °C) e successivamente con la futura implementazione a teleriscaldamento di IV generazione a basse temperature (temperatura di mandata pari a 65 °C). I risultati ottenuti sono poi valutati da un punto di vista energetico, ambientale ed economico. I risultati mostrano che il sistema solare decentralizzato permette un risparmio dell'8 % di energia primaria annuale con la configurazione ad alte temperature e del 12 % con la futura configurazione a basse temperature.

Parole chiave: HVAC, teleriscaldamento, bassa temperatura, solare termico, sostenibilità, efficienza energetica, edifici, simulazione dinamica, TRNSYS.

Abstract

The purpose of this thesis-work is the analysis of a district heating network in the new district of Merezzate, a newly built district of the city of Milan, which feeds into several multi-dwelling units composed by high-energy class buildings. The system is innovative of its kind as the apartments do not have heat exchangers for space heating nor storage for the production of domestic hot water, thanks to the innovative flat stations of the apartments which directly receive mains water at 65 °C. The main purpose of this thesis work is the creation of an energy model in a dynamic regime capable of simulating the entire district of Merezzate in order to evaluate the integration of solar energy distributed among buildings and network. The model takes into account all the significant quantities from supply and return temperatures, to mass flow rates and energies, reflecting them in all the network components and simulating their trend over time, depending on external conditions. The configuration of the network model is then validated using the real monitoring data provided by the system operator, A2A Calore & Servizi. The validated results deviate from the real data with an average error about 2%. Finally, an innovative solar thermal integration is evaluated. The new model is integrated with a decentralised solar thermal system which uses the district heating network as storage tank for the multi-dwelling units. The solar district heating system is studied with today's configuration at high temperatures (network supply temperature 100 °C) and subsequently with the future implementation of 4th generation district heating at low temperatures (supply temperature equal to 65 °C). The obtained results are evaluated from an energetic, environmental and economic point of view. The results proof that the decentralised solar system can save the 8 % of primary energy in high temperature configuration and 12 % with the future low temperature configuration.

Keywords: HVAC, district heating, low temperature, solar thermal, sustainability, energy efficiency, buildings, dynamic simulation, TRNSYS.

Abstract

1. Introduction and Aim of the Work

For several countries in European Union (EU), the large dependence on fossil fuels causes the enhancement of dependence on energy imports due to low energy resources [1]. Therefore, development of technologies for sustainable energy production becomes essential. European Union's policies are acting against these problems through reduction of primary energy consumption and development of energy system based on local renewable energy. These actions should reduce the energy imports and diversify energy sources [2].

The district heating is a technology for distributing heat from its production site to the end user. The growth of heated volumes in recent years has been rapid as the possibility of using waste heat or heat from cogeneration makes this technology attractive both from an environmental and an economic point of view. However, to maintain its attractiveness in the future, this technology will have to evolve, providing for intelligent integration into the network of thermal storage and distributed generation from renewable sources and increasingly efficient control systems. The European directives and the consequent Italian law push in this direction, offering incentives only to district heating networks that belong to the "efficient" category [2].

Within this context, the need of this thesis-work arises for numerical models capable of monitoring and simulating the operation of the district heating network and improving an existing project placed in Merezzate district with the aim of optimizing the operation and management of the network and estimate the performances of potential integration of solar thermal energy.

This thesis-work focuses on the analysis of the district heating simulation of Merezzate Plus project [3], a new district in the city of Milan, and tries to improve its the energy efficiency. Merezzate district is composed by eight multi-dwelling units with different high energy class buildings and different functions. Each multi-dwelling unit currently receives heat from the district heating through two plate heat exchangers. Nowadays, five multi-dwelling units are completed and work, therefore, just these five will be studied in this project.

The heated water can be directly used by consumers for space heating and as domestic hot water without the need for any other heat exchanger or storage, thanks to the innovative flat stations. The configuration will be implemented with a low temperature network, according to the Merezzate Plus project. The heat exchangers of each multi-dwelling unit will be removed and the district heating will directly serve the buildings. This would be one of the first use of this technology in Italy, the so called: 4th Generation of District Heating system.

For this reason, this thesis-work wants to propose a flexible simulator capable of describing all the significant quantities from supply and return temperatures, to mass flow rates and energies, reflecting them in all the network components and simulating their trend over time, depending on external conditions, i.e., thermal demands of the utilities, hot fluid delivery temperature and environmental conditions. The aim is to obtain a model that gives information both on the district heating side (primary side) and multi-dwelling unit side (secondary side), to evaluate the actual situation of the district network and simulate future interventions. Therefore, the district network model created will be validated, according to the monitoring data provided by A2A Calore & Servizi, to understand the validity of the results simulated with TRNSYS18 (a software used to simulate the behaviour of transient systems) [4], and the real improvement margins.

Once the model is validated, the aim of this thesis-work is to implement the Merezzate district through a decentralised solar thermal system which exploits the district heating network as a storage tank for the multi-dwelling units. The solar thermal optimisation and the flexibility of the simulation, together with a validated thermodynamic model, allow to integrate the future intervention for renovating the Merezzate district into the first 4th generation district heating in Italy. Therefore, the decentralised solar system model is also studied with a low temperature network configuration and the results will be compared with the currently high temperature network. The results from the simulations will be compared and studied from an energetic, environmental and economic point of view.

The outline of this thesis-work is as follow:

Chapter 1 introduces the purpose and the development of this thesis-work.

Chapter 2 defines the state of art of the 4th generation district heating, analysing the characteristic of the different DH generation and the decentralised solar system by reporting several existing cases and case studies.

Chapter 3 presents the methodology and the structure of this thesis-work, explaining the theory of the strategies and models that will be analysed in detail in the following chapters.

Chapter 4 provides a brief overview of the Merezzate district and technologies with today's configuration and with the next low temperature network.

Chapter 5 provides the pre-sizing data of the district network and redistributes them according to an hourly grid in order to analyse all the year.

Chapter 6 describes the TRNSYS modelling and sizing of the district heating network. The analysis is performed at today's configuration with a primary side delivery temperature of 100 °C.

Chapter 7 discusses the results from the previous simulation and validates the model according to the monitoring data provided by A2A company.

Chapter 8 analyses the implementation of a decentralised solar system from an economic and environmental point of view. It reports the evaluation of performances at high temperature conditions and at the next low temperature configuration.

Chapter 9 gives the conclusions, and suggestions are made for future work.

2. 4th Generation District Heating: State of the art

This Chapter focuses on the state of art of the technology of the project system: 4th generation district heating. It will cover the different types of district heating generations and the relative benefits and possible optimisation by analysing the state of art of several case studies of different district heating. The aim of this thesis-work is to improve the quality of the research by providing a simplified district network model to simulate different type of district heating and evaluate the effectively efficiency and relative benefits.

2.1 The District Heating

District heating is a system for efficiently distributing heat to a series of users through a network of pipes that use water as a heat transfer fluid. The distribution system consists in a supply line that connects the plant to the users and a return line that brings the cooled fluid back to the plant. The system physically connects the place of heat generation with the place where it is used, allowing the efficient use of heat that would otherwise be lost.

This technology allows to exploit heat from different sources. The production plant usually uses waste heat from other processes, such as the electricity production (cogeneration), while back-up boilers may be present to guarantee service continuity or cover thermal demand peaks [5]. The starting fuel can therefore be of any type (natural gas, fossil fuels, biomass or solid urban waste). Centralized heat production allows the implementation of more sophisticated systems to remove and capture the pollutants, reducing local pollution.

The picture in the next page shows a generic scheme of district heating operation.

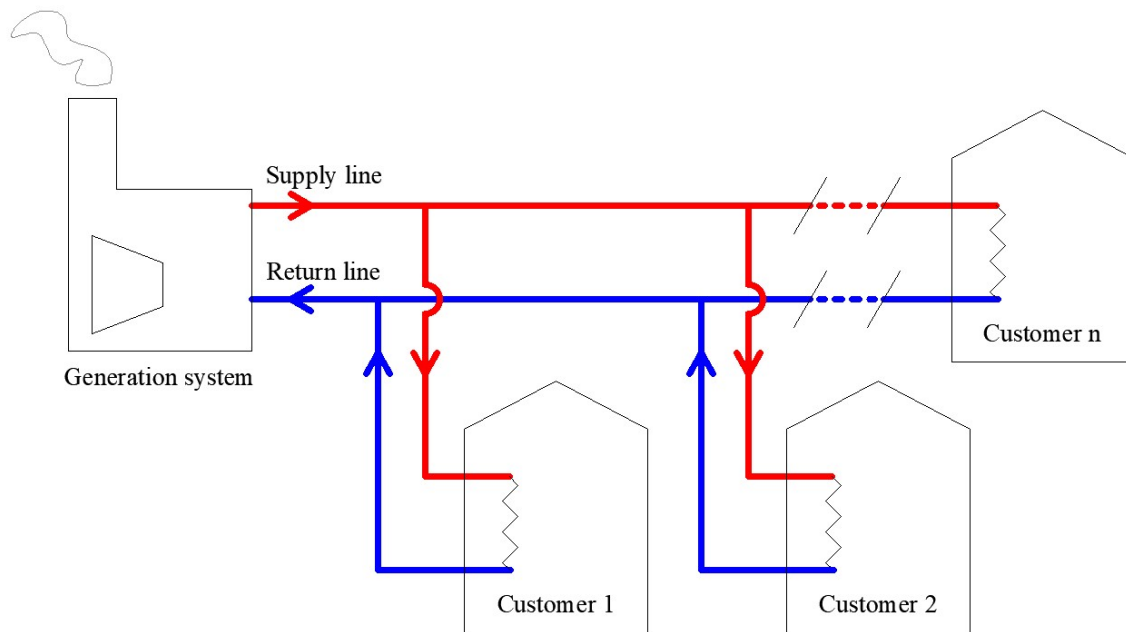


Figure 2.1 Scheme of the delivery of heat in DH networks [6]

The supply water is distributed from the generation system through the district heating until it reaches the costumers connected to the network. The district heating exchanges heat with costumer through a heat exchanger. The return water goes back to the generation system to be heated up again and restarts the cycle.

District heating appeared for the first time in the world at the end of the 19th century. New York has the first district heating (1876) and in a few years the technology has also taken hold in Europe, starting with cities like Hamburg and Paris. Today it has been used permanently for more than 50 years throughout North America, Europe (serving about 60 million citizens, with high peaks in the Eastern countries), Japan, Korea and China [7].

In Europe, the development prospects contained in the EU Commission's roadmap envisage an increase in the district heating service of around 2.1% between now and 2030 and 3.3% by 2050. If investments in renewable energy and district heating technology were upgraded, the expansion would be even greater with remarkable benefits, in fact if the 27 countries of Europe met 50% of its energy needs through the district heating between now and 2050, the use of fossil fuels would drop by 13% [8].

In an area with district heating the emissions are lower thanks to more advanced filtering systems and concentrated only near the production plant. Furthermore, district heating combined with cogeneration is very effective in reducing CO₂ emissions. District heating systems that use cogeneration plants allow the achievement of greater global energy efficiency. With this technology, in fact, the plant can produce electricity and simultaneously recover the thermal energy that is released during the thermodynamic process, which would be dispersed into the atmosphere as "waste" in conventional power plants [9]. A further possibility can be the exploitation of solar collectors or geothermal sources, which have an investment cost but eliminate the marginal costs due to fuel, as it will be shown in Chapter 8.

2.2 Transition to the 4th Generation DH

The district heating taken into account in this thesis-work is a high performances network and will be soon the first 4th generation DH in Italy. The new generation of district heating will use a low temperatures network which will benefit to the energy supply system, end users, and occupants [10]. In historical development of district heating, three generations developed successively as it will be presented in the this section.

The 1st generation DH systems used steam as the heat carrier. Typical components were steam pipes in concrete ducts, steam traps, and compensators. Almost all district heating systems established until 1930 used this technology. It operated with very high temperatures and was therefore not very efficient. There were also problems with reliability and safety due to the hot pressurised steam tubes. Nowadays, this generation is technologically outdated. However, some of these systems are still in use, for example in New York or Paris [11]. Other systems originally built have subsequently been converted to later generations.

The 2nd generation DH systems used pressurized hot water as the heat carrier, with supply temperatures mostly higher than 100 °C. Typical components were water pipes in concrete ducts, mostly assembled on site, large tube-and-shell heat exchangers, and material-intensive, large, and heavy valves. A main reason for these systems were the

primary energy savings, which arose from using combined heat and power plants. While also used in other countries, typical systems of this generation were the soviet-style district heating systems that were built after 2nd World War in several countries in Eastern Europe [11]. These systems emerged in the 1930s and dominated all new systems until the 1970s.

In the 1970s the 3rd generation DH was developed and was subsequently used in most of the following systems all over the world. The third generation uses prefabricated, pre-insulated pipes, which are directly buried into the ground and operates with lower temperatures, usually below 100 °C and compact substations using plate stainless steel heat exchangers. A primary motivation for building these systems was security of supply by improving the energy efficiency after the two oil crises led to disruption of the oil supply. Therefore, those systems usually used natural gas, biomass and waste as energy sources [11]. In some systems, geothermal energy and solar energy are also used in the energy mix.

This thesis work has the aim to simulate through a simplified and flexible network model the whole Merezzate Plus district considering both district network and multi-dwelling units. The successively implementation into the first 4th generation district heating in Italy gives to this thesis the opportunity to dimensioning, monitoring and optimizing the DH system operation and having an easy tool to predict the district's energy usage.

The direction of development for these three generations has been in favour of lower distribution temperature, material-lean components, and prefabrication. On the basis of the trends identified above, the future district heating technology should include lower distribution temperatures, assembly-oriented components, and more flexible materials [5]. The revolutionary temperature level, with supply temperature below 50~60°C, will become the most important feature of the 4th generation DH. Low temperatures have some benefits on the network such as a higher distribution efficiency due to less heat loss from the network, a lower risk of pipe leakages due to thermal stress, and the corresponding maintenance costs are reduced as well, a lower risk of water boiling in the network, which means lower risk of two phase-flow in pumps and the possibility to use plastic pipes in distribution areas with low pressures [12]. It also benefits the occupants and end users,

removing the potential risk of scalding human skin due to water leakages and better matching the future building heat demand and heat temperature. In addition, the 4th generation DH will take advantage of various heat sources, different level thermal storages, modern measuring equipment, and advanced information technology, to make itself more flexible, reliable, intelligent, and competitive.

However, the transition from the current 3rd generation DH to the future 4th generation DH is a challenging task. There are some technical issues associated with transition to the 4th generation DH such as supplying low temperature to new and existing buildings, integrating various heat sources including renewable sources and recycled sources, different TES (thermal energy storage) technologies, and smart DH systems. The implementation of Merezzate Plus into a 4th generation district heating opens also doors for some network optimization to improve the energy efficiency and sustainability through the integration of a decentralised solar thermal system. In fact, the low temperatures of the new generation DH will provide a higher output capacity from the connection to the solar heat collectors [12].

In the next Chapter the decentralised thermal system will be described and some different solar thermal district options will be presented.

2.3 Decentralised Solar Thermal DH

Solar thermal DH has been used as a label for district heating systems that have solar collectors as part of the integrated heat supply. This solar heat supply has been developed since the 1980s in Sweden [13], Denmark [14], and Germany [15]. The main advantage of solar district heating is its economy-of scale, as it can provide a lower levelized cost of solar heat with seasonal storage than smaller units [16].

Solar district heating plants can either be centralised or decentralised. Centralised plants are normally ground-mounted and cover a large land area, instead the decentralised solar district heating has the solar collectors located outside the central heat supply plants. These decentralised plants are often roof-mounted, which can be an advantage in urban

areas with high land-area costs. They were first introduced about two decades ago and, nowadays, appear mainly in Sweden, Denmark, Germany, and Austria [17]. Four different connection principles are available for connection of a local heat source to a district heating network. The most used feed-in connections are the return/supply (R/S) and return/return (R/R) connections. The other two possible connection alternatives: supply/return (S/R) and supply/supply (S/S) are rarely used [17]. The four principles for decentralised solar district heating will be studied carefully in Chapter 8. A fundamental principle for a well-functioning feed-in is that the feed-in heating energy must match the heating energy generated by the solar thermal system if no storage is used. It is often beneficial to avoid storage for practical and economic reasons [18].

The ultimate aim of this thesis-work is to evaluate a solution with a decentralised solar system by using the district network as a storage tank for the multi-dwelling units of Merezzate Plus. Some different connections with relative benefits will be studied in Chapter 8 in order to find the best optimisation for the next 4th generation district heating of Merezzate.

2.4 Milan District Heating

In the municipality of Milan, the district heating was developed since the 1990 and feeds today over 3000 buildings, including some historic places of the city such as Duomo, La Scala, Palazzo Marino, La Galleria, Palazzo Reale, Il Tribunale, and modern ones such as City Life, Cascina Merlata and Bicocca University, significantly reducing the CO₂ emissions and fine particles PM₁₀. The first plants were built in Bicocca area and Famagosta area. These first two projects were soon followed by other plants such as the West network in the Gallaratese area, which uses the recovered heat from the "Silla 2" waste-to-energy plant, and the district heating network in the Eastern area of Milan powered by the new "Canavese" plant and by the Linate airport plant [19].

The Milan district heating network is managed by A2A Calore & Servizi, a company of A2A Group, that has been designing and implementing heat production and conduction activities. The district heating provided by A2A is an efficient solution for heating

buildings while respecting the environment by using the resources available in the area. It can exploit heat generated by renewable sources (solar thermal, geothermal, biomass, wind etc), cogeneration or it can recover excess heat from industrial production and waste treatment cycles. The energy, produced or recovered, heats the water which is distributed to the homes thanks to a network of insulated steel pipes equipped with an automatic detection and localization system of failures, monitored 24 hours per day. The traditional boiler is then replaced by a heat exchanger that allows the heat contained in the water to be transferred to the internal distribution system of the building to heat the rooms and produce also domestic hot water [19].

A2A Calore & Servizi works mainly: in the production, distribution and supply of district heating; in the design, construction and operation of cogeneration plants and in heat distribution networks and in heat management and facility management. Merezzate Plus project was made in partnership with A2A and it is the company which provide for this thesis-work the pre-sizing data to create the dynamic network simulations and the monitoring data to check and validate the created model.

The following Chapter will focus on the methodology and the structure of this thesis-work, explaining the theory of the strategies and models that will be analysed in detail within this paper.

3. Methodological Approach

This Chapter focuses on the methodological approach of this thesis-work. In this section all the steps which conceptually make the structure of this work are explained in detail with applied tools. The methodology of this thesis-work can be schematised through the following steps:

- Aim of the work: the purpose of this thesis-work is to evaluate the integration of a decentralised solar thermal system in a district heating network.
- Tools: a thermodynamic model is created in TRNSYS thanks to the annual pre-sizing data redistributed through the BIN method.
- Validation: the model is validated with the real monitoring data provided by A2A.
- Implementation: the created model is used to evaluate the decentralised solar thermal integration in current and future scenarios.

These steps are deeply analysed in the following paragraphs.

3.1 Purpose of the Thesis

This thesis-work focuses on the analysis of the district heating simulation of Merezzate Plus project and tries to improve the energy efficiency of the whole district. The entire residential project and its relative district heating is analysed in Chapter 4, in order to fully understand its characteristics and potential improvements. The Merezzate district heating network and connection with the relative building complex of the project are described considering two different circuits: the district heating network (primary side) and the multi-dwelling unit circuit (secondary side).

The final purpose is to implement the Merezzate district through a decentralised solar thermal system which exploits the district heating network as a storage tank for the multi-dwelling units. The solar district optimisation and the flexibility of the simulation, together with a validated thermodynamic model, allow to integrate the future intervention for renovating the Merezzate district into the first 4th generation district heating in Italy.

Therefore, the solar district heating model is also studied with a low temperature network configuration and the results will be compared with the currently high temperature network.

3.2 Used Tools

This thesis-work wants to propose a flexible simulator capable of describing all the significant quantities from supply and return temperatures, to mass flow rates and energies, reflecting them in all the network components and simulating their trend over time, depending on external conditions, i.e., thermal demands of the utilities, hot fluid delivery temperature and environmental conditions.

The hourly energy needs are fundamental to calculate the mass flow rates and correctly size the network model. The pre-sizing data provided by A2A only provides annual energy needs for each multi-dwelling unit. Hence data are redistributed, according to an hourly grid. The BIN method [20] is used in Chapter 5 to redistribute the annual pre-sizing energy data for every building of each multi-dwelling unit, in order to calculate the hourly mass flow rates of the whole Merezzate district. The mass flow rates are used in the network model to describe the primary and secondary side of the district heating in Chapter 6. The employed software for the creation of the network model is TRNSYS which is a complete and extensible simulation environment for the transient simulation of systems, including multi-zone buildings [21].

TRNSYS, abbreviation of “Transient Simulation”, is a quasi-steady simulation software which simulates the system in long run. It is written in ANSII standard Fortran-77 and it is based on the solution of the energy balance equations (transmission, ventilation, internal gains etc...) of the various components of the building in order to find the quantities characterizing them. The model of the building is constructed as a network of nodes, resistances and capacities that define the relationships between the components [21], first of all the ambient air node. TRNSYS simulations are constructed by connecting individual component models (known as Types) together into a complete model. These individual components represent a piece of equipment that can be represented by a system

of equations to calculate its performance, such as pumps, pipes, chillers, solar collectors, etc... These are then connected together in the TRNSYS environment similarly to how they would be connected in real life [21]. The software can interconnect system components, types, in any desired manner, solving differential equations and facilitating information output. Each component is defined through a certain number of constant “parameters” and time dependent “inputs” and produces a time dependent “output” [21]. TRNSYS 18 is employed here.

The software allows the creation of dynamic model, exploiting the hourly energy needs, the variable return temperature from the multi-dwelling units simulated from two representative apartments and the outlet primary side temperature calculated at the previous instant. The aim of Chapter 6 is to obtain a model that gives information both on the district heating side (primary side) and multi-dwelling unit side (secondary side), to evaluate the actual situation of the district network and simulate the future interventions.

3.3 Validation of the Model

Once the Merezzate district network model has been designed, it is necessary to ascertain the validity of the used model to describe the components that constitute it and their interactions. To proceed with the validation of the work, it is necessary to compare the results calculated from the TRNSYS network model with the monitoring data, to understand their limits and potential improvements. The monitoring data used for this purpose are provided by the A2A Servizi & Calori and represent the Merezzate network from September to November 2020.

The results calculated from the pre-sizing data with the TRNSYS model show some optimization margins. For example, the mass flow rate used by the network could be much lower than the real one and the district heating could exchange more energy through the multi-dwelling unit substations.

To validate the model, the same conditions of the reality are applied. Therefore, another simulation will be done in Chapter 7, considering the same heat transfers calculated from the monitoring data. When the comparison is made with the same energies the model can be validated. The monitoring heat transfers are used as input file in the TRNSYS network model to check and validate the results. The created model and the performed simulation provide consistent results and a simplified scheme of the district heating.

3.4 Implementation of the Model

Once the model is validated, the aim of this thesis-work is to implement the Merezzate district through a decentralised solar thermal system which exploit the district heating network as a storage tank for the multi-dwelling units. The solar district optimisation and the flexibility of the simulation, together with a validated thermodynamic model, allow to integrate the future intervention for renovating the Merezzate district into the first 4th generation district heating in Italy. Therefore, the solar district heating model is also studied with a low temperature network configuration and the results will be compared with the currently high temperature network in Chapter 8.

The ideated solution consists in a solar thermal system integrated with the district heating, which works as an auxiliary heater for the multi-dwelling unit when temperatures reach the set-point and as a decentralised system for the whole network when temperatures do not reach the supply temperature.

The results from the simulations will be compared and studied from an energetic, environmental and economic point of view. The limits of this solution and the possible optimization for a decentralised solar system are analysed in the last paragraph of Chapter 8, where the obtained results are discussed to understand the margins of improvement.

4. Case Study: Merezzate Plus

In this Chapter the entire residential project and its relative district heating is analysed, in order to fully understand its characteristics and potential improvements. The real project taken into consideration for this purpose is Merezzate Plus in Milan. In this Chapter the Merezzate district heating network and connection with the relative building complex of the project will be described and carefully analysed.

4.1 Merezzate Plus Multi-Dwelling Units

Merezzate Plus is a new affordable housing district in the south-east area of the city of Milan. It is currently under construction, with 800 apartments 615 of which dedicated to social housing. It is designed to accommodate new lifestyles and met the highest environmental sustainability criteria. The buildings are arranged along a central avenue overlooked by an articulated system of open and permeable courtyards, which ends with the main square located to the north, in which local and urban services are concentrated.

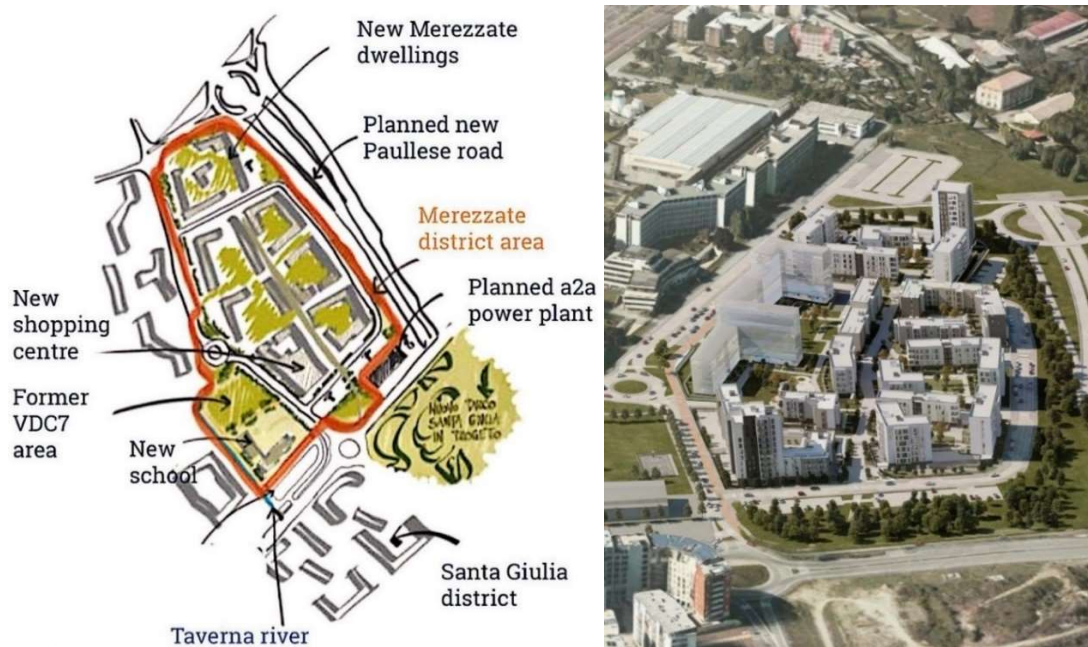


Figure 4.1 Merezzate Plus district area [22]

The relationship spaces generated in this way, create at the same time an urban and domestic environment with social and collective functions, such as commerce, local urban services and integrated services for living, to support a collaborative and young living. Supported by a community manager, the future residents will be able to collaborate to define and manage the spaces and collaborative services, thus creating an ecosystem of relationships capable of improving the daily life quality [23]. For the realization of this project 6 architectural firms, 4 engineering companies, and the best social and smart advisors were involved, as well as the partnership with A2A, that has made it possible to create a new way of supplying energy, simple, innovative and above all economical.

Merezzate district is composed by eight multi-dwelling unit (UDC) of different high-energy class buildings (E) and different functions, as it is shown in the Figure next page. Nowadays, five the following multi-dwelling units are completed: UDC 1, UDC 3, UDC 5, UDC 6, UDC 9. Therefore, just these five multi-dwelling units will be studied in this thesis-work (Figure 4.2).

Each residential unit is currently connected to the Merezzate district heating through a substation made of two plate heat exchangers with an exchange potential about 700 kW each, which split the primary (DH) and secondary (user) side of the system network. The heated water from the UDC goes directly to its buildings for space heating and DHW without needing any other heat exchanger or storage tank. The performing buildings in Merezzate district are well insulated low energy demanding, in classes between A1 and A3, served by the district heating network with an average non-renewable primary energy need equal to 40 kWh/m² (17 kWh/m² for DHW and 23 kWh/m² for space heating).

For the Merezzate Plus project the following partners are involved:

- A2A Calore & Servizi is the leading partner of this task and the developer of the low temperature district heating sub-network.
- Politecnico di Milano works in collaboration with A2A to develop the network model-based control system, capable to optimise the potential integration of high shares of RES (renewable energy source) on low temperature district heating networks.
- InvestiRE SGR is the real estate operator who built the building complex.

Case Study: Merezzate Plus



Figure 4.2 Merezzate Plus plan [24]

In the following paragraphs, the Merezzate network configuration will be analysed according to the Merezzate Plus project and the next ambitious improvement to 4th generation district heating will be also described.

4.2 Merezzate High Temperature Network

The first design of district heating system in Merezzate area contemplates the use of a high temperature network. This is the usual layout for district heating networks in Milan. The 3rd generation DH of Merezzate uses insulated pipes that operates with supply temperatures about 100 °C and return temperatures around 40 °C.

The delivery of heat in Merezzate has been designed through a new sub-network connected to the existing DH high temperature network “Milano Est”. The high temperature network in Merezzate district is fed by two heat generation plants:

1. The generation plant “Canavese”, which covers the eastern area of Milan, with the districts Città Studi, Argonne, Corsica, Lambrate up to the area of the Melloni Hospital and Il Tribunale. The plant, which started operating in 2007, is in the former AEM (anion exchange membrane) gas station, near Viale Forlanini.
In accordance with A2A's environmental policies, the plant has been equipped with the most modern technologies aimed at minimising its environmental impact. The plant is innovative in the use of geothermal energy from groundwater for heat pumps. The heat pump, which is electrically powered, extracts heat energy from the groundwater and returns it to the user connected to the district heating network. Gas engines produce electrical and thermal energy from the recovery of heat from the cooling circuit of the system [19]. The boilers integrate the production of thermal energy satisfying the peaks of demand, with two storage tanks.
2. The generation plant “Linate” supplies heating and electricity to Milan Linate airport. This service is flanked by another that makes the plant very important for the city of Milan: in fact, the heat produced by the plant is used to provide district

heating to a large urban area between the streets Salomone, Ungheria, Forlanini, Mecenate and Fantoli.

The plant is mainly made up of three cogeneration groups, equipped with the relative auxiliary systems. The first engine of each cogeneration group is an alternative internal combustion engine, powered by natural gas for the combined production of electrical and thermal energy. The thermal energy is produced by a system of thermal recovery from the exhaust gases of the engines, in the form of superheated water (about 120 °C in the delivery and 90 °C on the return) and the cooling fluids of the engines. In parallel to the circuit of thermal recovery from the motors, two additional boilers have been installed. A thermal storage system with a capacity of 10 MWt allows flexible and economical management of the cogeneration heat. In addition, to comply with current local regulations on emissions, the plant has been equipped with an SCR (selective catalytic reduction) plant for the control of nitrogen oxides [19].

Table 4.1 Merezzate heat generation plants by AIRU [25]

Heat Generation Plant	Generation Type	Total Installed Power	
Canavese	Endothermic Engine	15 MWe	13 MWt
	Gas Boiler	-	55 MWt
	Groundwater Heat Pump	-	15 MWt
Linate	Endothermic Engine	24 MWe	24 MWt
	Gas Boiler	-	60 MWt

The HT district heating exchanges heat with the multi-dwelling units (UDC) of Merezzate through the substations made by a double plate HX as presented in the previous paragraph.

In the following section the multi-dwelling unit substation is analysed.

4.2.1 Multi-Dwelling Unit Substation

Each residential unit is currently connected to the Merezzate district heating through a substation made of two plate heat exchangers with an exchange potential about 700 kW each, which split the primary and secondary side of the system network, as shown from the picture below. The secondary side distributes heat to all the apartments of the buildings of the multi-dwelling unit.

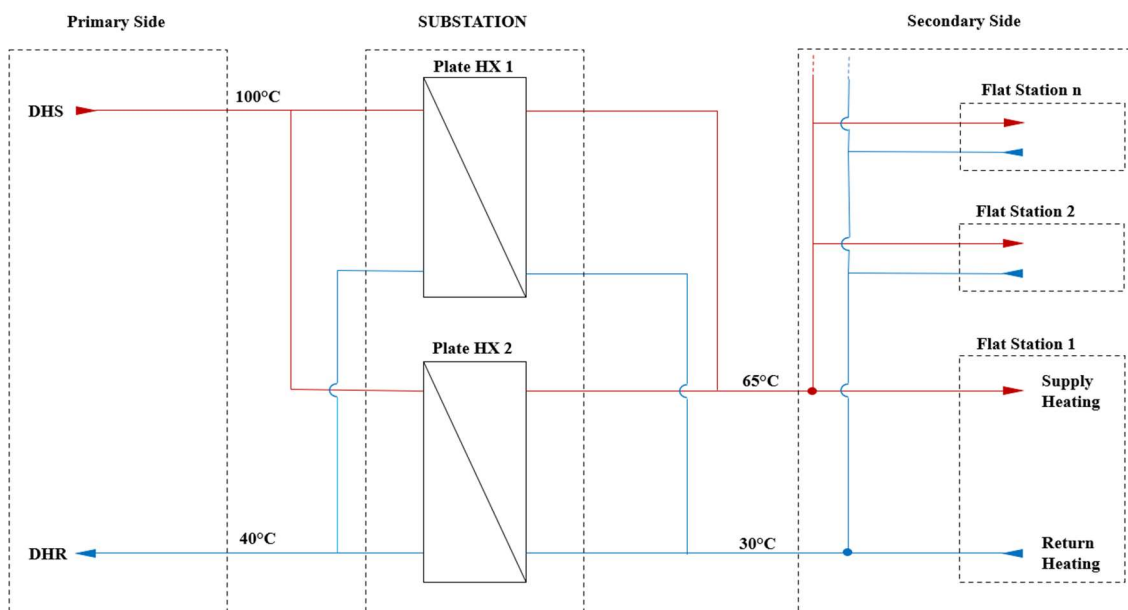


Figure 4.3 Scheme of a generic multi-dwelling unit substation

The temperatures of primary side are between 100 °C for the supply line (DHS) and 40 °C for the return line (DHR). Instead, the temperatures of the secondary side are around 65 °C for the supply heating and 30 °C for the return. The heated water of the secondary side is used both for space heating and domestic hot water, without using any other heat exchanger or storage tank, thanks to the innovative flat stations at each apartment.

In the following paragraph the innovative flat stations are explained and analysed.

4.2.2 Innovative Flat Station

The innovative flat stations of Merezzate buildings allow the direct use of heated water for space heating without needing any other heat exchanger and for domestic hot water without needing any storage tank. A simplified scheme of the innovative station is shown in Figure below.

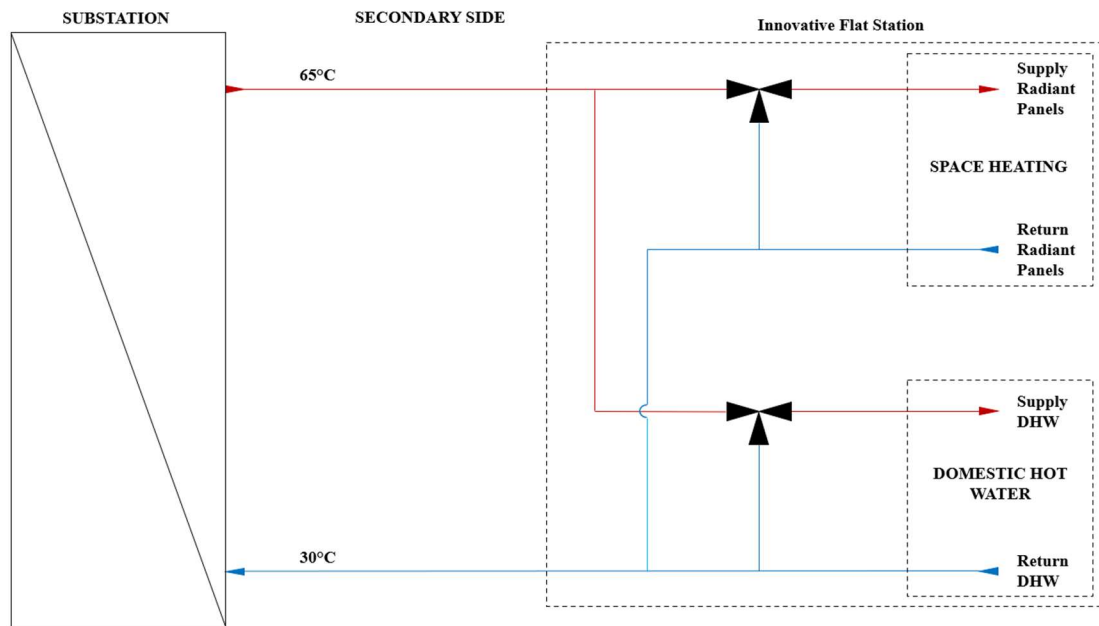


Figure 4.4 Simplified scheme of innovative flat station

The innovative flat station is the component of the secondary side which connects the apartments of each building to its relative multi-dwelling unit in Merezzate district. After the water is heated from the substation (double plate HX) of each multi-dwelling unit, the hot water is distributed to each building of that unit. The heated water is used both for space heating and DHW without needing heat exchanger or storage. This is possible because the temperature of the supply water in the secondary side is always higher than 60 °C to avoid the growth of legionella bacteria in the DHW. Moreover, the presence of mixing valves allows recirculation in order to match the temperature needed at each user.



Figure 4.5 Image of the flat station [26]

4.3 Merezzate Low Temperature Network

In the work of Merezzate Plus project there is also a new ambitious improvement of the concept concerning the district heating network. The main characteristic of the new district heating network is the implementation of a low temperature sub-network, fed by the main city network [6], which would be one of the first use of this technology in Italy: the so-called 4th Generation of District Heating systems.

The new Merezzate district heating (4th generation DH) will be a low temperature network designed to operate with a supply temperature around 65 °C and a return temperature of 30°C. This temperature levels are allowed thanks to the new high-energy class buildings (between A1 and A3) which are performing and have systems that operate at low temperatures which allow a better integration of renewables. The use of a low temperature network implies the supplying of the required thermal power with larger diameters to manage the increase of the flow. The low temperature network allows to supply heat directly in the domestic heating system without using the heat exchangers of the multi-dwelling unit substations thanks to the innovative flat stations. The instantaneous production of DHW is possible through a heat exchanger in the installed flat station.

A generic scheme of the next 4th generation DH without the multi-dwelling unit substation is shown in the following picture.

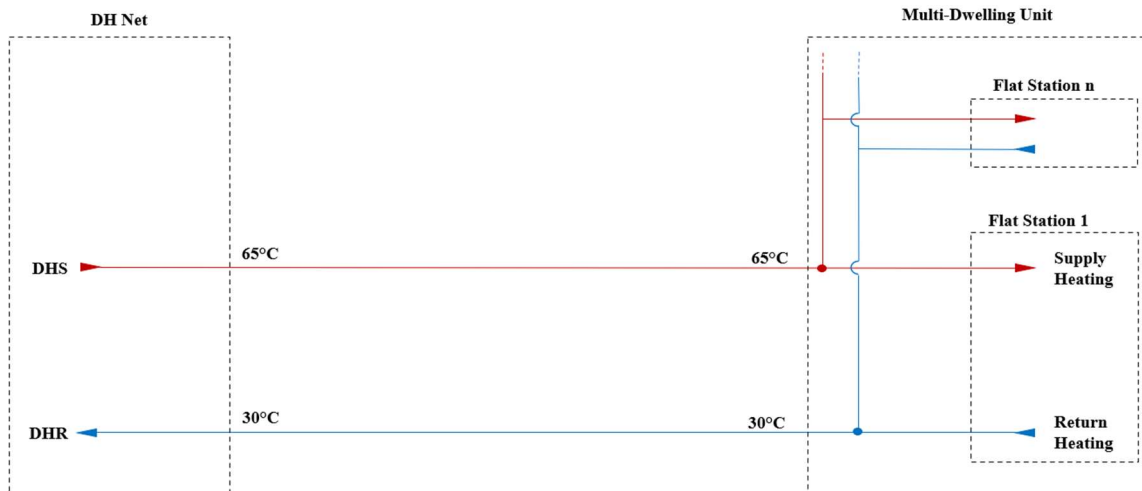


Figure 4.6 Scheme of the next 4th generation DH at low temperatures

The 4th generation DH represents a great improvement in terms of reduction of the heat losses in the network, both in the pipes across the insulation and through a better generation in the central plant. The working temperatures are 65 °C for the supply pipes and 30 °C for the return pipes. Therefore, the average temperature is closer to the external temperature and the heat dispersions are limited. The total energy saving for this sole change is estimated at 142 MWh/year, which is the 8% of the total energy produced and a cut of 44% of the total heat losses which would be forecast with the use of a high temperature network [6]. These results produce a new reduction of CO₂ emissions, out of the first strong curtailment in the building envelope design, following the “fabric first” strategy of Climate-KIC protocol (supported by the EIT: European Institute of Innovation & Technology, a body of the European Union).

For this reason, one of the aims of this work is the provision of a new flexible model able to simulate the next 4th generation DH. The low temperature in the network, together with the availability of a thermodynamic simulation tool, creates, indeed, an enabling premise able to integrate a high share of renewable heat sources on the network, as it will be seen with the solar thermal implementation in Chapter 8.

In the following Chapter the pre-sizing data of primary side provided by A2A will be analysed for each building of Merezzate multi-dwelling units.

5. Merezzate Plus Pre-Sizing Data

In this Chapter the pre-sizing data provided by A2A Calore & Servizi are presented in the following Tables. The data presented are referred to the buildings (E) grouped in their respectively multi-dwelling units (UDC) analysed in this thesis-work. Merezzate is a quiet cold climate, for this reason the cooling season will not be taken into account in this thesis, just the space heating and the domestic hot water will be analysed throughout all the chapters. The Merezzate network can be divided in two different circuits: the district heating network (primary side) and each single multi-dwelling unit network (secondary side), according to the previous chapters. All the pre-sizing data provided by A2A belong to the primary side, in order to estimate the heat exchange at each multi-dwelling unit and correctly dimension the plate heat exchangers.

Space heating and DHW data are shown in the following Tables for every building of each multi-dwelling unit analysed.

Table 5.1 UDC 1 pre-sizing data

Unit	Building	n° Flats	Power Need [MW]	Usable Heated Area [m ²]	DHW [kWh]	Heating [kWh]	Heating [kWh/m ²]
UDC1	E01	167	1.40	1487.76	25173	36711	24.68
	E02			1716.88	30760	43294	25.22
	E03			1288.16	24739	32581	25.29
	E06			2899.15	55840	68792	23.73
	E07			1913.90	33316	53483	27.94

Table 5.2 UDC 3 pre-sizing data

Unit	Building	n° Flats	Power Need [MW]	Usable Heated Area [m ²]	DHW [kWh]	Heating [kWh]	Heating [kWh/m ²]
UDC3	E08	127	1.10	2444.88	45049	63073	25.80
	E10			1076.61	21005	26372	24.50
	E11			1106.52	21615	25443	22.99
	E12			1531.06	28433	32539	21.25
	E13			1077.22	20645	25097	23.30

Table 5.3 UDC 5 pre-sizing data

Unit	Building	n° Flats	Power Need [MW]	Usable Heated Area [m ²]	DHW [kWh]	Heating [kWh]	Heating [kWh/m ²]
UDC5	E21	111	1.10	1344.19	25247	31224	23.23
	E22			1053.78	20458	26346	25.00
	E23			2610.35	50353	42433	16.26
	E24			824.15	16320	14267	17.31
	E25			2024.71	5969	61869	30.56

Table 5.4 UDC 6 pre-sizing data

Unit	Building	n° Flats	Power Need [MW]	Usable Heated Area [m ²]	DHW [kWh]	Heating [kWh]	Heating [kWh/m ²]
UDC6	E14	109	1.00	1601.89	30277	40495	25.28
	E15			1176.62	20516	29730	25.27
	E16			2140.37	40776	47108	22.01
	E17			1609.90	29863	38279	23.78

Table 5.5 UDC 9 pre-sizing data

Unit	Building	n° Flats	Power Need [MW]	Usable Heated Area [m ²]	DHW [kWh]	Heating [kWh]	Heating [kWh/m ²]
UDC9	E18	95	0.90	1146.17	20926	30344	26.47
	E19			2095.39	38652	49521	23.63
	E20			2479.20	37687	36467	14.71

Summing up all the multi-dwelling unit's data provided by A2A, an indicative amount of the total energy need by the whole Merezzate complex will be found as shown in the following Table.

Table 5.6 Merezzate district total pre-sizing data

Unit	Building	n° Flats	Power Needed [MW]	Usable Heated Area [m ²]	DHW [kWh]	Heating [kWh]	Heating [kWh/m ²]
ALL	TOT	609	5.50	36648.86	643619	855468	23.34

In the following chapters the annual data of each multi-dwelling unit will be redistribute according to an hourly grid thanks to the BIN method for space heating and normative

laws for DHW. These analysis steps are fundamental for having data for the overall analysis especially because the whole year will be taken into account in this thesis-work. The monitoring data will be provided for a very small period; therefore, it is crucial diversifying the data of each building in order to validate the model and provide hourly data for running the simulations. The small period of monitoring data is due by the fact that Merezzate Plus is a new urban district and people started living there from April 2020. Moreover, the heating season starts from middle of October, so there are not many data to validate the model.

The BIN method is applied in the following paragraph in order to calculate the hourly energy needs which will be used as input file in the thermodynamic model.

5.1 BIN Method

The BIN method (UNI/TS 11300-4) [20] is fundamental for the creation of a dynamic model to analyse different energy consumptions during the year. It requires the availability of the hourly frequencies with the relatively dry-bulb air temperatures of Linate weather station. This method considers the high variability of performance with the external temperature and proposes an analysis by outside air temperatures and time intervals. The previous annual data for space heating are redistributed, according to an hourly grid. The following analysis are based on data provided by Energy Plus [27] for the Milan station: Linate 160800. It will also be the file used during all the dynamic simulations within this thesis.

The results from the BIN method will be used in Chapter 6 in order to find the mass flow rate of primary and secondary side in the network model and show some optimization margins, comparing them to the monitoring data in Chapter 7.

All the buildings of Merezzate district use radiant panels for space heating. The radiant panels work with two different internal set-point according to the day hours and night hours. Therefore, two different balance temperatures are set, for applying the BIN

method. One is set equal to 16 °C for the day hours ($T_{balance_day}$) and one equal to 14 °C for night hours ($T_{balance_night}$).

After the temperature balance are set the part load ratio (PLR) is calculated for every hour according to the external ambient temperature (T_{amb}) and the minimum external temperature (T_{amb_min}), following the next formula:

$$PLR = (T_{balance} - T_{amb}) / (T_{balance} - T_{amb_min}) \quad (5.1)$$

When the PLR is calculated, the annual pre-sizing space heating ($Heating_annual$) is divided by the annual sum of PLR obtained (PLR_annual) for each building, in order to calculate the heating peak (Q_peak).

$$Q_peak = (Heating_annual) / (PLR_annual) \quad [kWh] \quad (5.2)$$

Then Q_peak is redistributed, by multiplying it for each hourly PLR, in order to find the energy consumptions ($Q_heating$) according to an hourly grid.

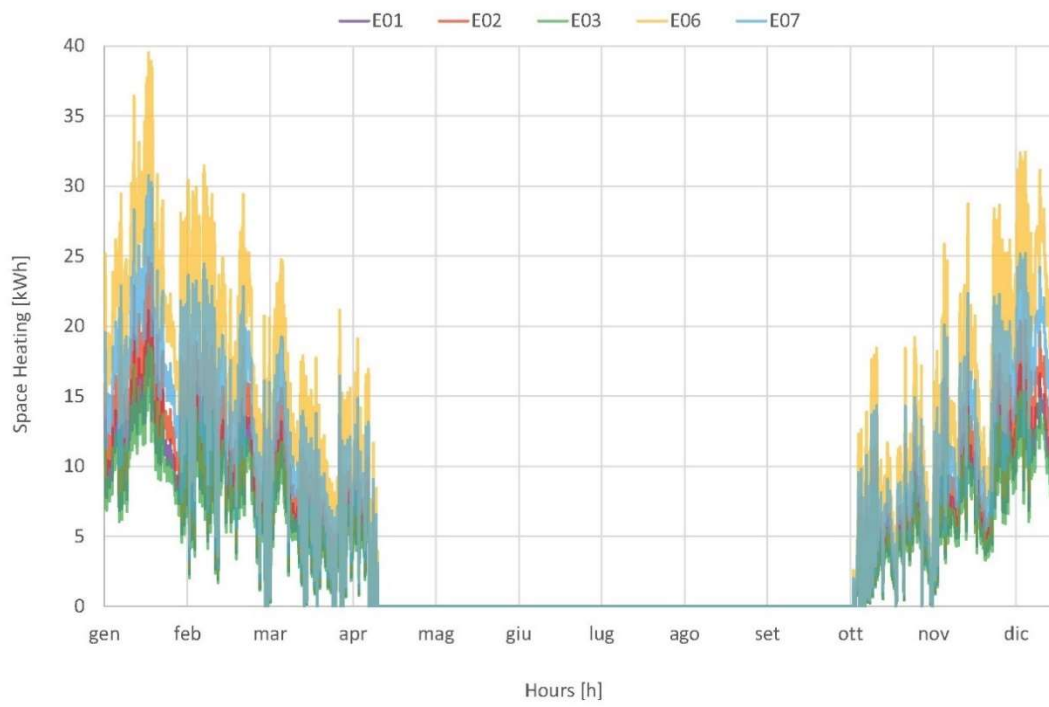
$$Q_heating = Q_peak \cdot PLR \quad [kWh] \quad (5.3)$$

The heating season is defined by the DPR 26/08/1993 n. 412 (and subsequent amendments) depending on the climatic zones. Milan is located in climatic zone E, which provides for an ignition period ranging from 15 October to 15 April. All the heating systems are connected to the Milan district heating, so it means radiant panels are activated from the 15th of October to the 15th of April.

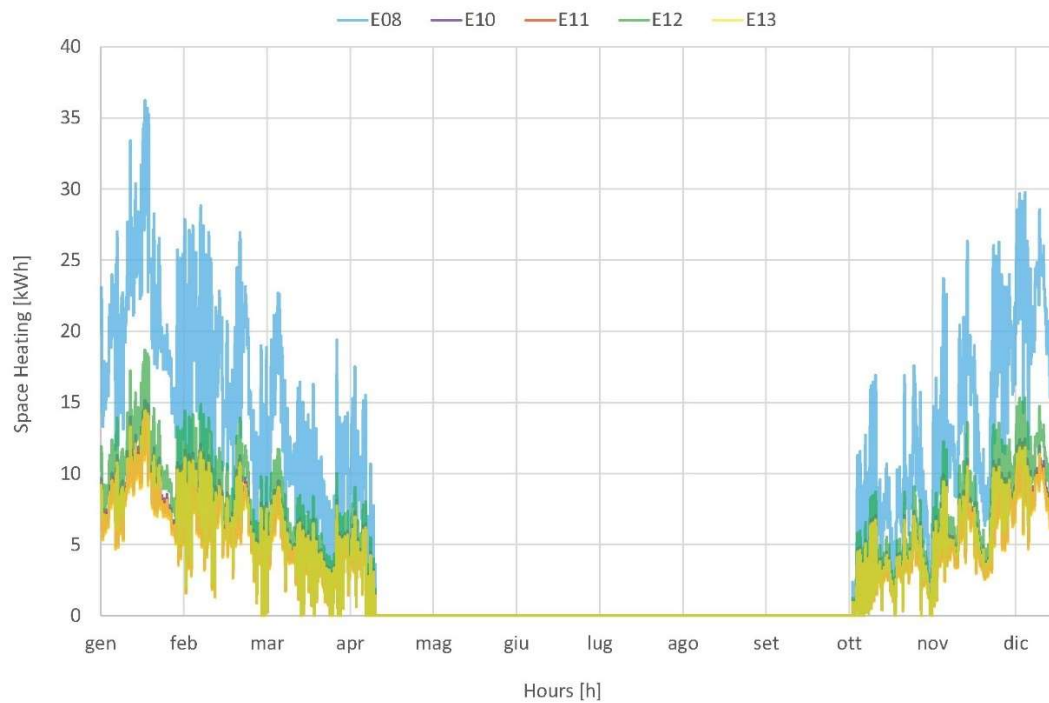
The hourly space heating obtained through the BIN method, are shown for every building of each multi-dwelling unit within this section.

The obtained results calculated by the BIN method to redistribute the annual energy need for space heating according to an hourly grid are shown in this Chapter for every building (E) of each multi-dwelling unit (UDC). During summer, the heating plants are off, according to the DPR 26/08/1993 and for this reason there are no results shown.

Merezzate Plus Pre-Sizing Data

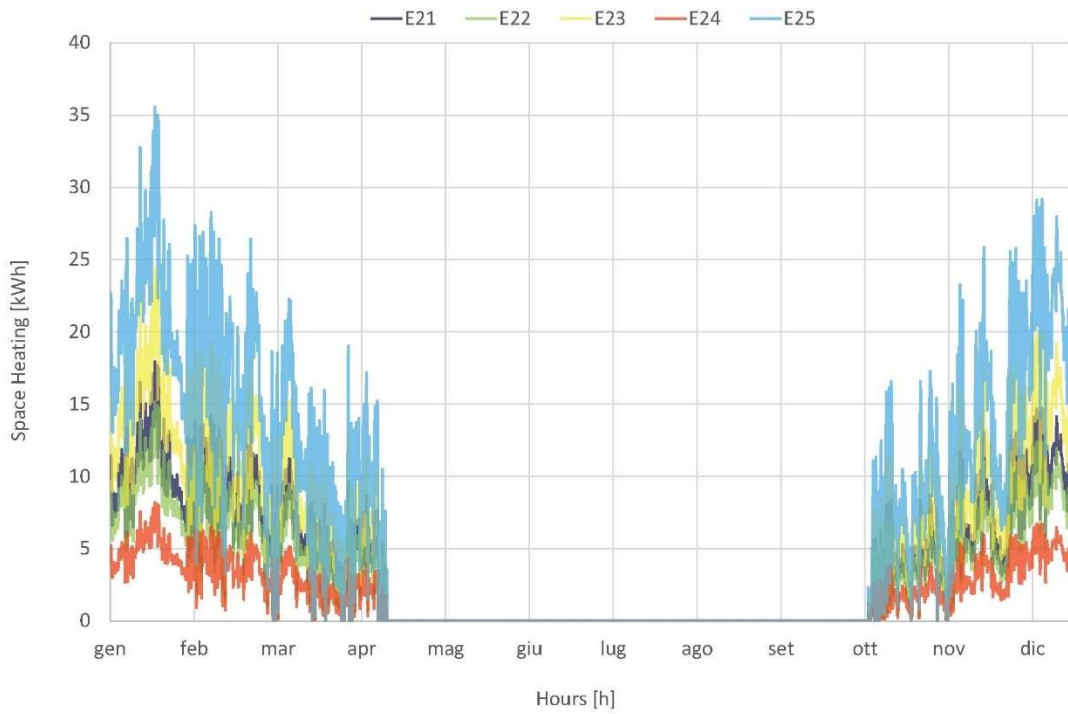


Graph 5.1 UDC01 space heating obtained by applying the BIN method

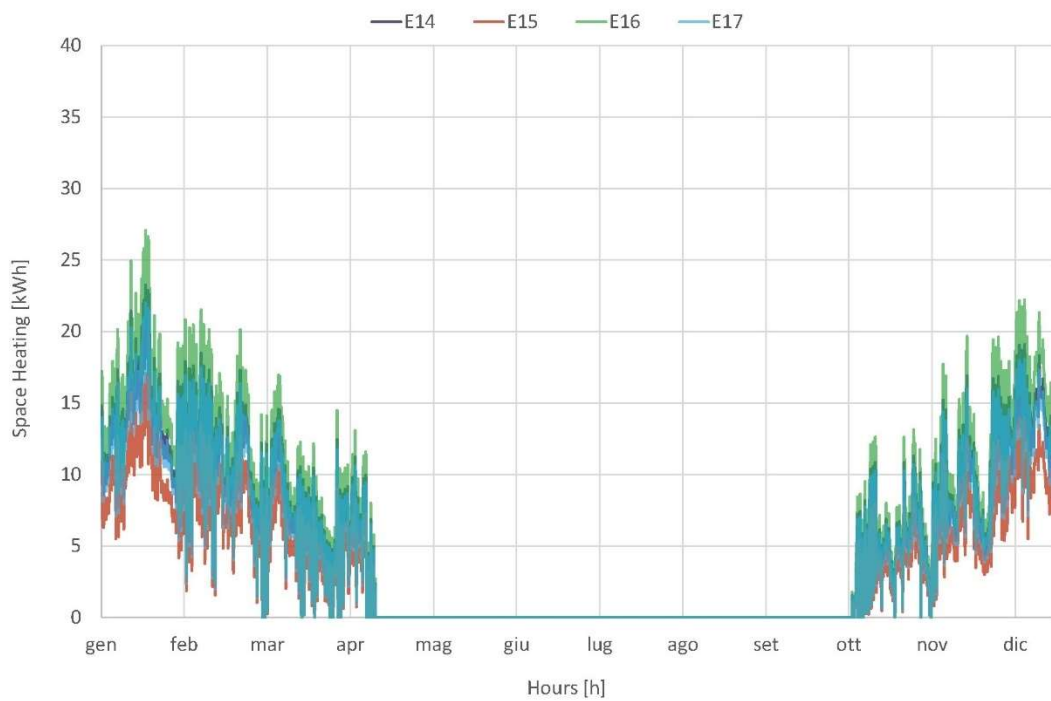


Graph 5.2 UDC03 space heating obtained by applying the BIN method

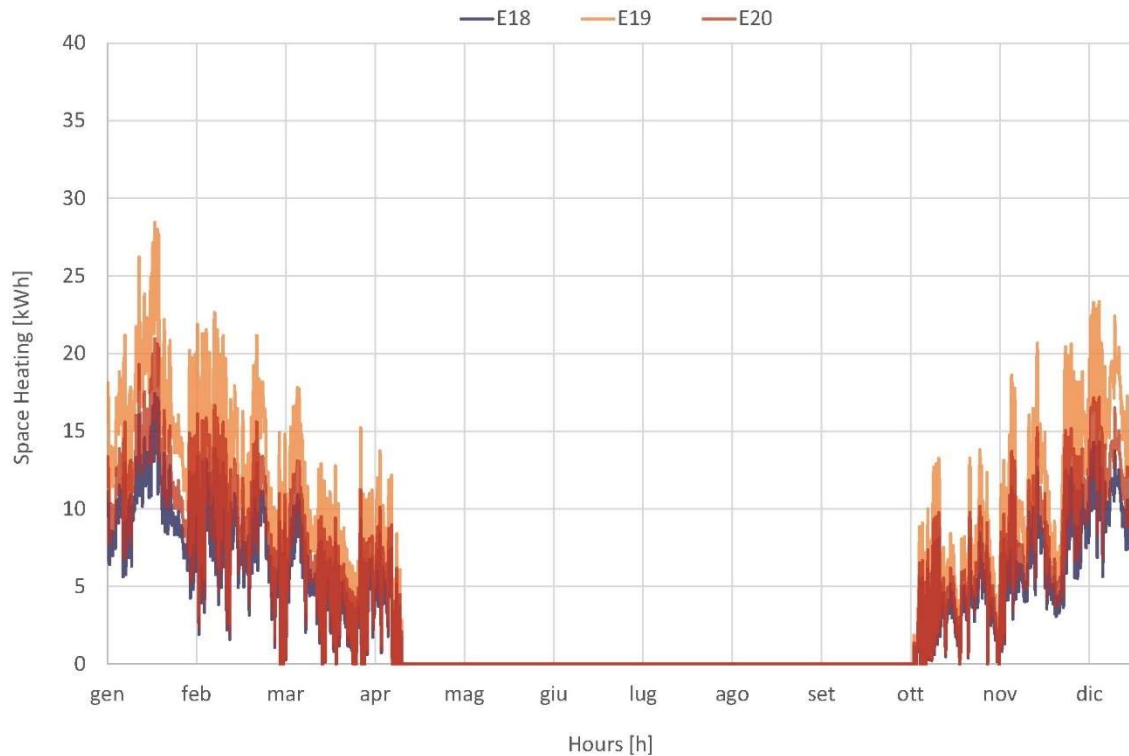
Merezzate Plus Pre-Sizing Data



Graph 5.3 UDC05 space heating obtained by applying the BIN method



Graph 5.4 UDC06 space heating obtained by applying the BIN method



Graph 5.5 UDC09 space heating obtained by applying the BIN method

After the space heating is redistributed according to an hourly grid, the domestic hot water has to be calculated in the following paragraph, according to an hourly week profile by following normative laws.

5.2 Domestic Hot Water

In this Chapter, a daily hourly profile will be calculated for the production of domestic hot water, according to the normative. There are two different way for calculating the DHW energy demand. The first method calculates the DHW consumption by people, instead the second one the finds the DHW consumption by meter square. Both ways will be calculated in this Chapter in order to find the optimal method for Merezzate situation, and the closest method to the pre-sizing data.

1. DHW Load (UNI 11300-2) per m²

The water consumed as litre per day (q) is calculated by the multiplication of the usable area (Su) for energy requirement factor (a)

$$q = a \cdot Su \quad [l/day] \quad (5.4)$$

where “a” factor is calculated as: $4.514 \cdot Su^{-0.2356}$ for $Su \ 51 < m^2 < 200$

Then the energy consumption (Q) is calculated by multiplying the water consumed per day (q) for the water density (ρ), its specific heat (c_p), the difference between the use temperature (T_{use}) and the mains temperature (T_{mains}), divided by 1000.

$$Q = \rho \cdot (q/1000) \cdot c_p \cdot (T_{use} - T_{mains}) \quad [J/day] \quad (5.5)$$

2. DHW Load (UNI 9182) per people

The water consumed as litre per day (q) is calculated by the multiplication of litre used per person per day (q_p) for the number of people (N_p)

$$q = q_p \cdot N_p \quad [l/day] \quad (5.6)$$

where q_p for an average flat is about 50 litre per person

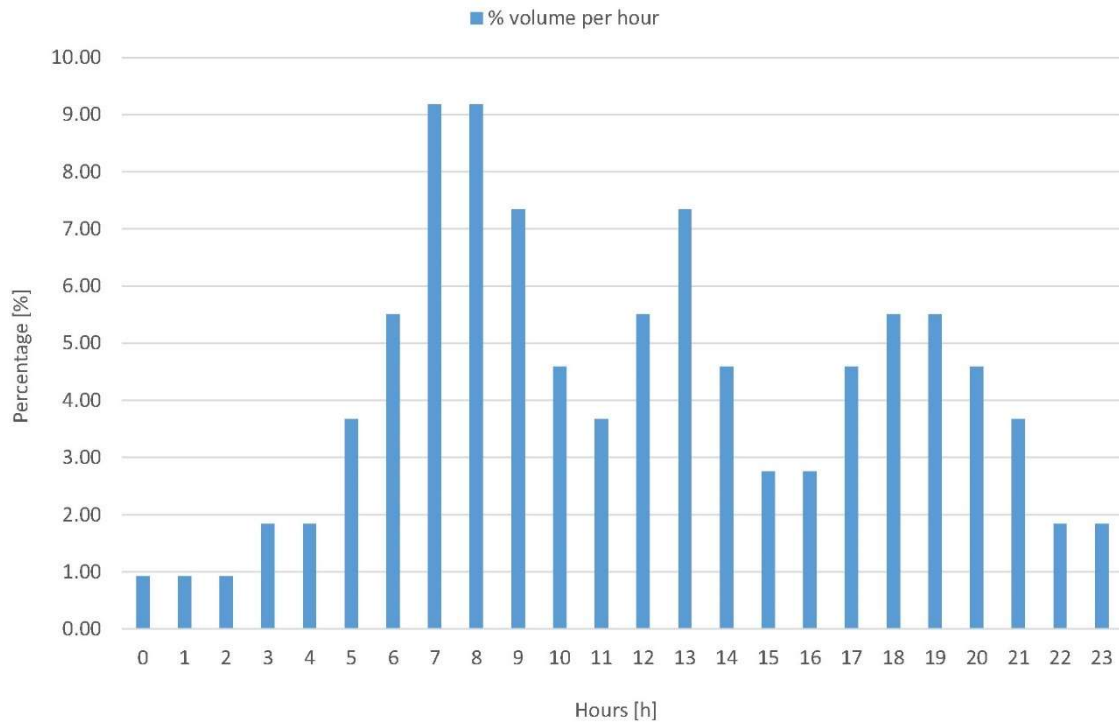
Then the energy consumption (Q) is calculated again by multiplying the water consumed per day (q) for the water density (ρ), its specific heat (c_p), the difference between the use temperature (T_{use}) and the mains temperature (T_{mains}), divided by 1000.

$$Q = \rho \cdot (q/1000) \cdot c_p \cdot (T_{use} - T_{mains}) \quad [J/day] \quad (5.7)$$

The DHW energy consumption per day is found in both ways. The results obtained are multiplied for 365 days per year, in order to find the annual consumption and compare them with the pre-sizing data. It is found that the DHW load per m² was more precise and closer to the A2A data.

After the most accurate way for calculating the DHW load is decided, the litres consumed per day are redistributed according to an hourly day profile. This is made following the residential building percentage volume per hours (%vol/h) as it is shown in the Graph next page.

Merezzate Plus Pre-Sizing Data



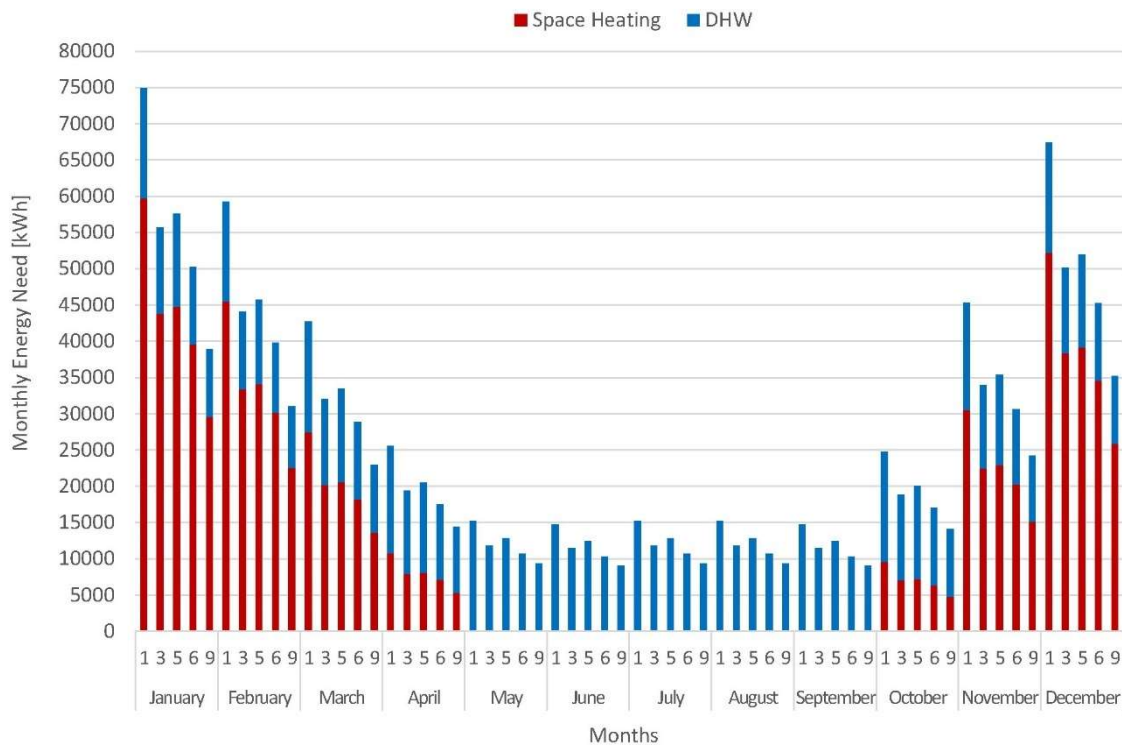
Graph 5.6 Residential daily profile for DHW

Finally, the DHW load per day is multiplied for the hourly percentage volume and the results are divided by 100. The DHW litre are now distributed through the hours in a day and the energy needed is easily found and transformed it in kWh to have comparable results with A2A pre-sizing data. When DHW and the space heating are found for each building of Merezzate the total hourly heating energy needs can be assumed for every multi-dwelling unit.

5.3 UDC Space Heating & DHW Hourly Energy

After the hourly profiles for space heating and domestic hot water of every building are calculated, the heating energy needs can be assumed through the year for each multi-dwelling unit. These data will be fundamental to create the thermodynamic model.

The monthly energy needs for space heating and DHW for each multi-dwelling unit are shown in the Graph below. The different heating energy needs for every UDC have compared each others.



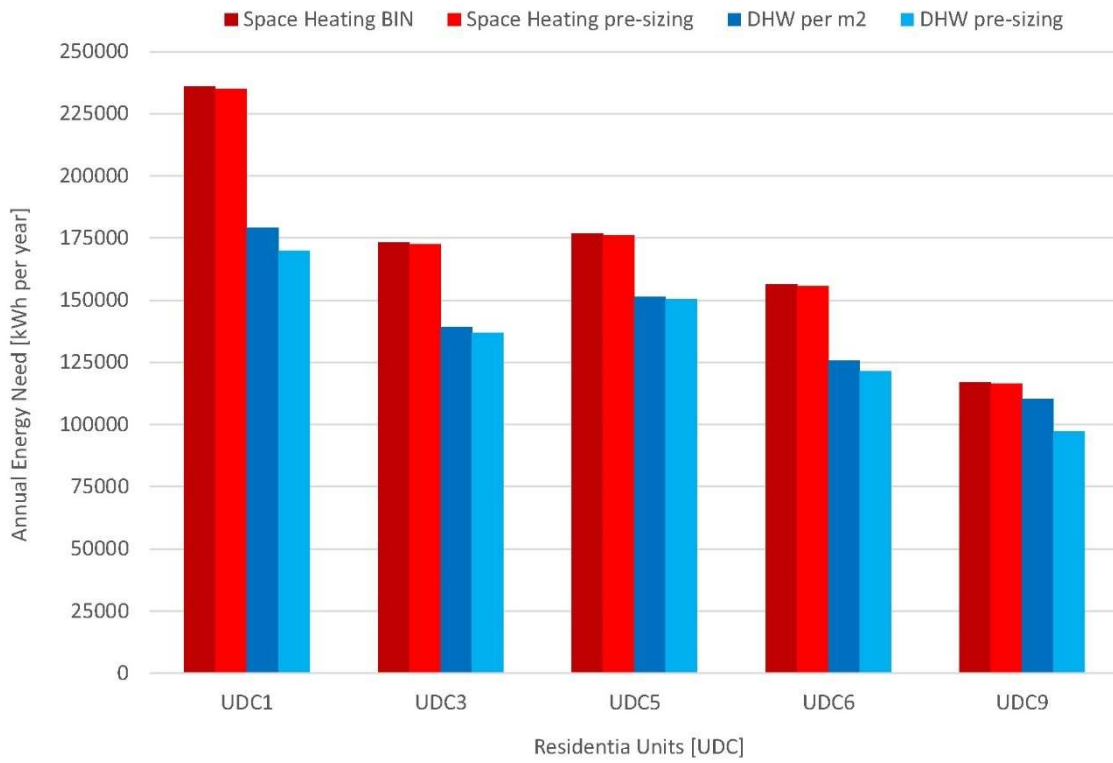
Graph 5.7 UDC space heating & DHW monthly energy needs

The Graph above shows the monthly sum of space heating and DHW of every building for each multi-dwelling unit. The total monthly results of each multi-dwelling units (UDC01; UDC03; UDC05; UDC06; UDC09) are then compared for every month.

After the monthly heating energy needs are studied, the obtained results from these calculations are then compared with the pre-sizing annual data provided by A2A company. In the following page the annual energy needs for space heating and DHW are compared for each multi-dwelling unit.

The data compared are almost the same, and the results are coherent with the pre-sizing data, according to the Graph 5.8.

Merezzate Plus Pre-Sizing Data



Graph 5.8 Annual energy needs compared with pre-sizing data

In the next Chapter the network simulation model will be created considering the heating hourly energy needs calculated in this Chapter, during the year.

6. TRNSYS Network System Modelling

This Chapter describes the modelling of the Merezzate multi-dwelling units and the connection with the district heating network. The employed software is TRNSYS which is a complete and extensible simulation environment for the transient simulation of systems, including multi-zone buildings [21]. The final aim is the construction of a validated model of the Merezzate Plus district that allows to accurately simulate the future integration of solar panels. Primary side and secondary side data are needed to create a correct network model. The energy needs analysed in the previous Chapter will be used here for calculating the mass flow rate in both circuits. The supply temperatures will be considered constant, according to the A2A pre-sizing data: 100 °C for primary side and 65°C for the secondary side. Instead, the primary side return temperature is calculated with the “delayed output device” which relates to the substations in order to calculate the outcoming temperature at the previous instant. The secondary side return temperature is calculated from the outlet temperatures of radiant panels, simulating some specific flats. Not all the apartments are simulated: the simulation of two existing flats is used. The results obtained are used as representative of the apartments of all the multi-dwelling units. The return temperature from radiant panels is then mixed up with the DHW return in order to have a dynamic outlet temperature in the secondary side. When these data are known, the components have connected each other, and the parameters set, all the Merezzate district network can be simulated.

This method allows the creation of dynamic model exploiting the hourly energy needs calculated in the previous Chapter, the variable return temperature from the multi-dwelling units and the outlet primary side temperature calculated at the previous instant.

6.1 TRNBuild Description

TRNBuild is the interface of TRNSYS tools for creating and editing all the geometrical information required by the TRNSYS model of the building. TRNBuild allows editing the walls and layer's materials and properties, to create ventilation and infiltration profiles,

to add internal gains (with a certain profile) and define radiant surfaces. Starting with some basic project data, the user describes each thermal zone and select the desired outputs [4]. This tool is used to create the building model, for simulating the two flats and the relative heating plants based on radiant panels. In the following Chapter the existing model of building 06 with flat 25 and flat 30 is analysed and the radiant panels system is added in order to find the return temperatures.

6.2 Apartments Simulation

The existing building model of the two flats is made by Prof. Scoccia and the assistants Filippini and Colombo [28]. The main structure of the apartments model consists of two interacting tools, Simulation Studio and TRNBuild. First the building and its structures are defined in TRNBuild (according to their orientations, properties and materials) and then all the system's components and the building itself are included in the Simulation Studio model. The first simulation ran shows the requirements that the system must cover. The results will represent the demand from the simulated building as served by an ideal system capable of always reaching the set point desired in the internal environment. Then in the next paragraph, the building and the real heating plant are simulated together in order to obtain the actual operating conditions of the radiant panel heating system, to meet the set point on the room air node. Finally, the results obtained from this simulation will be the input for the Merezzate DH network model in the last paragraph.

6.2.1 Building Descriptions and Flat Parameters

The analysis of this section focuses on the description of the two apartments n°25 and n°30 of building E06, which is part of the multi-dwelling unit UDC01. Each element requires some specifications and parameters to be defined, as explained in the previous paragraph. The building plan, the layers composition, the internal gains and losses will be covered within this Chapter.

The two analysed apartments are located on the 4th floor (flat n°25) and 5th floor (flat n°30), with only one facing outwards to the South-East. They border to the South-West and North-East with two other apartments and to the North-West with a common area, which includes a stairwell and elevators.

The plan type of building E06 is shown in the following Figure. The plan shows a typical floor (4th floor or 5th floor) and the studied flat (n°25 or n°30) is indicated in orange.

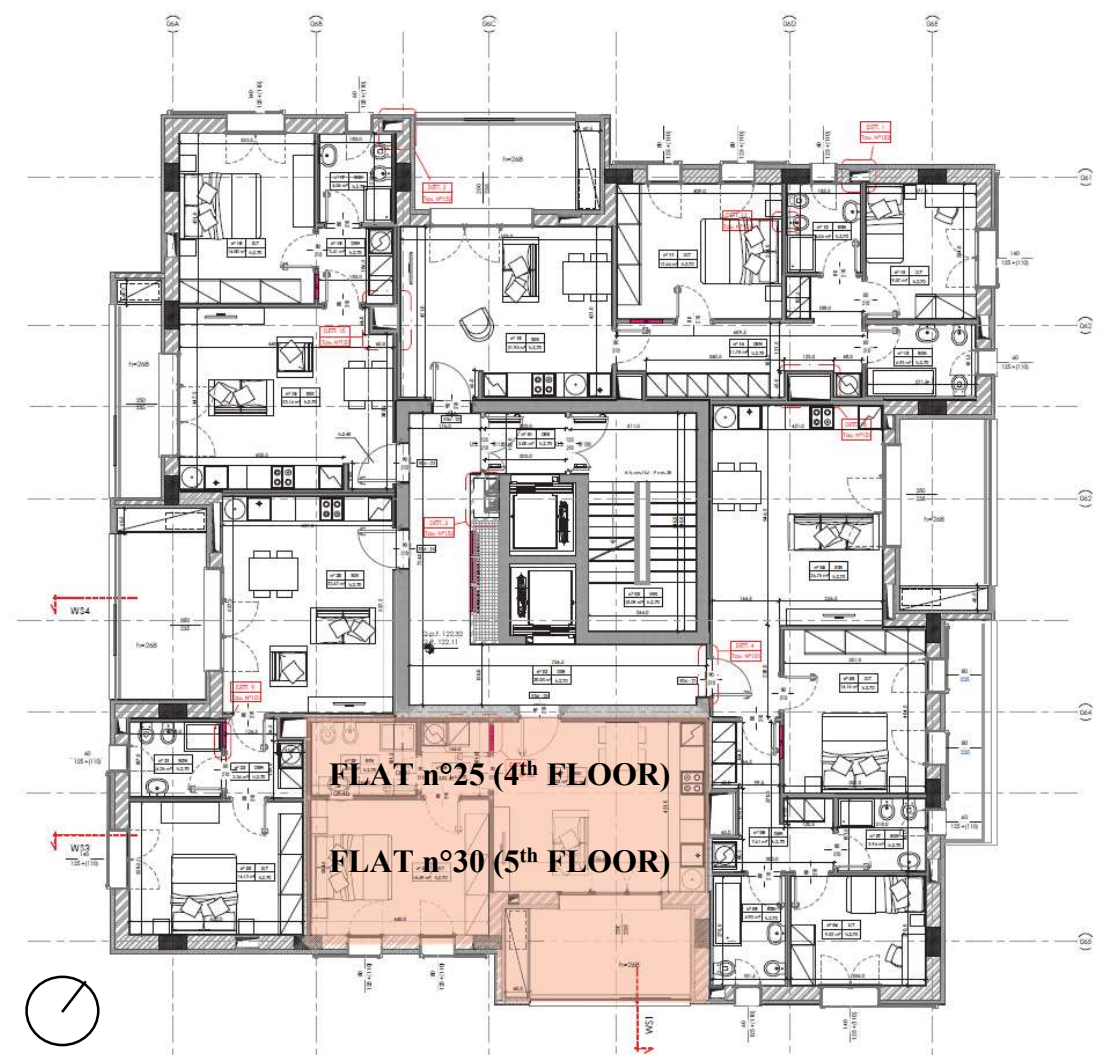


Figure 6.1 Plant type of building E06 [23]

The geometry of the apartments was created in Sketch-Up 3D which can be read by the TRNBuild software.

The model is schematized as follows (Figure 6.2): the two apartments have same dimensions, with a total area of 46.90 m² each, 23.40 m² of living area and 23.50 m² for the sleeping area. There is also a loggia, modelled as a shield [28]. The stairwell and lifts are surrounded by a common area of 28.50 m². There is only one side facing with the external environment (South-East), while the other sides are adjacent to the remaining apartments. For this reason, it was decided not to model the entire building but to set an adiabatic condition where an area bordered with the remaining apartments [28]. The conceptual scheme of the model created in TRNBuild is shown in the Figure next page (Figure 6.2).

In the following Table the stratigraphy used in the model is presented with the relative thermal transmittances.

Table 6.1 Transmittances of the apartment's layers [28]

Building Component	U [W/m²K]
External Wall [M1]	0.215
Internal Wall between Stairwell [M2]	0.623
Partition between Apartments [M4]	0.254
Internal Partition [M7]	0.47
Inter-Floor Slab between Apartments [S2]	0.443
Inter-Floor Slab towards Stairwell [P5]	0.307
Window 80x125 [W2]	1.36
Window 250x235 [W11]	

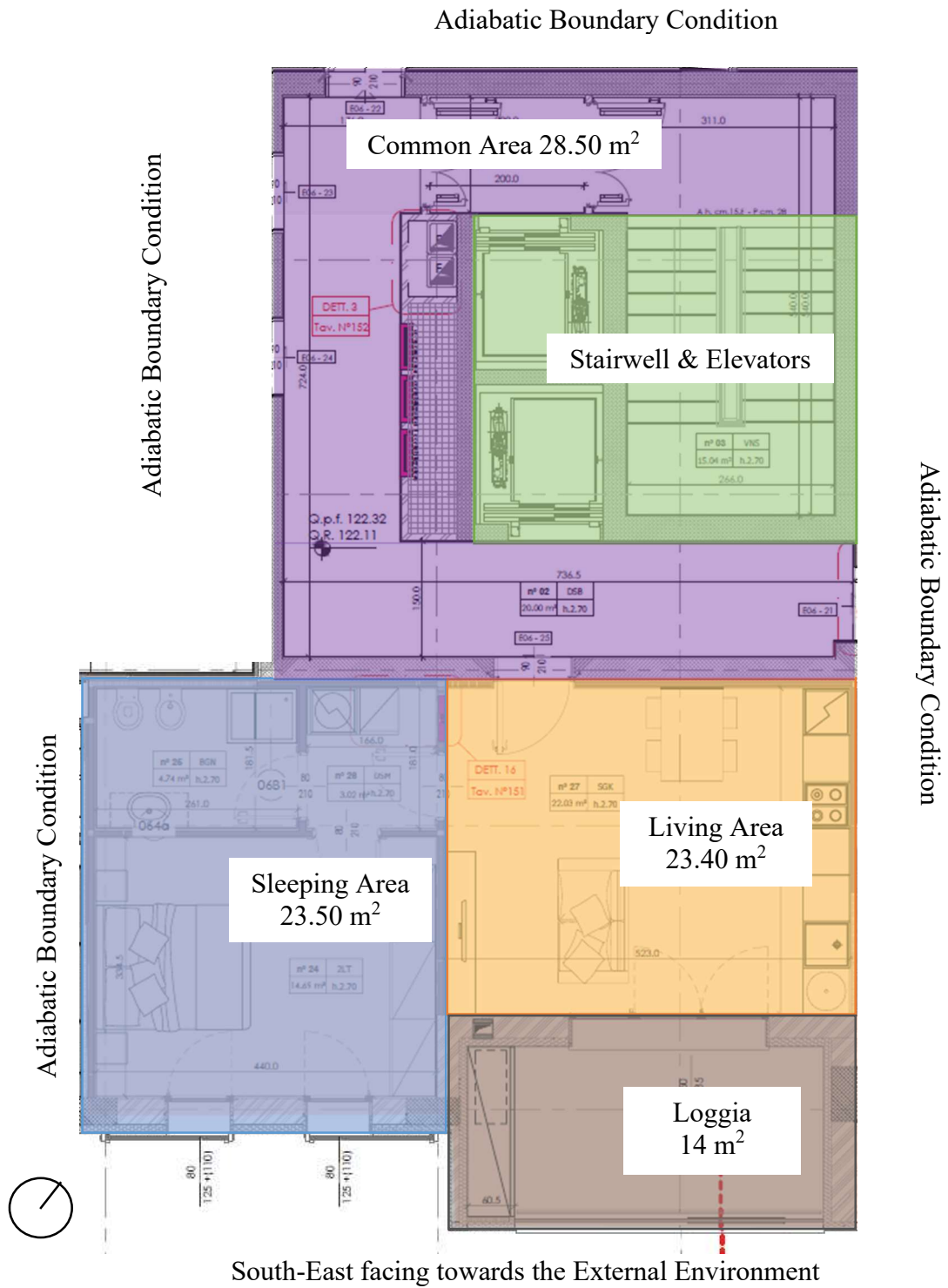


Figure 6.2 Geometric modelling scheme of flat n°25 and flat n°30 [28]

For the internal loads due to the presence of people, 60 W/person of sensible heat (of which 33% convective and 67% radiative) and 40 W/person of latent load were considered. Two different occupancy profiles have been hypothesized (max 2 people), one for the living area and one for the sleeping area [28]. For internal loads due to equipment a maximum load of 4.39 W/m² is considered on the entire apartment then it was assumed to divide this load by attributing 2/3 to the living area and 1/3 to the sleeping area, resulting in a maximum of 5.87 W/m² and 2.92 W/m² [28]. A constant infiltration of 0.05 vol/h is set and a constant natural ventilation (at external temperature and relative humidity) equal to 0.25 vol/h is set too [28].

It is set an ideal heating and cooling system able to maintain the temperature and relative humidity inside the area according to the indicated set-point [28], to analyse the energy needs of the apartments. The heating season is defined by the DPR 26/08/1993 n.412 (and subsequent amendments) depending on the climatic zones. Milan is located in climatic zone E, which provides for an ignition period ranging from 15 October to 15 April. The remainder of the year is considered in the simulations as a cooling season. The heating system has a set point temperature of 20 °C during the day and a setback of 16 °C during the night. The cooling system instead provides a set point temperature of 26 °C constant during the day. Relative humidity control is also assumed with a set point equal to 50% [28].

6.2.2 Apartments TRNSYS Model

The main components of the system are: the TRNBuild building studied in the previous Chapter, the Linate weather, the heating and cooling set points profile and all the calculators to obtain the energy needs. The scheme of TRNSYS system model is shown in the Figure next page.

The climate file used in the simulations (.tm2 format) is based on data provided by the Meteonorm weather station in Milan Linate 160800.

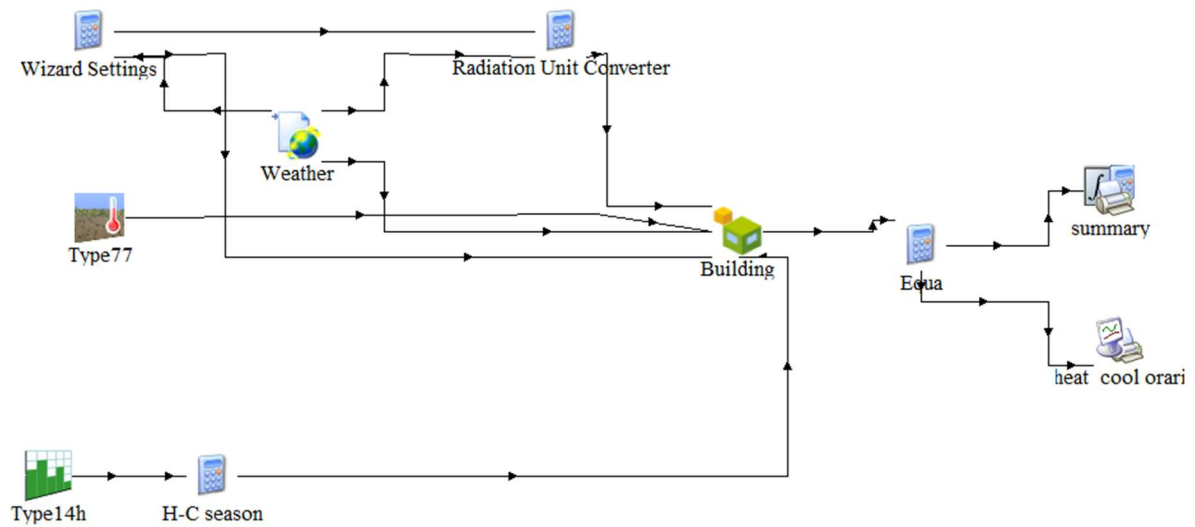


Figure 6.3 TRNSYS system model representation [28]

A specific TRNSYS type represents each component of the system, as reported in the Table below. Some components have been simulated through tailored made models implemented through TRNSYS calculators: special types are used as equations and functions editors.

Table 6.2 Building E06 TRNSYS components for energy needs

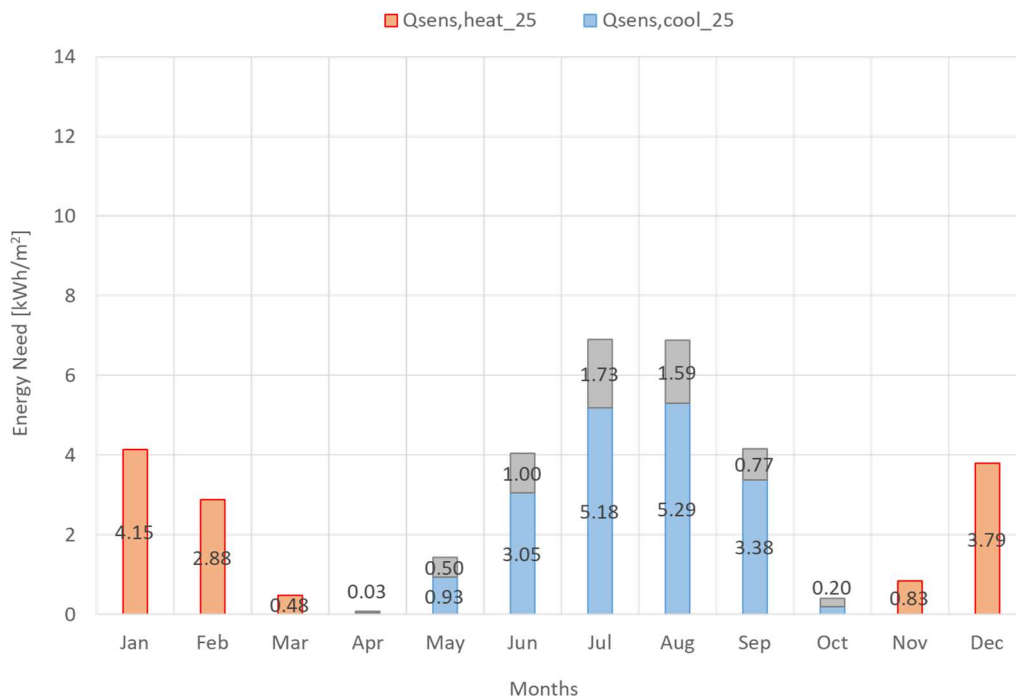
Component	TRNSYS Type
Weather Data Processor	Type 15-6
Soil Temperature Profile	Type 77
Time Dependent Forcing Function	Type 14h
Multi-Zone Building	Type 56
Simulation Summary	Type 28b
Online Graphical Plotter	Type 65c

The multi-zone building receives weather information, such as solar radiation and environmental temperature, from the Type 15-6, representing the climate conditions of Milan. All the data are processed by the calculator in order to find the energy needs and the monthly energy balance as we are going to analyse in the following paragraph.

6.2.3 Flat n°25 Energy Needs & Energy Balance

The monthly energy needs and energy balance are found for flat n°25 and flat n°30 thanks to the previous simulation, considering all the heating gains, ventilation, infiltration and comfort set temperatures analysed in the previous section. Here, the results obtained for the model are shown just for flat n°25, according with their identical position and dimensions, they will have similar energy needs.

The monthly energy needs of apartment n°25 are shown in following chart. The envelope is well insulated, and the cooling needs are bigger than the heating needs. The heating needs are also lower than the pre-dimensioning data performed by the utility company that have designed the DH plant. This difference could be caused by A2A because companies usually over-dimension the projects to avoid future demand issues when people start living in there.



Graph 6.1 Monthly energy needs of flat n°25 [29]

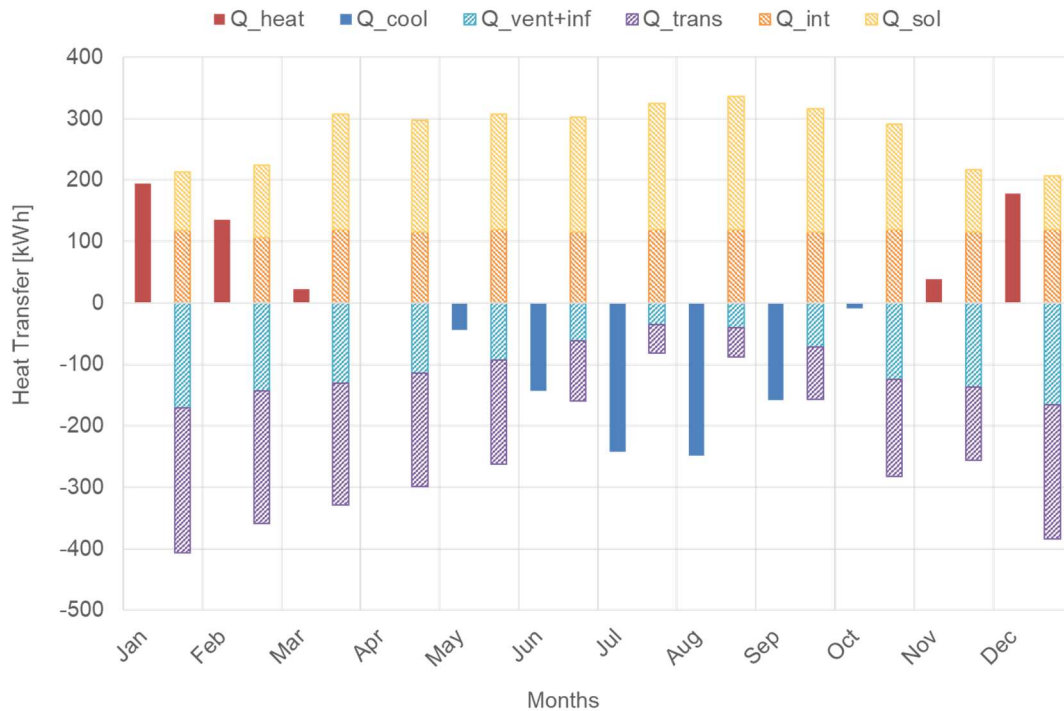
High-energy class buildings often have higher consumption in reality than the project, due to the rebound effect (higher setpoints and higher DHW consumption), according to

the prof. Filippi’s speeches (Politecnico di Torino). The designers, therefore, tend to align the project with empirical data given by experience rather than the expected from theory. A parallel project is underway to analyse the consumption of individuals based on the monitoring of sensors placed in some sample apartments to understand the reason of this difference.

Table 6.3 Annual energy needs comparison

Annual Energy [kWh/m ²]	
Flat n25	13.16
Flat n30	12.56
Pre-dimensioning	23.73

The last analysis performed by existing simulations of Prof. Scoccia [29] is the monthly energy balance of the two apartments. The red and blue columns are the requirements that the plant must cover equal to the sum of the effects of dispersions and gains. The results of the flat n°25 are shown in the Graph below.



Graph 6.2 Monthly energy balance of flat n°25 [29]

The results shown so far represent the demand required by the simulated building alone as served by an ideal system capable of always reaching the desired set point in the internal environment. In the next paragraph, the building and the real heating plant are simulated together in order to obtain the actual operating conditions of the radiant panels, to meet the set point on the room air node. The results obtained will be the input for the simulation of the Merizzate DH network.

6.2.4 Radiant Panels Modelling

In this paragraph the heat transfer from radiant panel systems is analysed for flat n°25 and flat n°30. The building model is the same used before integrated in TRNSYS with the radiant controllers to activate the panels according to the internal comfort temperature. The radiant floor is modelled by the integration of an “active layer” (with a radiant panel plant) on the floors of the simulated apartment inside TRNBuild. The layer is called “active” because it contains fluid filled pipes that add heat to the surface [30].

The radiant plant is modelled on TRNSYS following the next steps.

Due to the finite distance between pipes, a two-dimensional temperature field develops in the plane of the thermo-active construction element cross-section (Figure 6.4 and Figure 6.5). Thermal input or output along piping loops causes a change in the water temperature within the pipe. This change affects the construction element temperature in the z direction. This means that all three dimensions have to be taken into account for the calculation of a thermo active construction element system [30].

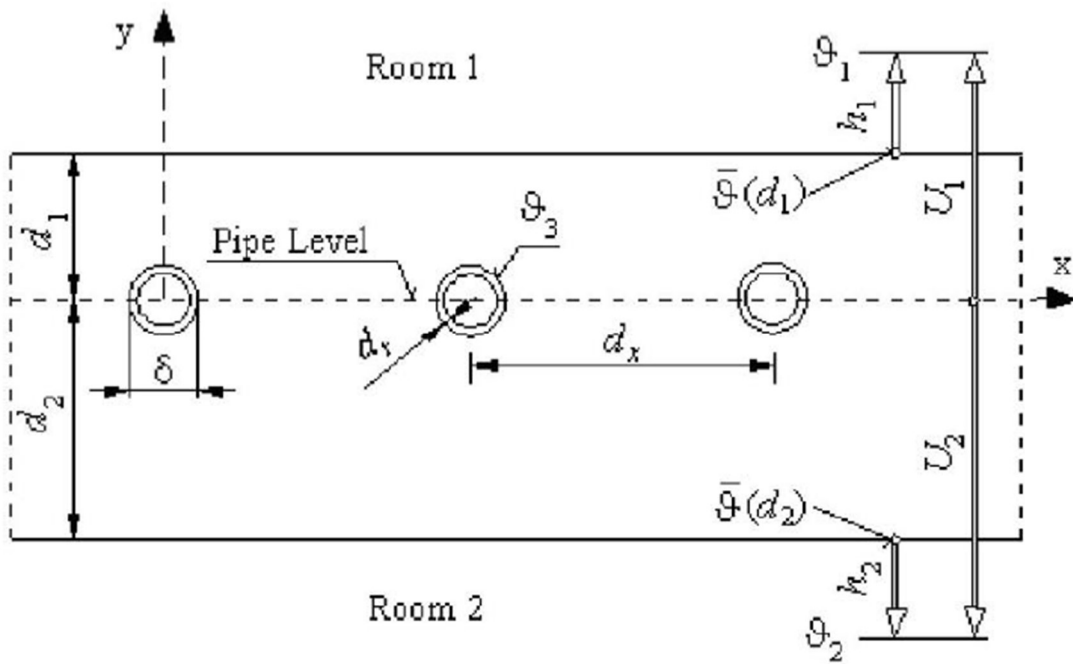


Figure 6.4 Structure of the thermo active construction element system [30]

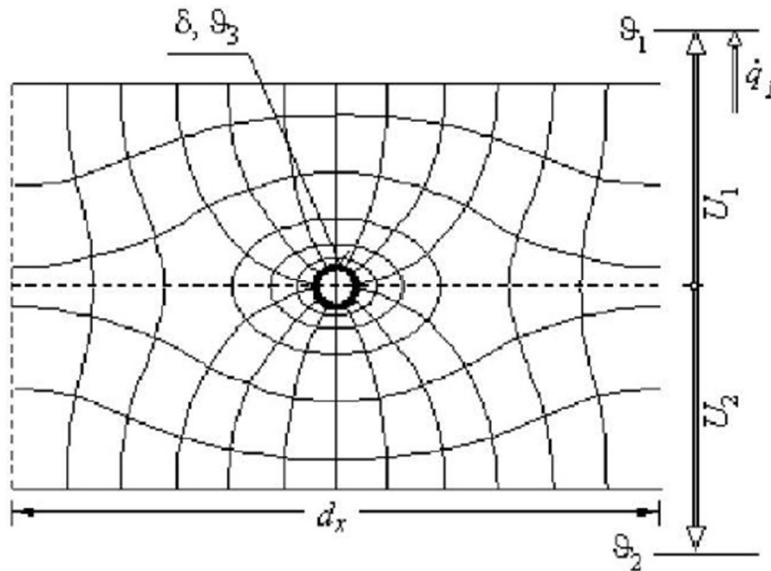


Figure 6.5 Heat flow in a cross section of a thermo active construction element [30]

The stationary solution for temperature distribution in the x-y plane results, as described in the following formula for heat flow on the surface towards room 1, according to previous pictures:

$$\dot{q}_1 = \Phi \cdot U_1 \cdot (\vartheta_3 - \vartheta_1) + (1 - \Phi) \cdot \frac{U_1 \cdot U_2}{U_1 + U_2} \cdot (\vartheta_2 - \vartheta_1) \quad (6.1)$$

The first term to the right of the equation sign describes the heat flow between temperature ϑ_3 on the outside surface of the pipe and temperature ϑ_1 within room 1. The temperature difference is multiplied by the proportionality factor $\Phi \cdot U_1$, which represents the coefficient of thermal transmittance for the pipe configuration. The physical variable Φ is used as correction factor. This variable resembles the shape factor and can be derived from the partial differential equation for thermal conduction [30].

For the configuration of pipes, Φ becomes:

$$\Phi = \frac{2 \cdot \Pi \cdot \lambda_b \cdot \Gamma}{d_x \cdot (U_1 + U_2)} \quad (6.2)$$

Where:

$$\Gamma = \left[\ln \left(\frac{d_x}{\Pi \cdot \delta} \right) + \frac{2 \cdot \Pi \cdot \lambda_b}{d_x \cdot (U_1 + U_2)} + \sum_{s=1}^{\infty} \frac{g_1(s) + g_2(s)}{s} \right]^{-1} \quad (6.4)$$

To check the evidence of this formula, it can be calculated with $\Phi = 0$ as a borderline case, which means that the calculation is done for a construction element without pipes. The result is equal to the heat flow in the upper half of the construction element determined by the familiar calculation method using the U value [30]:

$$\dot{q}_1 = \frac{U_1 \cdot U_2}{U_1 + U_2} \cdot (\vartheta_2 - \vartheta_1) \quad (6.5)$$

The heat flow for the second side of the room can be determined in a similar way as the previous case:

$$\dot{q}_2 = \Phi \cdot U_2(\vartheta_3 - \vartheta_2) + (1 - \Phi) \cdot \frac{U_1 \cdot U_2}{U_1 + U_2} \cdot (\vartheta_1 - \vartheta_2) \quad (6.6)$$

These two equations can be represented by a network of resistances in a triangular arrangement as in the following Figure.

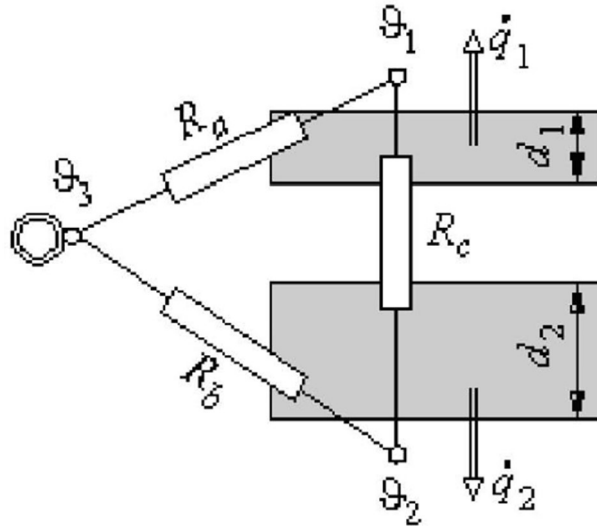


Figure 6.6 Network of resistances with triangular arrangement [30]

The three resistances can be described as follows:

$$R_a = \frac{1}{\Phi \cdot U_1} \quad (6.7)$$

$$R_b = \frac{1}{\Phi \cdot U_2} \quad (6.8)$$

$$R_c = \frac{U_1 + U_2}{U_1 \cdot U_2 \cdot (1 - \Phi)} \quad (6.9)$$

The triangular network can be transformed into an equivalent star network (Figure 6.7) using the following relations [30]:

$$R_1 = \frac{R_a \cdot R_c}{R_a + R_b + R_c} \quad (6.10)$$

$$R_2 = \frac{R_b \cdot R_c}{R_a + R_b + R_c} \quad (6.11)$$

$$R_x = \frac{R_a \cdot R_b}{R_a + R_b + R_c} \quad (6.12)$$

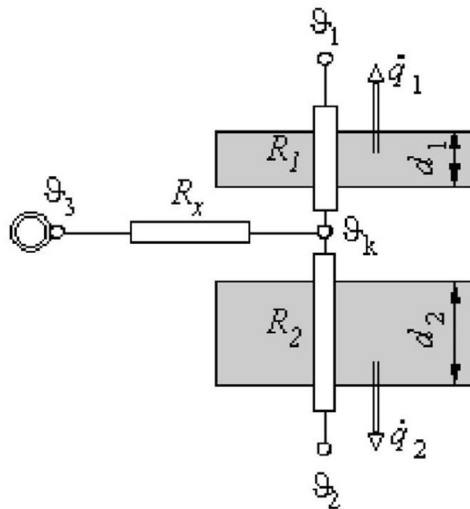


Figure 6.7 Network of resistances with star arrangement [30]

Inserting the equation of R_a (6.7), R_b (6.8) and R_c (6.9) into the equations of R_1 (6.10), R_2 (6.11) and R_x (6.12), the following results are achieved for the star resistances:

$$R_1 = \frac{1}{U_1} \quad (6.13)$$

$$R_2 = \frac{1}{U_2} \quad (6.14)$$

$$R_x = \frac{(1 - \Phi)}{\Phi \cdot (U_1 + U_2)} \quad (6.15)$$

Due to the transformation of the triangular network into the equivalent star network the information on the pipes can be expressed by one single resistance, that is the R_x resistance. This means that the resistance of each construction element now depends solely on its U value. Despite the multi-dimensional nature of the problem, the equations of R_1 and R_2 prove that thermal transmittance through both halves of the construction element can be calculated by means of the one-dimensional equation for thermal conductance. When ϕ is replaced in R_x (6.15) by the equations of ϕ (6.2) and Γ (6.4), the following equation is achieved after several transformations [30]:

$$R_x = \frac{d_x \cdot \left[\ln \left(\frac{d_x}{\pi \cdot \delta} \right) + \sum_{s=1}^{\infty} \frac{g_1(s) + g_2(s)}{s} \right]}{2 \cdot \pi \cdot \lambda_b} \quad (6.16)$$

The summation term here, served the purpose of adaptation to the boundary conditions when used in the differential equation. If:

$$\frac{d_i}{d_x} > 0.3 \quad \text{and} \quad \frac{\delta}{d_x} < 0.2$$

the summation term is negligible for practical applications. Therefore, the equation of R_x can be simplified to the following:

$$R_x \approx \frac{d_x \cdot \ln \left(\frac{d_x}{\pi \cdot \delta} \right)}{2 \cdot \pi \cdot \lambda_b} \quad (6.17)$$

Thus, the resistance R_x depends only on two geometric variables: the distance between pipes d_x and the pipe diameter δ , and on the thermal conductivity of the material layer λ_b in the pipe plane. The transformation from triangular to star-shaped network results in the additional temperature ϑ_k for the centre point of the star-network. This temperature equals the mean temperature in the pipe plane when $y = 0$. This temperature is called core temperature [30].

Based on the above calculations of the thermal resistance the Thermo-Active Building element might be described:

Table 6.4 Resistance in x-direction & criteria [30]

Floor heating systems	$R_x = \frac{d_x \cdot \left(\ln \left(\frac{d_x}{\pi \cdot \delta} \right) + \sum_{s=1}^{100} \frac{g_1(s)}{s} \right)}{2 \cdot \pi \cdot \lambda_b}$ $g_1(s) = -\frac{\frac{\alpha_2}{\lambda_b} \cdot d_x - 2 \cdot \pi \cdot s}{\frac{\alpha_2}{\lambda_b} \cdot d_x + 2 \cdot \pi \cdot s} \cdot e^{-\frac{4 \cdot \pi \cdot s}{d_x} \cdot d_2}$	$d_x \geq 5.8 \cdot \delta$ $\alpha_2 = \frac{\lambda_{Insulation}}{d_{Insulation}} < 1.212 \frac{W}{m^2K}$ $\frac{\delta}{2} \leq d_2$ $\frac{d_1}{d_x} \leq 0.3$
-----------------------	---	--

The radiant panels are modelled following the previous equations behind the active layer, according to the TRNSYS guide [30]. To correctly set the active layer, the pipe spacing ($d_x = 0.15$ m), pipe outside diameter ($\delta = 0.017$ m), and pipe conductivity ($\lambda_b = 1.26$ kJ/hmK) are added according to the TRNSYS guide & A2A project. After finishing the floor definition, some more active layer specification can be modified for each specific radiant floor like the inlet mass flow rate (310 kg/h), inlet temperature (37 °C), number of loops (2) and additional energy gain (0) at the fluid level [30]. The number of loops is used to calculate the pipe length:

$$\text{pipe length} = \frac{\text{floor area}}{\text{pipe spacing} \cdot \text{number of loops}}$$

The inlet mass flow rate is considered constant and equal to the nominal flow rate according to the project (310 kg/h) and the inlet temperature of radiant panels is equal to 37 °C as from A2A's data.

The radiant panels are activated according to the heating season defined by the DPR 26/08/1993 n.412 for climatic zone E and according to the inside comfort temperature.

They are regulated by some new controllers (type 2b) in order to always reach the set temperatures inside the apartments. New controllers are added in order to reach the set temperature of 20 °C during the day and 16 °C during the night, coherently with the same hypothesis used for the calculation of the energy needs. The new component and its type are reported in the Table below.

Table 6.5 TRNSYS controller component

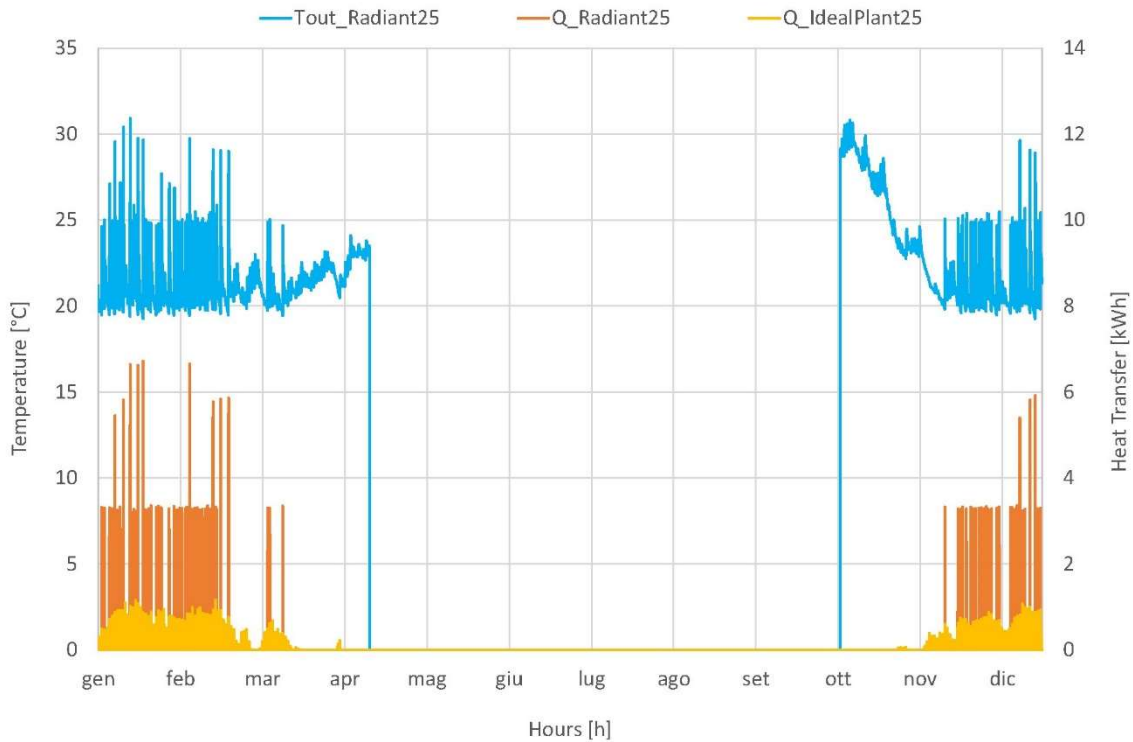
Component	TRNSYS Type
Differential Controller	Type 2b

Now that radiant panels are modelled in TRNSYS and TRNBuild the obtained results will be analysed in the following Chapter.

6.2.5 Flat n°25 Radiant Panel Results

The outlet temperatures obtained from the simulation of flat n°25 are presented in the following chart. The heat transfer from radiant panels and the heat transfer calculated from the previous simulation (Figure 6.3) considering an ideal heating plant, are compared on the right axis.

The radiant panels usually work with a ΔT of 5-7 °C, therefore it was expected an average return temperature around 30 °C, according also to A2A data. Instead, the average outlet temperature from the simulation is about 22.3 °C. This could be caused by the high performances of the building and by the simulator which considers perfect energy exchange.



Graph 6.3 Radiant panels outlet temperature & heat transfer for flat n°25

The outlet temperatures from radiant panels ($T_{out_Radiant25}$) are usually lower than 30 °C and it seems the heating system is activated few times per day, according to the Graph above. The comparison between the ideal heating plant ($Q_{IdealPlant25}$) and the modelled radiant panels ($Q_{Radiant25}$) highlights a significantly difference in the heat transfer. The actual system is active fewer time with a very higher heat transferred, compared to the ideal plant. The next step is to analyse the operation of the controllers used in the TRNSYS model, in order to check if the system is correctly activated and the ambient temperatures are included in the assumed comfort ranges.

In the next chart (Graph 6.4) a shorter period is studied to check the ambient temperatures of the living and sleeping area in order to analyse the radiant controllers. The considered months for this analysis are December, January and February. The heat transfers are always shown on the right axis to understand better when the radiant system is activated and the difference with the previous ideal plant.

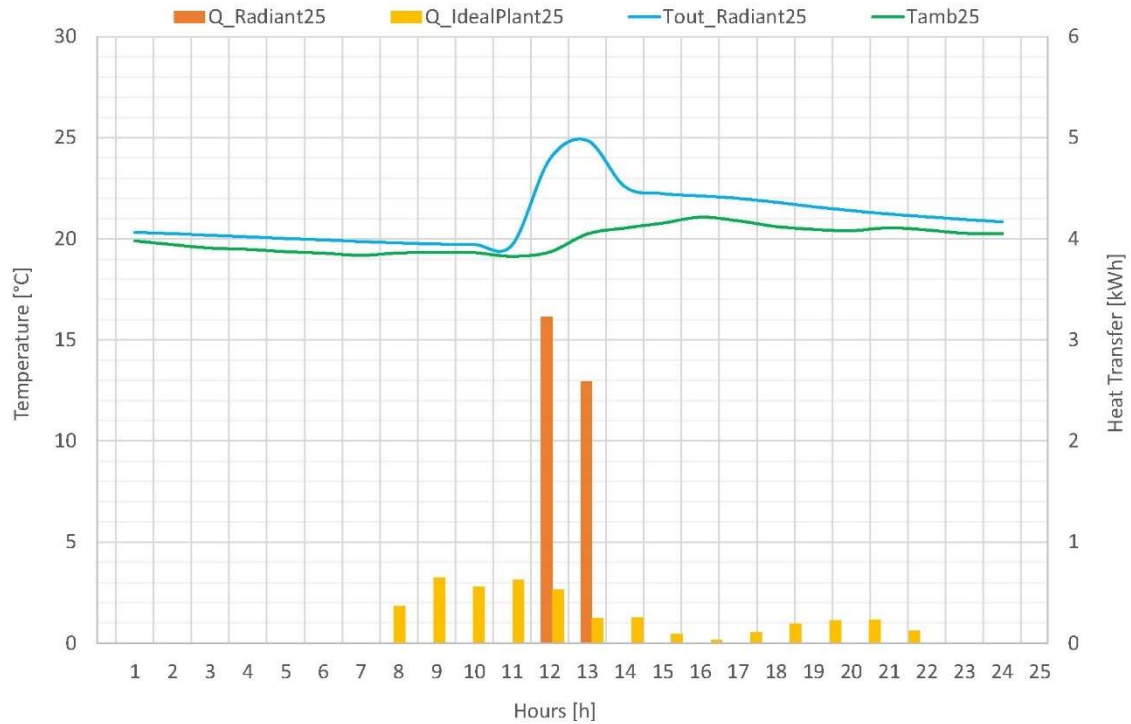


Graph 6.4 Radiant panels data analysed in a short period for flat n°25

The radiant controllers correctly work and the ambient temperatures in the living area and sleeping area are always included in the pre-established range. Therefore, it seems the radiant panels are truly activated few times for reaching the set temperatures. The heat transfer of the ideal plant appears more distributed during these months compared to actual radiant system, without underling any peaks.

Another more accurately zoom will be performed to study the heat transfer difference. A daily analysis will be made to understand how many times the plant is actually activated during the day and how it affects the outlet radiant temperatures.

The next chart (Graph 6.5) shows the trend of radiant outlet temperatures and heat transfers during the day. The selected day for analysing these parameters is the 5th of December. The heat transfer of the ideal plant and the actual radiant system are shown in the right axis.



Graph 6.5 Radiant panel outlet temperatures and heat transfers during the day

The radiant panels are activated few hours during the day as it was expected from the previous Graphs. The comparison between the actual and the ideal plant highlights that the ideal plant is activated more time during the day exchanging less heating each time. This is due to the setting of the radiant plant, in fact, it is considered a high constant mass flow rate, according to the project, which allows to activate the panels just a couple hours in a day. The designers probably used an empirical data given by the experience for sizing the radiant plant, rather than the expected values for a high energy class building, as explained in the paragraph 6.2.3. Another analysis will be performed to confirm this theory, changing the ambient set-point temperatures, and comparing the annual total consumption.

When activated the panels affect the outlet temperature of the radiant plant, increasing the return temperature which reaches values about 25 °C. If the radiant panels were activated more time in a day the outlet temperatures would increase, reaching closer

values to the expected set-point of 30 °C. This effect could be correlated with the rebound effect explained before, when the dimension of the radiant plant is higher than it was needed.

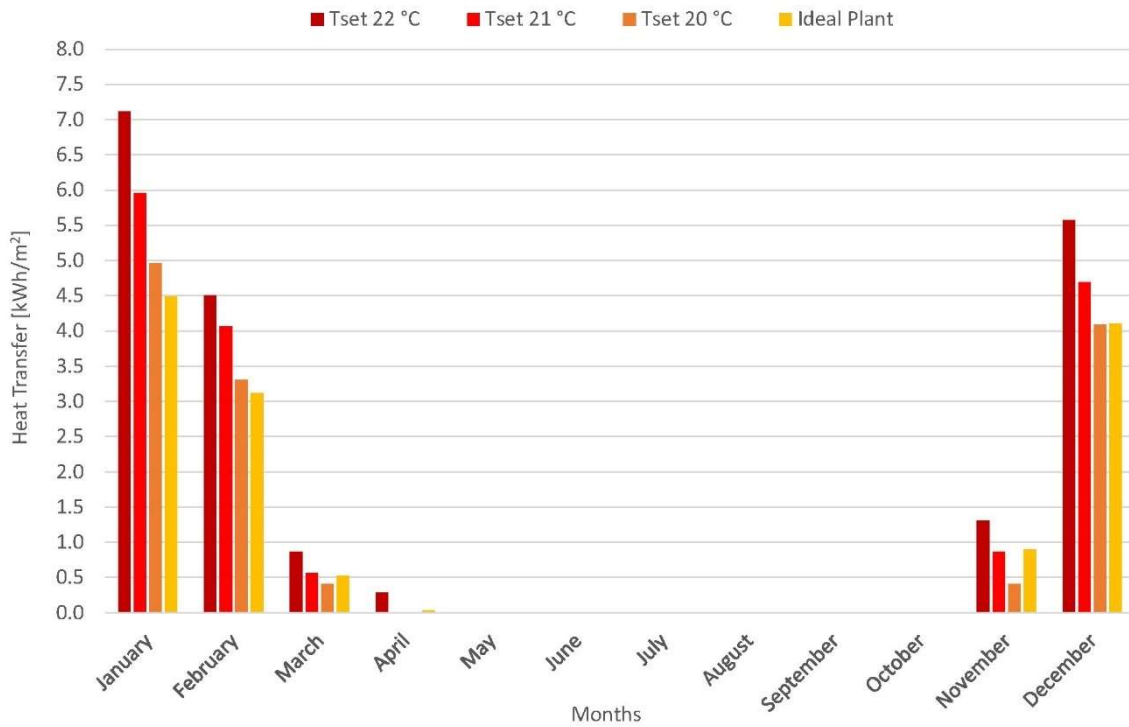
In the next Table are shown the results of annual heating energy per meter square of different ambient set-point simulations. It is considered a set-point temperature of 21 °C and another of 22 °C to demonstrate that the total consumptions will increase, becoming closer to the pre-sizing data.

Table 6.6 Annual heating comparison of different set-point for flat n°25

Annual Heating [kWh/m²]	
Pre-dimensioning	23.73
Ideal Plant	13.16
Tset: 20 °C	13.16
Tset: 21 °C	16.14
Tset: 22 °C	19.65

The heating energy consumption has an annual increase around 3 kWh/m² for each extra degree, according to Table 6.6. When the ambient temperature is set to 22°C the annual energy consumption is very close to the pre-sizing data. This analysis motivates the hypothesis of the over-sizing plants and the rebound effect. The monitoring data of buildings will be needed to really support and prove this theory.

In the following Graph the monthly heating energy results are shown for the different ambient set-point temperatures.



Graph 6.6 Monthly heating comparison of different set-point for flat n°25

A parallel project is underway to analyse the actual building consumptions based on the monitoring of sensors placed in some sample apartments to understand the reason of the difference between pre-sizing data and simulated ones. Therefore, this topic will not be explored anymore within this thesis.

It will be always considered an ambient set-point temperature of 20 °C for the next simulations. It is assumed that the outlet temperature from radiant panels is pretty much the same for every multi-dwelling unit (UDC) and it will be used as input data for the district network simulation model. Therefore, in the next simulations the outlet temperature of radiant panels will be mixed up with the return temperature in the secondary side equal to 30 °C according to the project data.

6.3 Merezzate District Heating Modelling

In this Chapter a dynamic model of the Merezzate network is created in order to have a complete scheme of the whole district heating system. At first, the multi-dwelling unit substations are modelled, considering the pre-sizing data calculated in Chapter 5 for space heating and DHW loads and the radiant return temperatures from the previous paragraph. The substations are fundamentals because they generate the input data for the district heating network. The second step is to model the district network, assembling all the components and calculating the heat losses. The results obtained from the TRNSYS simulation will be discussed in the next Chapter, comparing them with the monitoring data provided by A2A.

6.3.1 Work Introduction

The Merezzate district network can be subdivided in two different circuit: the district heating primary side and the multi-dwelling unit secondary side, as explained in Chapter 4 and according to the Figure 4.3. The secondary side generates the input data, through the multi-dwelling unit substation, for the primary side. The work within the Chapter 6.3 is structured as following:

- The multi-dwelling unit substations are modelled considering the pre-sizing loads for space heating and DHW and the dynamic return temperature from the radiant panels.
- The secondary supply temperature is assumed constant equal to 65 °C, according to the data project.
- When heating loads, supply and return temperatures are known, the substation heat exchangers are sized following the reference of the TRNSYS component.
- The modelled substations use the data from the secondary side as input to generate the data not known a priori of the primary side.
- The mass flow rate and return temperature in the primary side are calculated considering the secondary side input data and a constant supply temperature equal to 100 °C, according to the data project.

- The Merezzate district network is then modelled assembling all the network components and the calculating the heating losses.
- When all the significant quantities are known in all the components the TRNSYS simulation of the district network is run.

The Merezzate district heating network is shown in the Figure 6.8. The red lines indicate the supply flow rate with an inlet temperature of 100 °C and the blue lines describe the return flow rate with an expected outlet temperature around 40 °C from the data project. The multi-dwelling units (UDC) exchange heat with the district network through the substations which are shown in the Figure below with the light red rectangles.



Figure 6.8 Merezzate district heating network

In the following paragraph the multi-dwelling unit substations are modelled:

6.3.2 Multi-dwelling unit Substation Modelling

The multi-dwelling unit substations are modelled following the scheme in Figure 6.9. The mass flow rates are calculated from the heating needs for space heating and domestic hot water of the pre-sizing data from the BIN method:

$$m_{\text{space heating}} = \frac{Q_{\text{space heating}}}{c_{p_w} \cdot (65^\circ\text{C} - T_{\text{out_radiant}})} \quad (6.18)$$

$$m_{\text{DHW}} = \frac{Q_{\text{DHW}}}{c_{p_w} \cdot (65^\circ\text{C} - 30^\circ\text{C})} \quad (6.19)$$

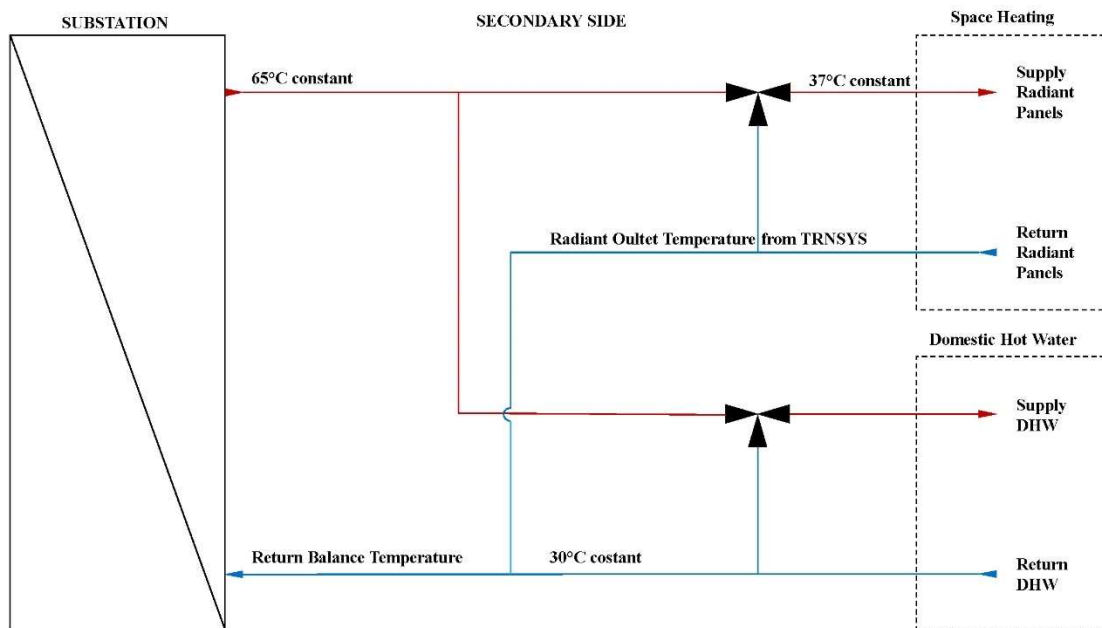


Figure 6.9 Multi-dwelling unit substation modelling scheme

After the mass flow rates for space heating and DHW are calculated the total mass flow rate and the final return temperature in the secondary side (Return Balance Temperature in the Figure 6.9) can be calculated, according to the following formula:

$$m_{\text{return TOT}} = m_{\text{space heating}} + m_{\text{DHW}} \quad (6.20)$$

$$T_{\text{return balance}} = \frac{(m_{\text{space heating}} \cdot T_{\text{out radiant}}) + (m_{\text{DHW}} \cdot 30 \text{ }^\circ\text{C})}{m_{\text{return TOT}}} \quad (6.21)$$

Now all the data in the secondary side are known and they can be used as input for the primary side.

In the following paragraph the substation heat exchanger will be modelled according to the project data and TRNSYS mathematical reference.

6.3.3 Substation Heat Exchanger Sizing

A zero-capacitance sensible heat exchanger is modelled with a counter flow configuration. Given the hot and cold side inlet temperatures and flow rates, the effectiveness is calculated for a given fixed value of the overall heat transfer coefficient (UA). The TRNSYS component relies on an effectiveness minimum capacitance approach to modelling the heat exchanger [31]. Under this assumption, it is needed to provide the heat exchanger's UA and inlet conditions. The model then determines whether the cold (multi-dwelling unit side - secondary circuit) or the hot side (district heating side - primary circuit) is the minimum capacitance side and calculates an effectiveness based upon the specified flow configuration and on UA [31]. The heat exchanger outlet conditions are then computed.

The overall heat transfer coefficient is the value characterizing the heat exchanger, main component of the substation. It is influenced by the thickness and thermal conductivity of the mediums through which heat is transferred. The larger the coefficient, the bigger is the heat transferred from its source to the product being heated.

The overall heat transfer coefficient is calculated following the NTU method:

$$NTU = UA / C_{\min} \quad (6.22)$$

Where:

NTU = number of transfers unit

C_{\min} = minimum heat capacity [kW/K]

C_{\min} is calculated as the minimum value between the heat capacity of hot fluid (primary side) and the heat capacity of the cold fluid (secondary side). The heat capacity is calculated multiplying the mass flow rate per its specific heat.

$$C_{\min} = \min [m \cdot c_{p,c}; m \cdot c_{p,h}] \quad (6.23)$$

Where the mass flow rates of primary and secondary side are calculated as:

$$m = Q / [c_p \cdot (T_1 - T_2)] \quad (6.24)$$

Q is the transfer rate of each substation and it is equal to 700kW for UDC01 and 600kW for the others.

The NTU value for a counter flow heat exchanger is calculated by the following formula:

$$NTU = \frac{1}{C_r - 1} \cdot \ln \left(\frac{\varepsilon - 1}{\varepsilon \cdot C_r - 1} \right) \quad (6.25)$$

Where C_r is the heat capacity ratio equal to C_{\min} / C_{\max} for each network side, and ε is the effectiveness of the heat exchanger, which is a dimensionless quantity between 0 and 1 and it is calculated as: Q / Q_{\max}

$$Q_{\max} = C_{\min} \cdot (T_{h1} - T_{c2}) \quad (6.26)$$

After all the values are known the overall heat transfer is easy calculated as:

$$UA = NTU \cdot C_{\min} \quad (6.27)$$

The results calculated from the NTU method are: $UA = 35 \text{ kW/K}$ for the multi-dwelling unit UDC01 and an $UA = 30 \text{ kW/K}$ for the other multi-dwelling units.

After the substation heat exchangers are modelled all the data are checked to understand which values are known and which are missing.

6.3.4 Substation Data for Primary and Secondary Side

After the substations are modelled, the data from the secondary side can be used as input to generate the data in the primary side. A scheme of the substation heat exchanger describes the data in both sides (Figure 6.10). The input values are fundamental for the correct functioning of the system. The data of the following scheme are analysed to understand which of them are known and which have to be calculated.

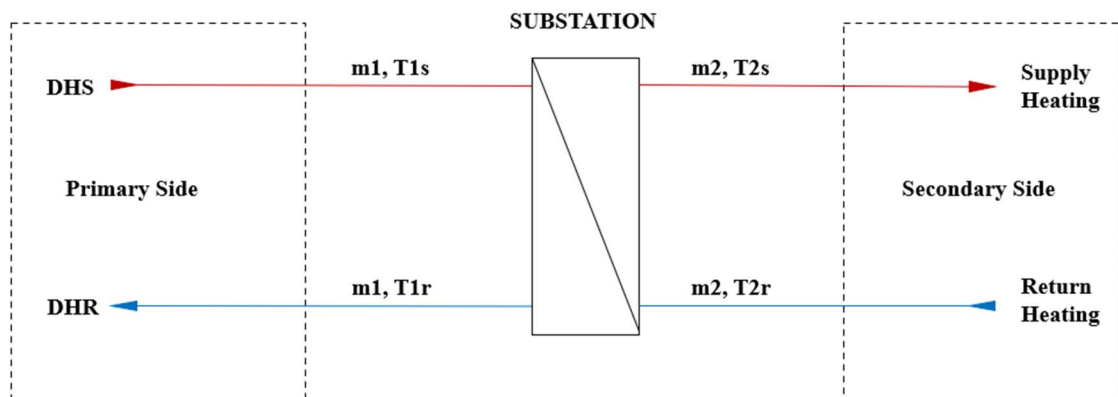


Figure 6.10 Scheme of the substation heat exchanger

Secondary side data:

- $m_2 = m_{\text{return TOT}}$ calculated in the paragraph 6.3.2
- $T_{2s} = 65 \text{ }^\circ\text{C}$ assumed constant
- $T_{2r} = T_{\text{return balance}}$ calculated in the paragraph 6.3.2

Primary side data:

- $m_1 = \frac{Q_{\text{TOT}}}{c_{p_w} \cdot (T_{1s} - T_{1r})}$
 where: $Q_{\text{TOT}} = Q_{\text{space heating}} + Q_{\text{DHW}}$ from pre-sizing data
- $T_{1s} = 100 \text{ }^\circ\text{C}$ assumed constant
- $T_{1r} = \text{unknown}$

The return temperature of the primary side is the missing data to find the mass flow rate and make the simulation work, according to the analysis above. For this reason, it will be used the “delayed output device” to calculate the temperature at the previous instant in TRNSYS. This type allows to create a dynamic network model also in the primary side. The mass flow rates are calculated now from the energy needs of pre-sizing data and dynamic return temperatures in both sides.

After all the data are known and all the component analysed, the Merezzate network can be created on TRNSYS.

6.3.5 Merezate Network TRNSYS Model

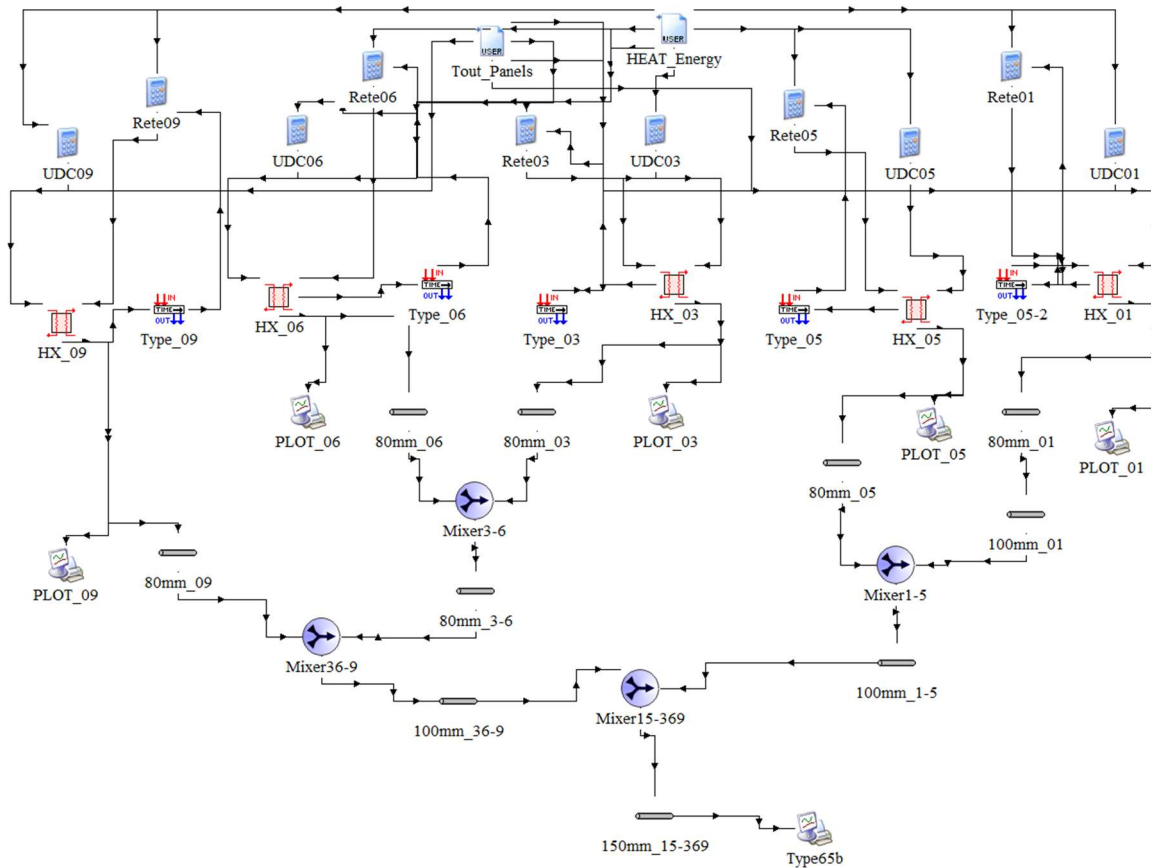


Figure 6.11 TRNSYS Merezate district network model

The main components are used in this TRNSYS model to simulate the whole district heating of Merezate. All the substations are modelled as heat exchangers with the overall heat transfer coefficient calculated in the previous paragraph 6.3.3. There are input data files which read the heating energy needs of the pre-sizing data from BIN method and radiant outlet temperatures previously calculated. The whole district network is designed with proper pipe sizes and linear heat transfer coefficient in order to simulate the relative thermal losses, with mixers to create the same district profile according to the Figure 6.12. Every heat exchanger is connected to a plotter in order to monitor the mass flow rates and outgoing temperatures.

Another fundamental component added to this model is the “delayed output device” (type 150) as studied in the previous paragraph. It relates to the substations in order to calculate the outcoming temperature from the district at the previous instant.

The new components and their types are reported in the Table below.

Table 6.7 Merezzate district TRNSYS components

Component	TRNSYS Type
Input Data Reader	Type 9a
Heat Exchanger: Counter Flow	Type 5b
Delayed Output Device	Type 150
Pipe	Type 31
T Piece Connector	Type 11h

The pre-sizing energy needs are used to calculate the mass flow rates in the primary and secondary sides. It is considered a constant supply temperature equal to 100 °C for the primary side, and an outlet temperature calculated by the “delayed output device”. Instead, a constant supply temperature of 65 °C is considered for the secondary side and the balance return temperature resulted by mixing the radiant return temperatures with the DHW return.

Now that all the components of Merezzate network are assembled, the last step is the calculation of the heat transfer coefficients for every pipe of the district in order to calculate the total thermal losses.

6.3.6 Pipes Thermal Losses

In this Chapter the pipes used in the Merezzate district network are analysed and for each different diameter pipe the thermal energy losses are calculated.

All the pipes of the district heating network are shown in the picture next page (Figure 6.12). The most used diameters, according to that Figure, are:

- Pipe DN 80 to regulate the connection with the multi-dwelling unit substation.
- Pipe DN 100 always used to connect the multi-dwelling unit each other along the district network.
- Pipe DN 150 used to connect the whole district network to the A2A thermal energy power plant.

The complete dimensions with diameter and thickness for the materials of the pipes are shown in the following Table:

Table 6.8 Used pipes dimensions

Nominal Diameter DN [mm]	Steel Pipe Diameter DN [mm]	Steel Pipe Thickness DN [mm]	Sheath Pipe Diameter DN [mm]	Sheath Thickness [mm]
80	88.9	3.2	160	3
100	114.3	3.6	200	3.2
150	168.3	4	250	3.9

After all the pipes are studied, all the thermal energy losses have to be calculated, in order to properly model the pipes for the TRNSYS simulation.

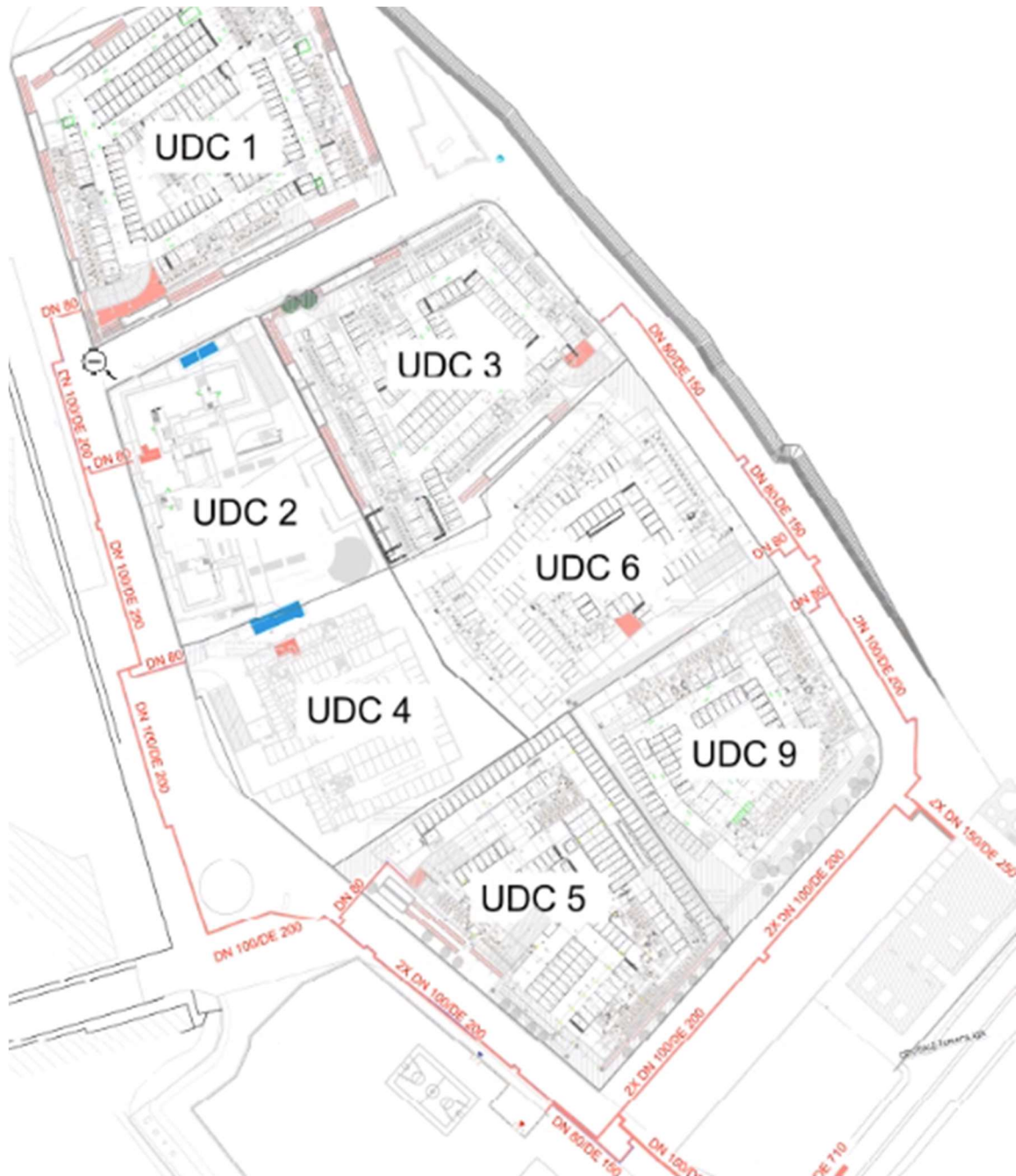


Figure 6.12 Pipes of Merezzate Network

At first, all the thermal conductivity of each used material are studied, according to the values of the Table next page:

Table 6.9 Pipe materials thermal conductivity

Thermal Conductivity [W/mK]			
λ Steel	λ Insulation	λ Sheath	λ Ground
76	0.026	0.43	1

Then, the thermal resistance of each material is calculated, according to the following formula:

$$R = \frac{\ln\left(\frac{D}{D-2t}\right)}{2\pi \cdot \lambda} \quad (6.28)$$

Where:

R = thermal resistance of the material studied [mK/W]

D = diameter of the material [m]

t = thickness of the material [m]

λ = thermal conductivity of the material [W/mK]

Therefore, according with the previous Table of materials (Table 6.9) and the previous formula (6.28), the thermal resistances (R) are calculated for each material and the total resistance is found for every pipes. The global coefficient of thermal exchange is calculated as $1/R_{TOT}$. All the global coefficient of thermal exchange are shown in the following Table for each type of pipe.

Table 6.10 Pipes global coefficient of thermal exchange

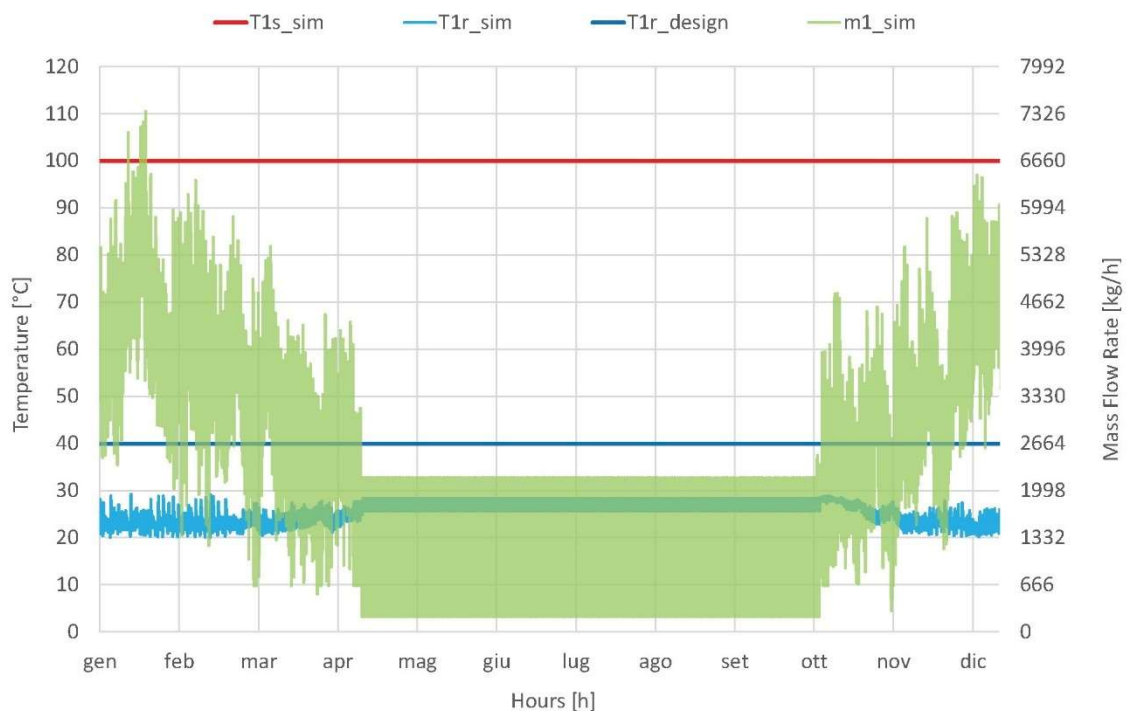
Global Coefficient of Thermal Exchange [W/mK]						
Pipe	R Steel	R Insulation	R Sheath	R Ground	R_{TOT}	K Pipe
DN 80	0.00016	3.36331	0.01415	0.63402	4.01163	0.24927
DN 100	0.00014	3.22575	0.01204	0.59998	3.83790	0.26056
DN 150	0.00010	2.22827	0.01173	0.56629	2.80639	0.35633

Once all the thermal losses are set in the TRNSYS model, the simulation can be run. The Merizzate network results will be shown in the following paragraph.

6.3.7 Merizzate District Heating Results

The primary side results of the Merizzate district network are analysed in this Chapter.

The following Graph shows the supply temperature ($T1s_sim$), the return temperature ($T1r_sim$) and the mass flow rate ($m1_sim$) calculated from the previous simulation. The return temperature is also compared with the design outlet temperature ($T1r_design$) expected from the project data.



Graph 6.7 Merizzate network primary side results

The return temperatures in the primary side are lower than expected, according to the design data. It seems the model is simulated in an operating regime different from what

is foreseen by the project. A comparison between the results and monitoring data is needed in order to make some more analytic considerations.

The return temperature in the primary side is lower during winter than the summer period due to the activation of the radiant plants. The supply temperature is always equal to 100 °C because it was considered as constant input to calculate the mass flow rate.

In the next Chapter the results of the secondary side will be analysed in order to clarify the situation and understand the reason of this difference. The data values coming out from the substation will be studied and the TRNSYS model will be then validated comparing the obtained results with the monitoring data provided by A2A Calore & Servizi.

The validation of the model is a key step of this thesis-work, because it is crucial to understand how the model really works and why the obtained results are different from the design data.

7. Model Validation

Once the Merezzate district network simulation has been designed, it is necessary to ascertain the validity of the used model to describe the components that constitute it and their interactions. To proceed with the validation of the work it is necessary to compare the results calculated from the TRNSYS network model with the monitoring data, to understand their limits and potential improvements. The monitoring data used for this purpose are provided by the A2A Servizi & Calori and represent the Merezzate network from September to November 2020.

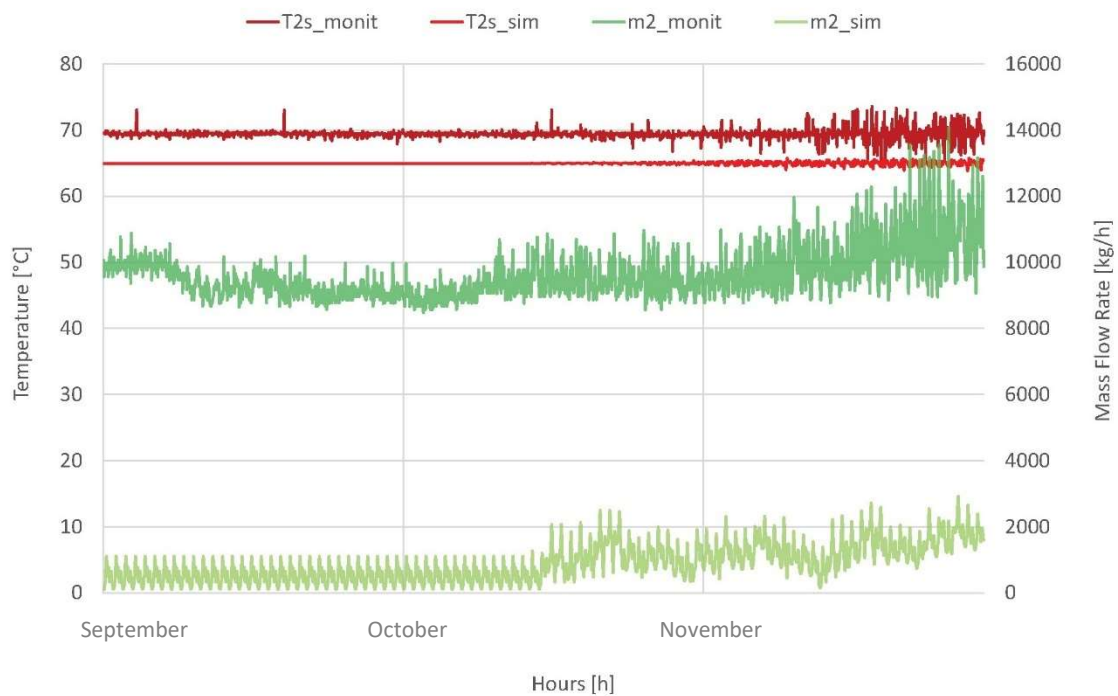
7.1 Substation Results compared with the Monitoring Data

In this Chapter, the monitoring data provided by A2A are compared with the substations model results. Hourly temperatures, mass flow rates and energies are known for the primary and secondary side of each residential substation. The A2A data date back from September to November 2020: the period when the buildings started to be inhabited.

All the results simulated with TRNSYS are compared with the monitoring data, with the aim to validate the built model by checking the supply and return temperatures and the mass flow rates from each Merezzate substation.

The secondary side data of the multi-dwelling unit UDC01 are analysed in the Graph 7.1 next page. The supply temperatures (T_{2s_sim}) and the mass flow rates (m_{2_sim}) of UDC01 from the network model are compared with the supply temperatures (T_{2s_monit}) and mass flow rates (m_{2_monit}) provided by A2A.

Model Validation



Graph 7.1 UDC01 model results compared with monitoring data

The results obtained from the TRNSYS model are different from the actual situation. The actual mass flow rate in the secondary side is much higher than the simulated one. Instead, the monitored supply temperatures are 5 °C higher than the simulated ones.

This Graph shows the results of the substation UDC01 if the data went as they should, but the reality seems very different. The mass flow rates flowing in the secondary side are almost 6x times higher than the simulated ones. Moreover, the heating district exchange less energy with the multi-dwelling unit substation. To correctly validate the model, it has to be put in the same conditions of the reality. Therefore, another simulation will be done considering the same heat transfers calculated from the monitoring data. When the comparison is made with the same energies the model can be validated.

In the following Chapter, the monitoring heat transfers are used as input file in the in the following network TRNSYS model to check and validate the results in the secondary side.

7.2 Model Validation

In this Chapter the monitoring data about the heat transfer at each substation are used as input file in the Merezzate TRNSYS network modelled before, to check the situation in the secondary side. Since the performances of the simulated multi-dwelling units are very different from the real ones, they are compared with real loads, to validate the substation and the network model.

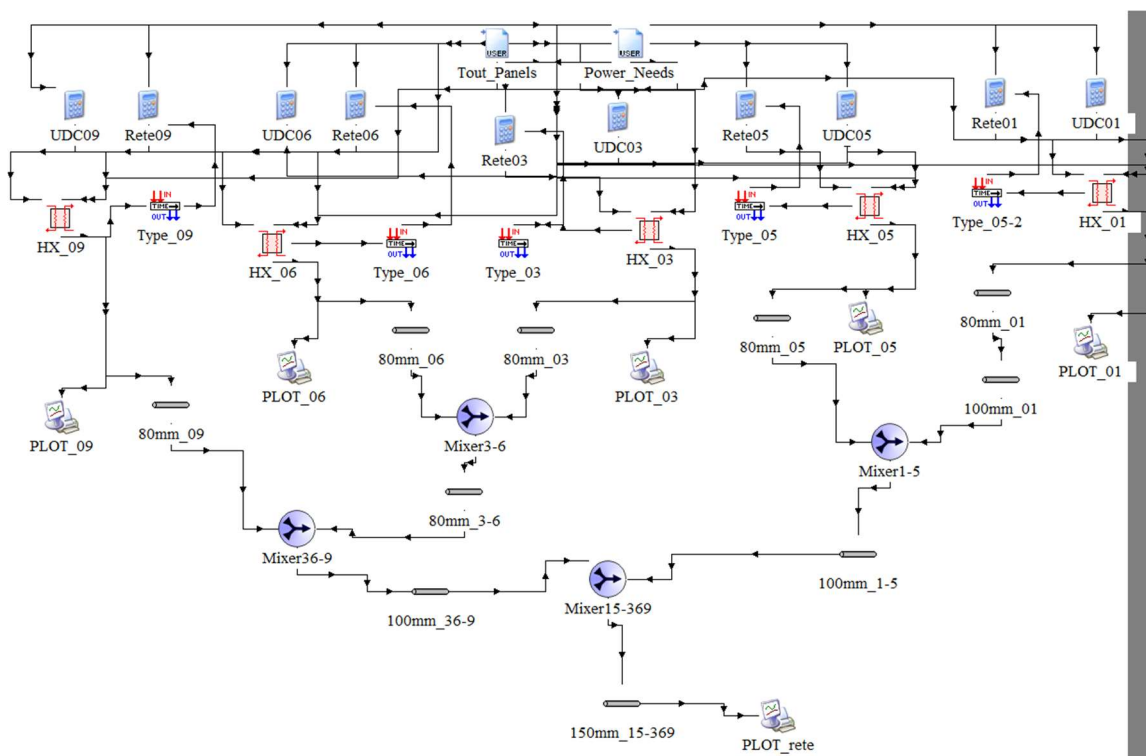
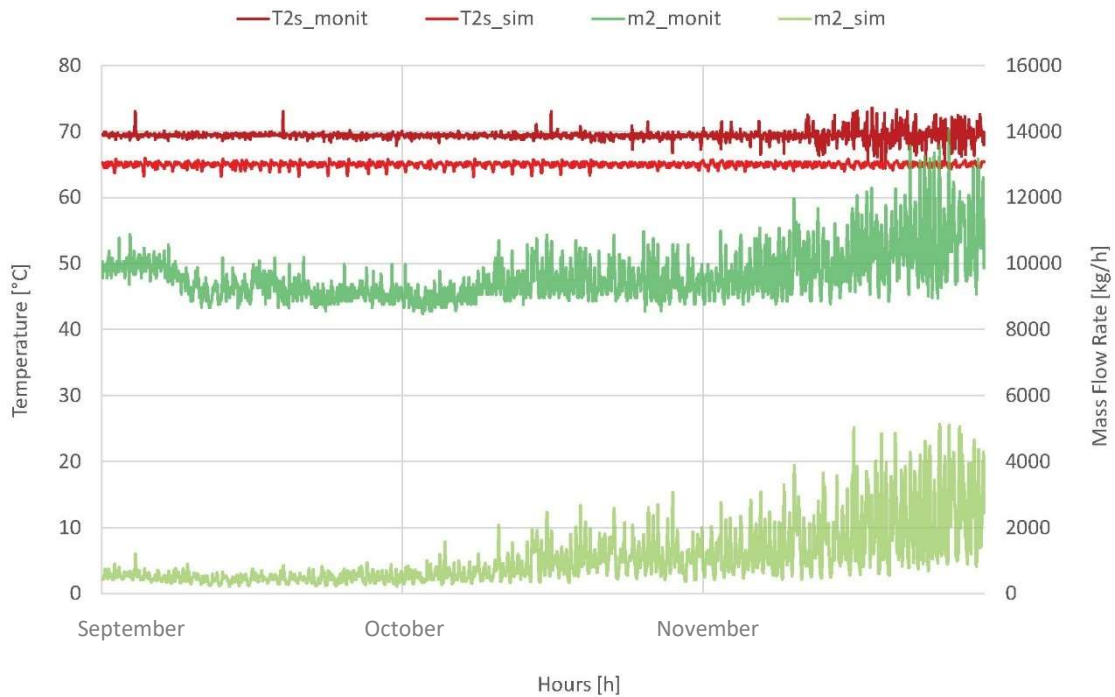


Figure 7.1 TRNSYS network model with monitoring heat transfers

A higher mass flow rate is expected in secondary side. This is probably due to some recirculation in the secondary circuit (this hypothesis will be verified in the next paragraph). There is no precise information regarding the multi-dwelling unit network (secondary side) because all the data are provided by A2A which mainly deals with the district heating network (primary side).

The obtained results for the multi-dwelling unit UDC01 (Graph 7.2) are shown in the following Graph.



Graph 7.2 UDC01 results from actual energy compared with monitoring data

The simulated mass flow rate in the secondary side is now around 3x times lower than the actual one. This can be due to a recirculation in the secondary side with the supply line. Supply temperatures are also higher than the designed ones. It is shown just one multi-dwelling unit because this problem occurs in all substations.

The monitoring data are still different from the simulated one, there is probably something different in the secondary side that was not simulated correctly. There must be recirculation in the secondary side to have instant DHW production, however, it seems much higher than expected. Assuming a recirculation mass flow rate and checking the return temperatures in the secondary side could be a good analysis to understand the reason of these results.

There is a by-pass valve in the flat station to allow the recirculation for having instant DHW production. In this section the by-pass valve is simplified with a recirculating mass calculated in the secondary side equal to the difference between the mass flow rate simulated ($m2_sim$) and the monitoring one ($m2_monit$). The difference between these two flows is modelled as recirculating mass ($m2_rec$) from the supply circuit. The recirculating mass is then mixed with the return flow rate. The return balance temperature ($T2r_mix$) is compared within this paragraph with the return temperatures from A2A in the secondary side.

A new simplified scheme of recirculation in the secondary side is shown in the picture below (Figure 7.2).

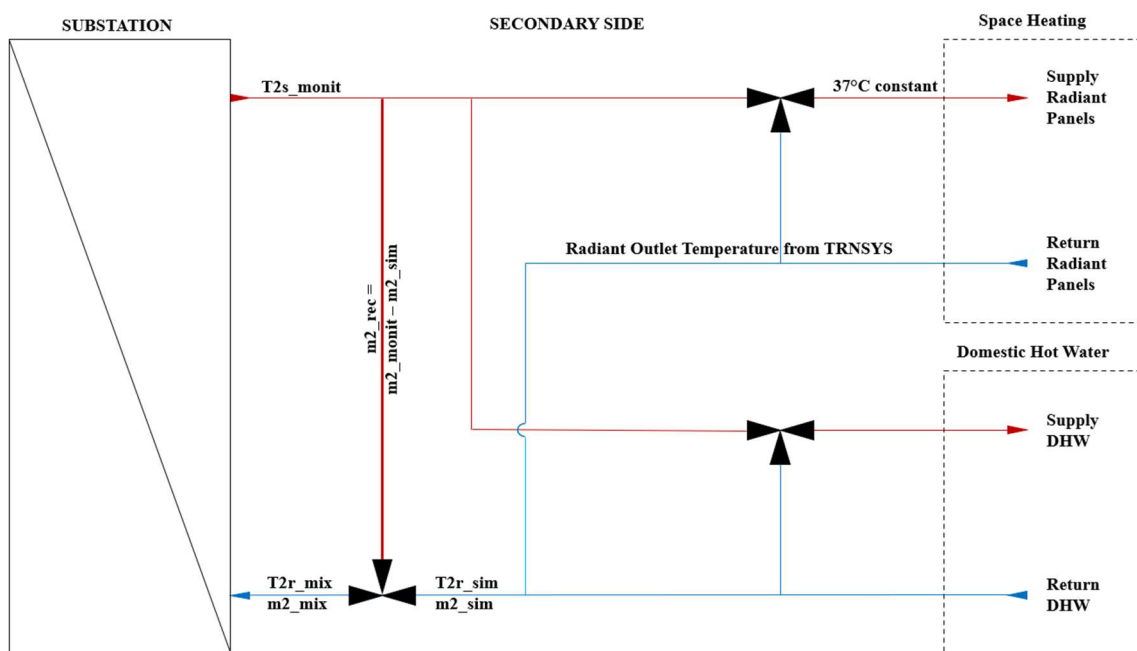


Figure 7.2 Secondary side scheme with recirculation

The recirculating mass is calculated as:

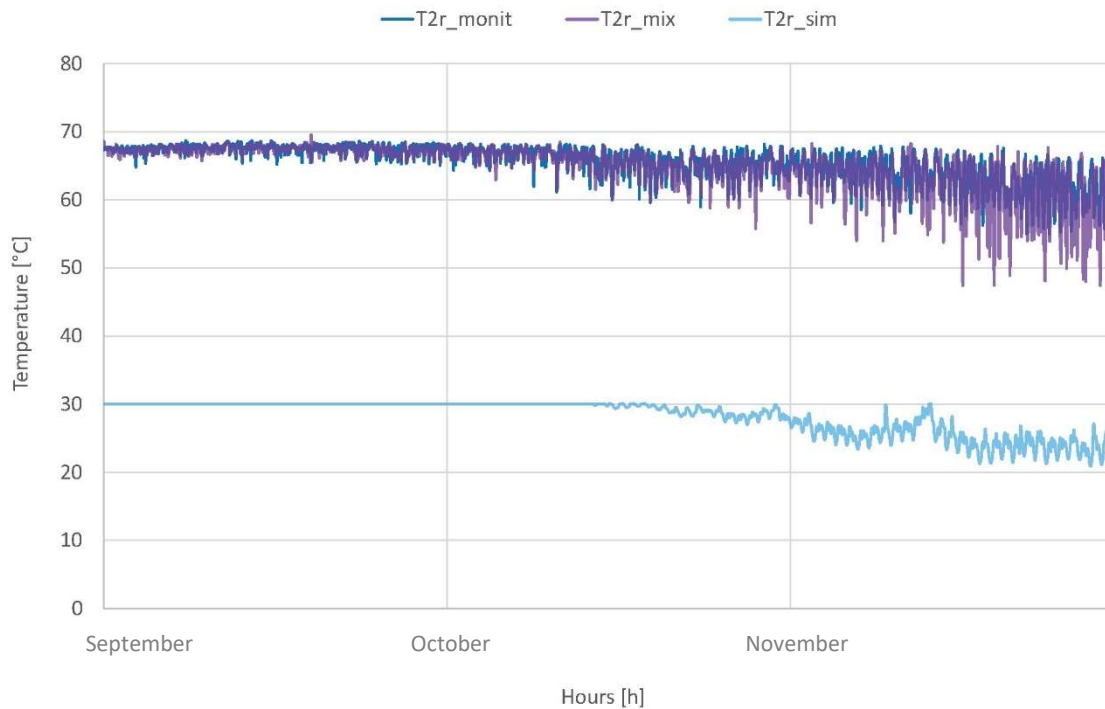
$$m2_rec = m2_monit - m2_sim \quad (7.1)$$

Instead, the return balance temperature is calculated as:

$$T2r_mix = (m2_sim \cdot T2r_sim + m2_rec \cdot T2s_monit) / m2_mix \quad (7.2)$$

Where the T2s_monit is the monitoring supply temperature of the secondary side and m2_mix is the same mass flow rate monitored (m2_monit).

The UDC01 mixed temperature (T2r_mix) given by the recirculation in the secondary side is analysed and compared with the monitoring return temperature (T2r_monit) and the first simulated outlet temperature (T2r_sim), in the following Graph.

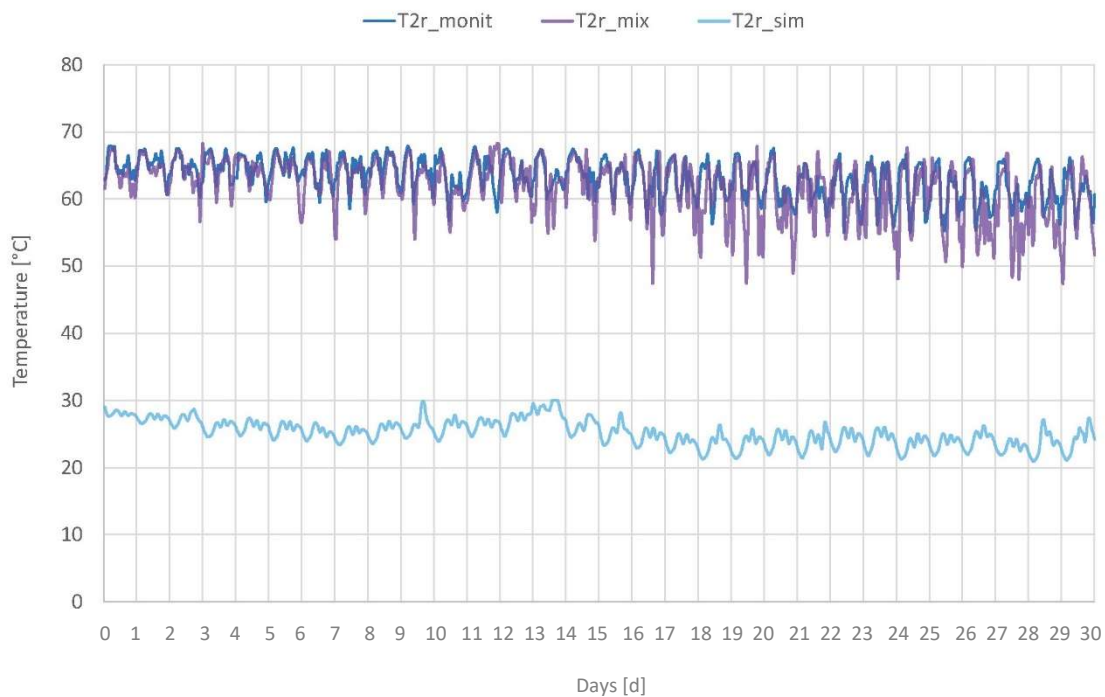


Graph 7.3 UDC01 recirculation results compared to the monitoring data

The return mixed temperature is almost the same of the monitoring outlet temperature. The two Graphs are practically overlap. The previous simulated return temperature is also shown in chart to understand better the difference between the network simulation

considering a secondary side scheme as in Figure 4.4 and the network simulation considering the new secondary side scheme with recirculation as in Figure 7.2.

A smaller period is also zoomed to show better the comparison and understand better the return temperature trends. November is the chosen month to allow some time for the heating system to run. The comparison during November is shown to in the following Graph.

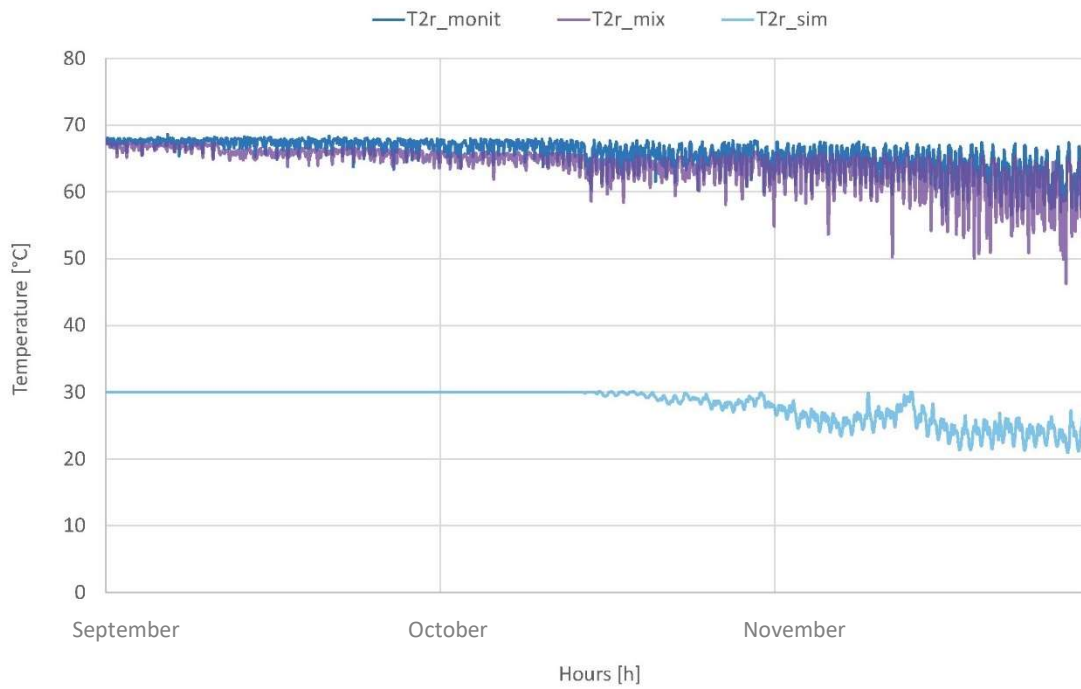


Graph 7.4 UDC01 recirculation results compared to monitoring data during November

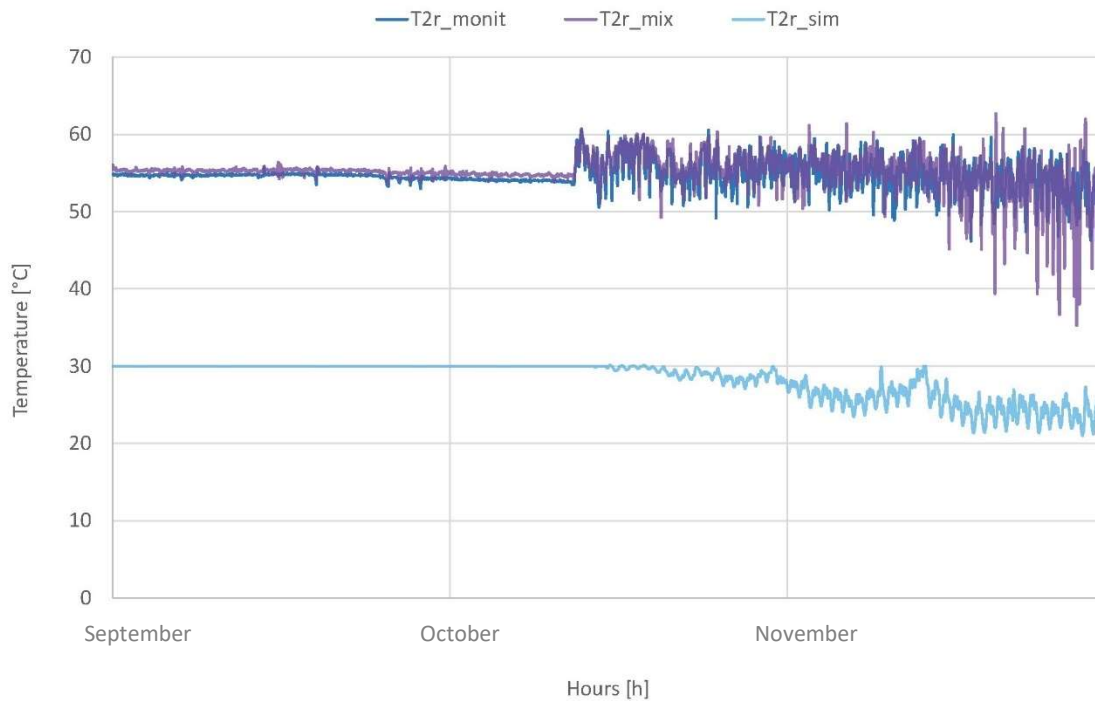
The return mixed temperature and the monitoring temperature have the same trends during November, according to Graph 7.4. The mixed temperatures seem a bit lower during the end of the month. The other mixed temperatures are analysed to understand if there is a tendency to also have lower results in the other multi-dwelling units.

The comparison between the recirculation results and the monitoring temperatures are shown for each multi-dwelling unit in the following Graph.

Model Validation

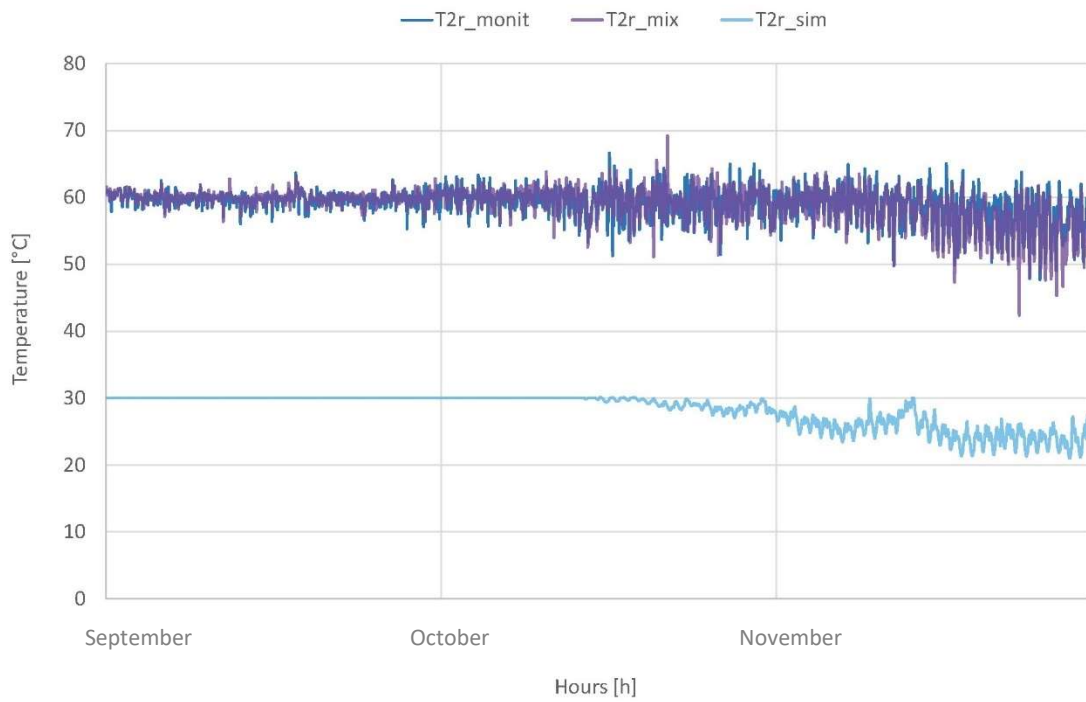


Graph 7.5 UDC03 recirculation results compared to the monitoring data

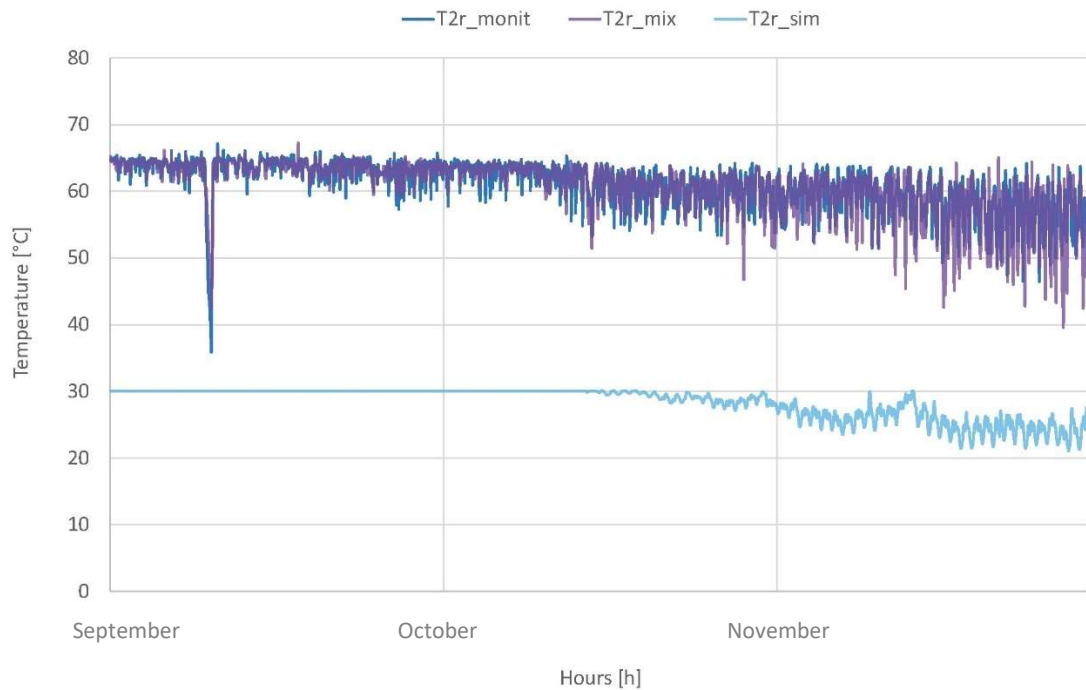


Graph 7.6 UDC05 results with recirculation compared to the monitoring data

Model Validation



Graph 7.7 UDC06 recirculation results compared to the monitoring data



Graph 7.8 UDC09 recirculation results compared to the monitoring data

The mixed temperatures are very close to the reality for every multi-dwelling unit. The average differences between the recirculation results and the monitoring data are shown in the following Table.

Table 7.1 Average difference between recirculation results and monitoring data

Average [°C]	UDC01	UDC03	UDC05	UDC06	UDC09
T2r_mix - T2r_monit	-0.59	-1.80	0.41	-0.14	-0.19

It is highlighted a general tendency to have a lower average temperature in the mixed return line. This probably happens because it is considered a supply temperature around 65 °C in the secondary side, but it is actually sent about 70 °C. This theory can be confirmed by the multi-dwelling unit UDC05 which is the only one that have an average mixed temperature higher than monitoring one, in fact there is an actual supply temperature lower than 65 °C. Moreover, the multi-dwelling units which shows the least discrepancy are where the supply temperatures are closer to the ones considered. UDC06 and UDC09 have an average difference less than 0.20 °C indeed. Anyway, the results seem consistent with the actual data. A Table with summary errors is shown below to understand better the validity of these data (Table 7.2).

Table 7.2 Percentage difference between recirculation results and monitoring data

Error [%]	UDC01	UDC03	UDC05	UDC06	UDC09
MAX	21.60	24.05	29.81	27.36	28.15
Average	1.84	2.89	2.12	2.13	2.51
min	0.00	0.00	0.00	0.00	0.00

The average discrepancy between the mixed temperature and the monitoring data is lower than 3% for each multi-dwelling unit, according to the Table 7.2. It means the new simplified scheme designed (Figure 7.2) is consistent to correctly describe the actual

situation. Now that the secondary side is validated, the next step is to check the primary side. Another simulation is run, considering all the secondary side monitoring data and the actual energy and supply temperature for the primary side, in order to check the mass flow rate and the return temperature in the primary circuit.

7.3 Validation of the Network Model

In this Chapter the monitoring data of the secondary side of each substation are used inside the TRNSYS network simulation modelled before, to check the primary side. The monitoring heat transfers and the supply temperatures are used in the primary side to check the return temperatures and the mass flow rates of the network as shown in Figure 7.3. Therefore, the previous TRNSYS network model (Figure 7.1) is used, substituting the secondary side pre-dimensioning data, primary side energies and supply temperatures with the monitoring data for each multi-dwelling unit, as it is described in the scheme below.

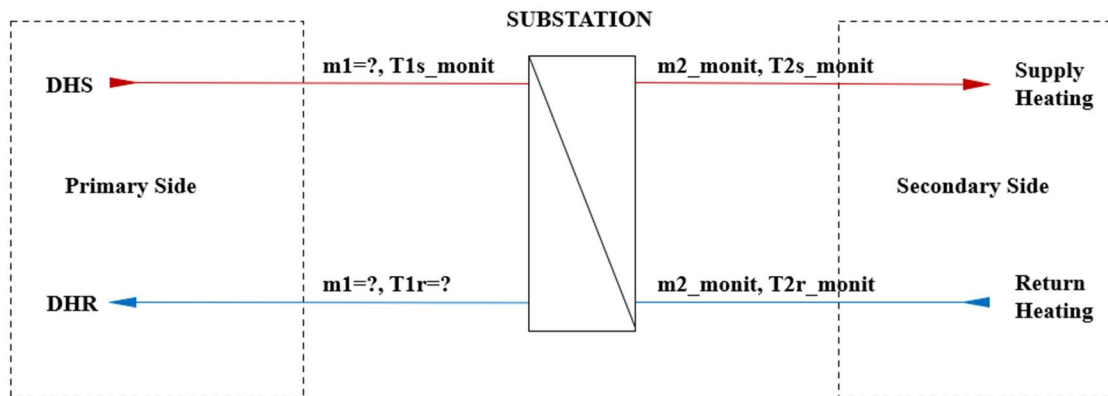
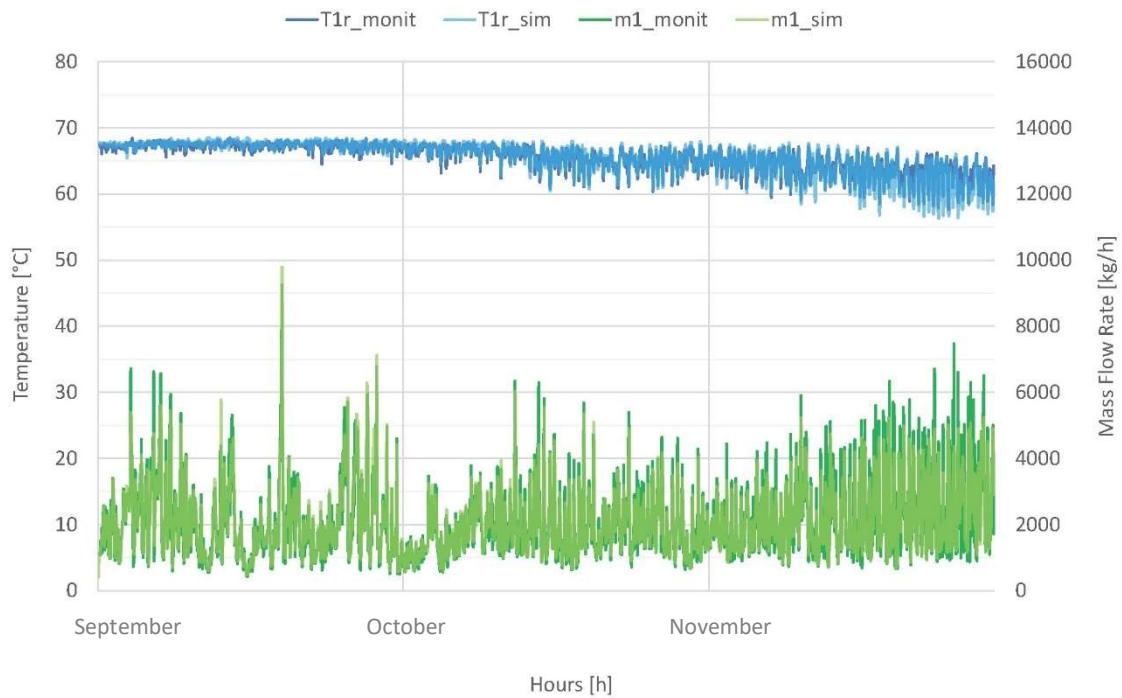


Figure 7.3 Scheme of validation of the network model

The Delayed Output Device (Type 150) is fundamental in this validation, because it calculates the return temperatures of the primary side at the previous instant. This component also balances the mass flow rate in the primary circuit according to the

monitoring energy used. Mass flow rates and return temperatures of the primary side are checked in this network simulation in order to validate the model.

The results obtained from the TRNSYS model are validated with the monitoring data provided by A2A, in the following charts.

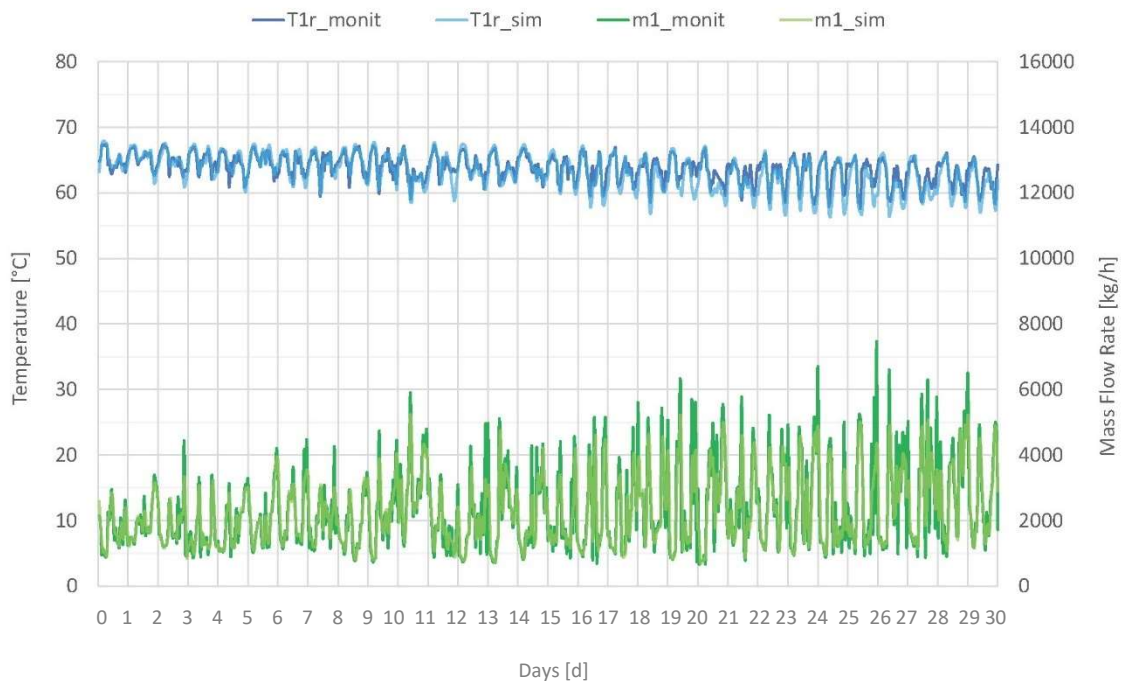


Graph 7.9 UDC01 primary side validation

It is immediately clear that the model is correctly designed now, and the simulation provide results consistent with the actual network. The return temperatures (T1r_sim) and mass flow rates (m1_sim) simulated are the same of the monitored ones (T1r_monit & m1_monit).

A smaller period is also zoomed to show better the validation between the simulated results and the monitoring data. The month of November is chosen also here to allow some time for the heating system to run. The comparison during November is shown to in the following picture.

Model Validation



Graph 7.10 UDC01 primary side validation in November

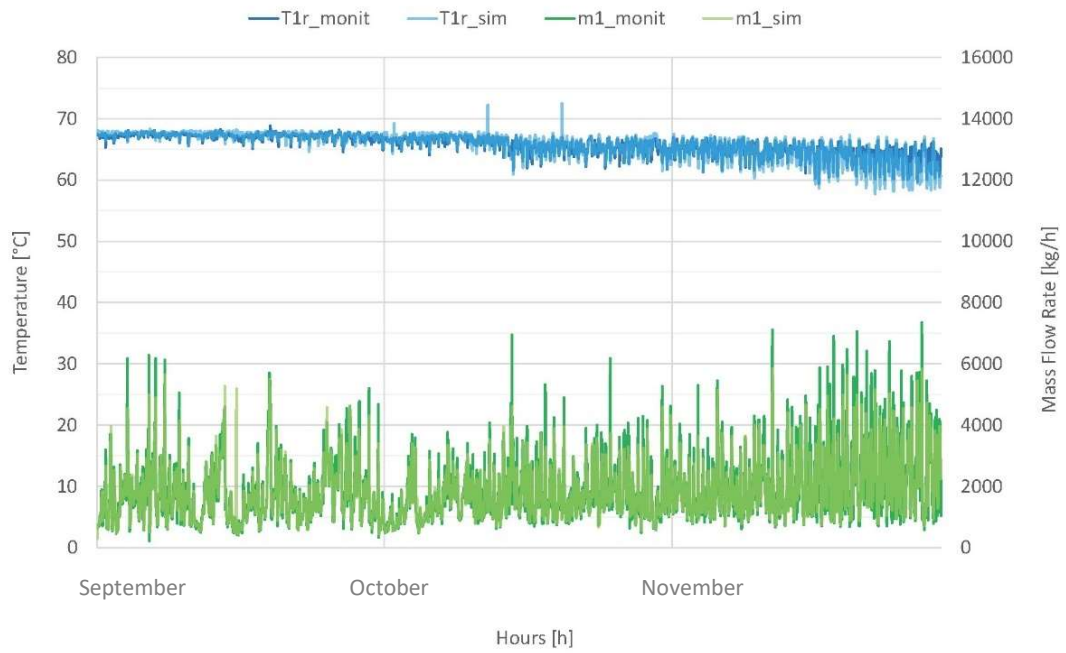
The simulated results perfectly overlap with the monitoring data. The simulated return temperatures are practically the same of the monitored ones. The mass flow rates are very close to the actual data except for the peaks. This is probably due to the hourly timestep used during the simulation because it assumes a constant value for the whole hour, when the data change every second in the reality. A summary Table of the mass flow rate differences for each multi-dwelling unit is shown below to understand if the average values are consistent with the actual situation. It is immediately clear that mass flow rates are practically the same and the average difference is always lower than 3%. The model probably does not cover some mass flow rate peaks due to the hourly grid used. Anyway, the simulation made is consistent with the actual situation.

Table 7.3 Average difference between simulated results and monitoring data

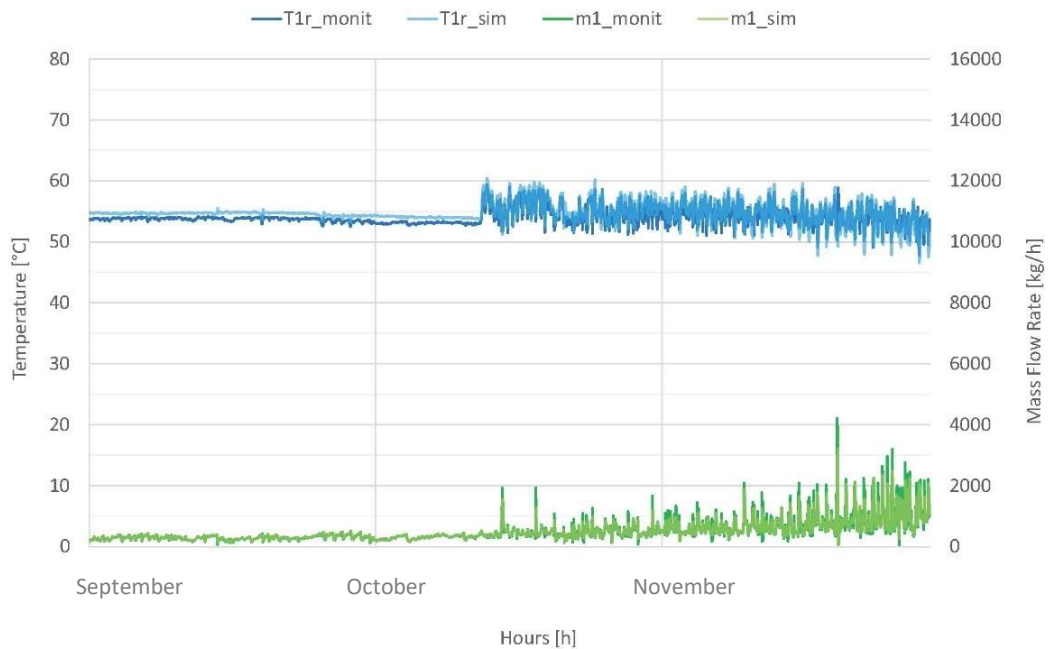
m1 Average Error	UDC01	UDC03	UDC05	UDC06	UDC09
m1_sim - m1_monit [kg/h]	-3.72	-48.23	2.97	29.28	-8.34
Average [%]	0.18	2.55	0.60	2.25	0.74

Model Validation

The other multi-dwelling unit results are shown in the following Graphs.

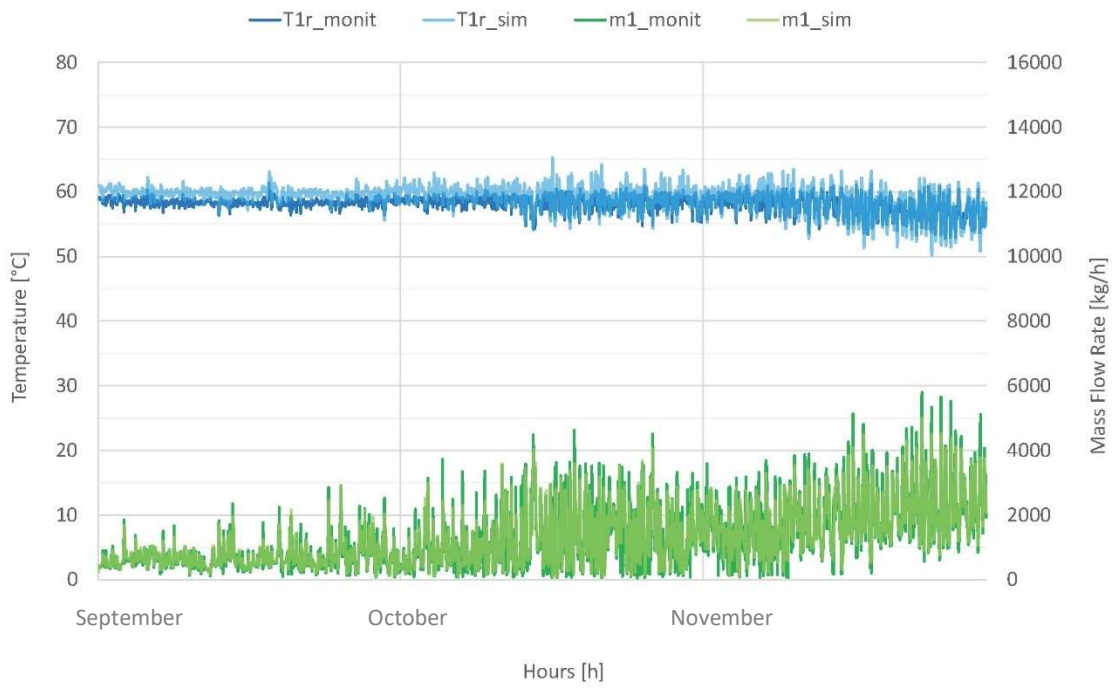


Graph 7.11 UDC03 primary side validation

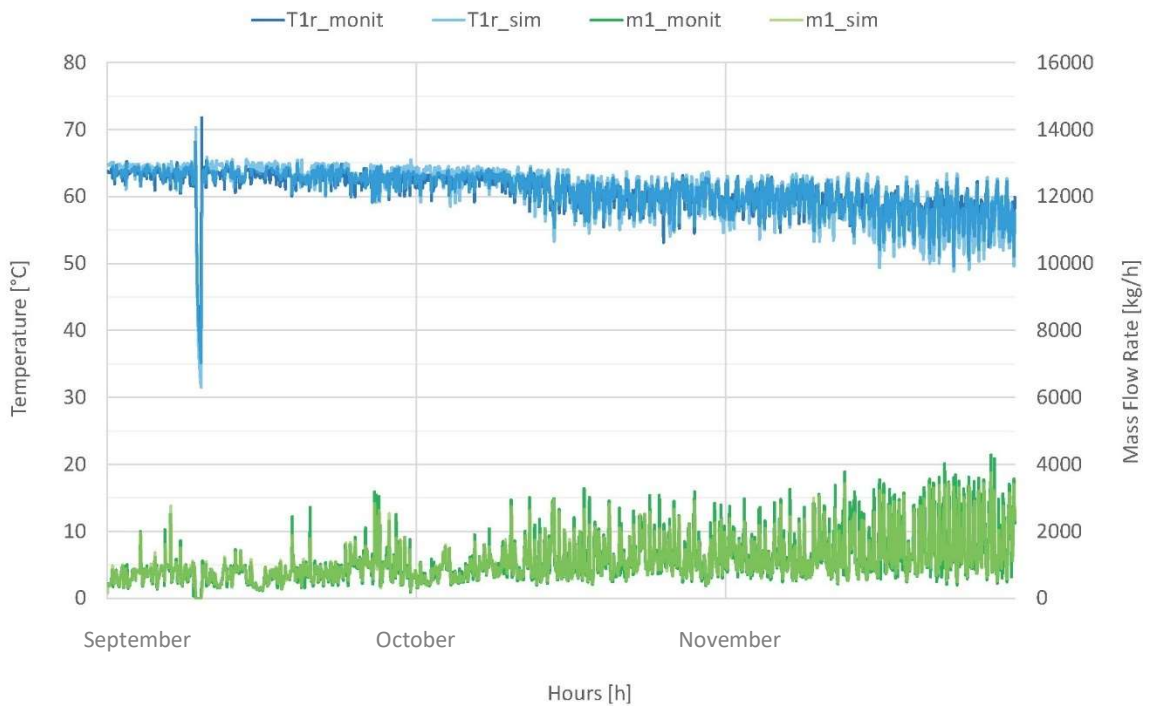


Graph 7.12 UDC05 primary side validation

Model Validation



Graph 7.13 UDC06 primary side validation



Graph 7.14 UDC09 primary side validation

A Table with summary errors of the primary side return temperatures is shown below to understand better the validity of these data (Table 7.4).

Table 7.4 Percentage difference between simulated results and monitoring data

T1r Error [%]	UDC01	UDC03	UDC05	UDC06	UDC09
MAX	10.41	9.21	16.16	9.85	22.24
Average	1.10	1.06	1.79	2.25	1.77
min	0.00	0.00	0.00	0.00	0.00

The average difference is always lower than 2% except for the UDC06. The TRNSYS model is considered validated, according to the Graphs and the summary error Tables shown in the previous pages. The obtained results are practically the same of the monitored ones, therefore, the simulation model correctly describes the actual situation.

After the analysis performed in this Chapter the actual district network is deeply analysed in both sides (primary and secondary side). The model created on TRNSYS and the simulation performed, provide consistent results and a simplified scheme of the district heating. The Merezzate network model can be used to inform the implementation of all future projects in the area.

The results obtained till now and the validated TRNSYS model will be used in the next Chapter to design a possible implementation of the Merezzate district.

The ideated solution consists in a solar thermal system integrated with the district heating. The solar system works for each unit of building as an auxiliary heater before the heat exchanger and as a decentralised system for the whole network when the temperatures do not reach the supply set point.

The solar thermal system analysis is shown and described in the following Chapter.

8. Decentralised Solar Thermal Model

This Chapter focuses on the analysis of a decentralised solar system for the multi-dwelling unit UDC05. The solar thermal integration in district heating is studied with nowadays DH network and with the next implementation of 4th generation DH. The different feed-in systems are analysed with their relative benefits and the best configuration is simulated through the TRNSYS network model. The results will be discussed in the last paragraph, considering the stagnation hours, the produced energy, the reduction of non-renewable primary energy and the investment costs.

8.1 Solar Thermal DH and different Feed-in Connections

Solar energy is one of the most renewable and eco-friendly energy sources, promising sustainable solution. The common technology used for heating application is the solar thermal collector. It converts solar radiation into exploitable thermal energy through an intermediary fluid flowing in a heat exchanger [32]. Its working fluid is a mixture composed by water and glycol (33.3 %). The presence of glycol permits to avoid the freeze of the water in the tube by decreasing its freezing point. Its percentage within the water should be minimized because it reduces the efficiency of entire solar field due to its higher viscosity. For large-scale applications, the common solar collector types are: flat plate collectors (FPC) and evacuated tubular collectors [33]. The most utilized is the FPC for its high value of price/performances ratio, as proposed in the Solar District Heating Guide [33].

Solar energy reaches its highest potential with long sunlight hours and high solar radiation intensity. However, solar radiation is intermittent and affected by variable weather conditions and seasonal fluctuations [34]. Due to the nature of solar radiation, heating demand and solar energy availability are seldom in phase. Moreover, high delivery temperatures cannot be achieved through stationary non-concentrating collectors, the flat-plate and vacuum tube [35].

The integration of heat from solar energy technologies can be realised by feeding in energy both at centralised or at multiple decentralised locations from the consumer side. As distribution networks serve as thermal transmission grids, the interaction between the energy feed-in (i.e. production) and withdrawal (i.e. consumption) at multiple locations within distribution networks should be incorporated [36]. The use of the grid to accumulate the energy allows a better exploitation of the solar energy by distributing it among several buildings [36]. Modelling the interactions between these subsystems is challenging. The network configuration changes compared to solar system with storage tank and the feed-in connections become crucial. Some of 20 DH-connected solar thermal facilities in Sweden were mapped out in this study and it was found that their performance was lower than expected [33]. There were signs that this was caused by fluctuations in feed-in heating energy and flow. One main finding is that a fundamental principle for a well-functioning feed-in is that the feed-in heating energy must match the heating energy generated by the solar thermal system if no storage is used. It is often beneficial to avoid storage for a practical and economic reasons [37]. This Chapter aims to study the potential of district heating system with solar thermal based on decentralised system, by developing a modelling framework for design and simulation of such network.

A distributed heat source can be connected in four different ways [37], as anticipated in Chapter 2.3:

- In a return/supply system (R/S) the water is withdrawn from the return pipe, heated to a correct temperature, and fed back into the supply pipe.
- In a return/return system (R/R) the water is withdrawn from the return pipe, heated to any temperature higher than the temperature on the return line, and fed back into the return pipe.
- In a supply/return system (S/R) the water is withdrawn from the supply pipe, heated to any temperature, it has already a higher temperature than the temperature in the return line, and fed back into the return pipe.
- In a supply/supply system (S/S) the water is withdrawn from a supply pipe, heated to any temperature higher than the temperature on the supply line, and fed back into the supply pipe.

The use of S/R and S/S is not very common since they feed the DH system with high temperature on the return line or a higher temperature than necessary on the supply line. They can be used some hours per year as an overheat protection system for a local heat source that can be hard to shut down. R/R and S/S system cannot produce any flow on the DH main line this disadvantage is very important to consider when system is planned. On the other hand, R/S and S/R system can produce the needed flow in the DH system both in the service and on the main line [37]. A feed-in system never guarantees heat to all customers in the DH system. It is the central heat generation system that has the responsibility to provide heat to all customers.

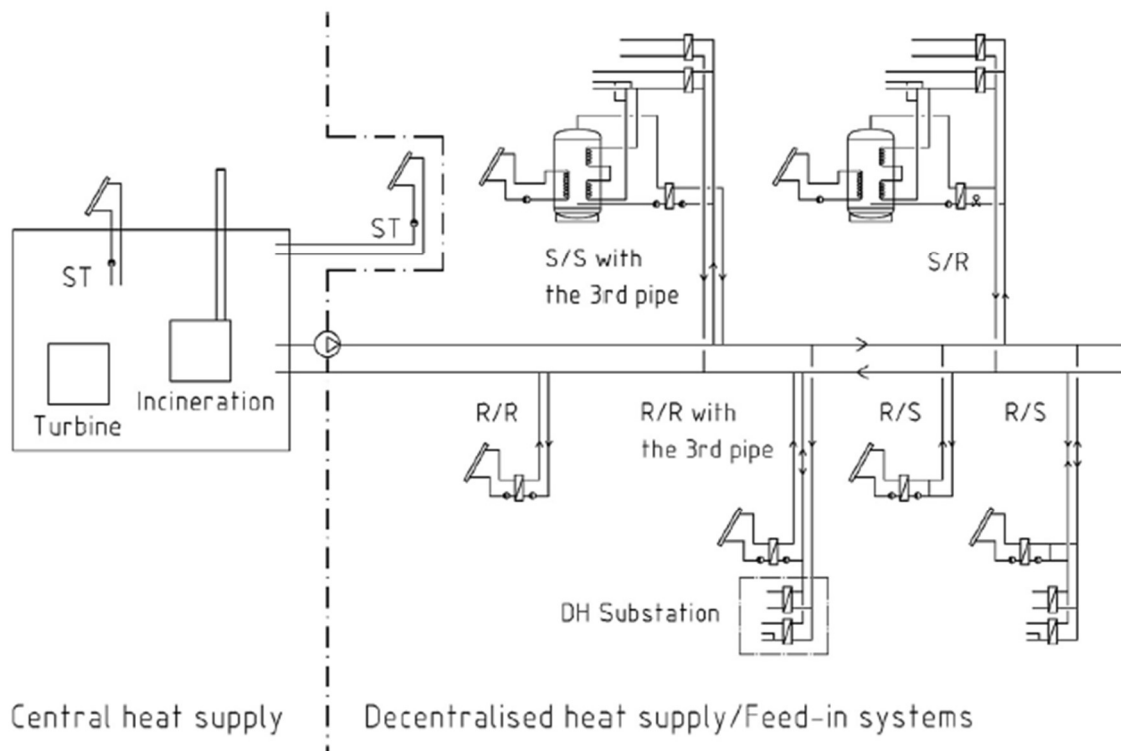


Figure 8.1 Generic scheme of the four different feed-in connections [17]

The main performances and specific characteristics of each feed-in connection are resumed in the following Table:

Table 8.1 Main characteristics of the four different feed-in connections [37]

Distributed Heat Generation	R/R	R/S	S/R	S/S
Most common	X	X		
Can create a flow in the DH network		X	X	
Need a feed-in pump		X	X	
Can function without a pump	X			X
Increase DH return temperature	X		X	
Simple control strategy	X		X	X
Must produce a temperature above a certain level		X		
Can be used as an over-heat protection system without an extra pipe (the 3 rd pipe)		X	X	
An extra pipe is needed (the 3 rd pipe)	X			X

The solution studied in this thesis-work will be the supply/return feed-in connection because the solar field is integrated to the DH network with a S/R configuration. The decentralised solar system withdraws the water from the supply line of the primary network and send it back to the return line. The water is used by the multi-dwelling unit thanks to the substation and then is post-heated by the solar field. If the water reaches the supply set point temperature goes again to the substation and can be used by the users. If the water does not reach that set point it goes back to the return of the primary network. This solution is chosen because the configuration can remain unchanged with the next 4th generation district heating. This integration is picked from a construction point of view to also simplify the work on site. In fact, the substations will be removed soon and the low temperature network will flow in the Merezzate district. This solar integration will remain the same with the next LT configuration and the decentralised solar system is ready to work. For this reason, the proposed solution will be studied and simulated at today's configuration and with the next 4th generation DH. In the following Chapter the solar thermal system is analysed for the multi-dwelling unit UDC05.

8.2 Solar Field Sizing

For this thesis work, the selected solar collector type is the FPC. The adopted model for the feasibility study is RIELLO CSAL 25 RS [38], whose specific characteristics are reported in the following Table.

Table 8.2 Characteristic of the selected model of FPC [38]

Intercept Efficiency (η_0)	0.784	-
Slope Coefficient (a_1)	4.08	W/m ² K
Curvature Coefficient (a_2)	0.0084	W/m ² K ²
Slope of Collector (β)	55	°

These technical parameters refer to the aperture area of the solar collectors. The solar collectors should be specific orientated according to the geographical coordinate in order to maximize the solar output. In this case, they are oriented towards the south direction with an azimuth angle (γ) equal to 0°, typical orientation adopted in this hemisphere. While the inclination depends specifically on the latitude of the installation place. Therefore, the assumed inclination angle (β) is equal to the latitude of Milan (45°) increased of 10°. A correct value of β permits the maximization of solar energy captured by collector when the incidence angle (θ) is not zero. When θ is greater than 25°, it influences the trend of Incidence Angle Modifier (IAM), causing the decay of collector performances complies the variation of θ .

From these parameters, the efficiency of the solar collectors is obtained through the following two equation 8.1 and 8.2 according to the Standard European EN12975 [39].

$$\eta_{coll} = \eta_0 - a_1 \left(\frac{T_m - T_{amb}}{G} \right) - a_2 \frac{(T_m - T_{amb})^2}{G} \quad (8.1)$$

$$T_m = \frac{T_{in} + T_{out}}{2} \quad (8.2)$$

Where:

T_m = mean temperature [$^{\circ}\text{C}$]

G = solar irradiance [W/m^2]

T_{in} = inlet temperature of collector [$^{\circ}\text{C}$]

T_{out} = outlet temperature of collector [$^{\circ}\text{C}$]

The efficiency curve of the selected model is represented in the following Figure.

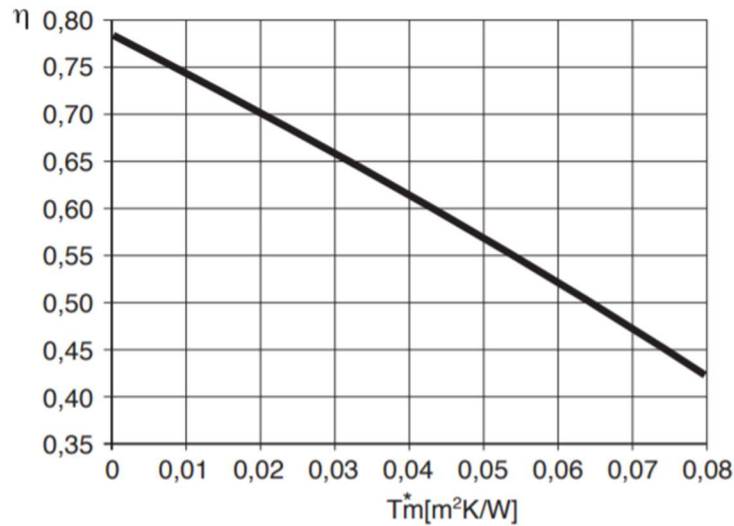


Figure 8.2 Efficiency trend complies to T_m referred to absorber area [38]

$$T_m^* = (T_m - T_{amb})/G \quad (8.3)$$

The nominal power curve refers to $800 \text{ W}/\text{m}^2$ while the peak power is calculated by the standard with an irradiation of $1000 \text{ W}/\text{m}^2$ [38].

Therefore, the total power produced by solar field is computed through the following equation:

$$P_{coll} = A_{sf} \cdot \eta_{coll} \cdot G \quad [\text{W}] \quad (8.4)$$

The Asf is considered equal to 100 m^2 for multi-dwelling unit UDC05 to guarantee the correct supply of the heating demand but also to avoid the oversizing of the solar field. The oversizing provokes the solar system stagnation, damaging the system. The stagnation hours are the no-working time of the solar collectors, due to the exceed of heating produced compared to the heating needed by user. During the stagnation, the temperature in the solar collectors can achieve up to $200 \text{ }^\circ\text{C}$ causing the boiling of the working fluid and damaging the primary loop. The solar collector chosen has a 33.3% of glycol in the water/glycol mixture which maintains its characteristics in an interval of temperature between $170 \text{ }^\circ\text{C}$ and $-15 \text{ }^\circ\text{C}$ [38]. The number of stagnation hours raises by increasing the solar area or reducing the solar panels mass flow rate. The stagnation hours are always checked and maintained lower than 50 hours ($h_{\text{stagn}} \ll 50 \text{ h}$) during all the simulations in order to not damage the solar system.

To correctly dimension the solar HX is fundamental sizing its overall heat transfer coefficient (UA). The overall heat transfer coefficient is the value characterizing the heat exchanger. It is influenced by the thickness and thermal conductivity of the mediums through which heat is transferred. The larger is the coefficient, the bigger is the heat transferred from its source to the product being heated. In a solar heat exchanger, the relationship between the overall heat transfer coefficient (U) and the solar irradiance (G) in nominal condition can be described by the following equation:

$$G \cdot \eta_{\text{coll}} \cdot A_{\text{tot_coll}} = U \cdot A_{\text{HX_sol}} \cdot \Delta T_{\text{LM}} \quad (8.5)$$

Where:

Nominal solar irradiance: $G = 800 \text{ W/m}^2$

Nominal collector efficiency: $\eta_{\text{coll}} = 0.6$

Nominal logarithmic mean temperature difference: $\Delta T_{\text{LM}} = 8 \text{ K}$

With these assumptions the $U \cdot A_{\text{HX_sol}}$ can be simplified as $60 \text{ W/m}^2\text{K} \cdot A_{\text{tot_coll}}$

Therefore, the final UA used within the simulations will be equal to:

$$U \cdot A_{\text{HX_sol}} \approx 3.6 \cdot 60 \text{ kJ/hm}^2\text{K} \cdot A_{\text{tot_coll}} \quad (8.6)$$

After the solar field and the solar heat exchanger are dimensioned the different configuration of decentralised solar district heating will be analysed in the following Chapter. The first case will be done with the high temperature network and the second case with the next low temperature configuration. A constant mass flow rate equal to 30 kg/hm² will be considered for the solar panels in both cases, as suggested from the technical datasheet [38].

8.3 Decentralised Solar District HT Configuration

The first analysis on the decentralised solar DH is made with the today's high temperature configuration. The solar thermal system is used as a sustainable supply source to cover the multi-dwelling unit heating demand. The return water (≈ 40 °C) from the substation is heated up by the solar heat exchanger connected to the solar collector and goes to the network in 2 different ways. If the water reaches more than 80 °C it goes into the substation and can be used by multi-dwelling unit. If it does not reach the set point temperature the water is pre-heated and goes back to the return primary side of the network. Therefore, the solar field can be exploit by the multi-dwelling unit or the network.

Solar thermal exploited by user:

- If $T > 80$ °C it goes to substation by the supply line from the primary side and it will exchange heating to the consumers.

Solar thermal exploited by Network:

- If $T < 80$ °C it goes to the DH return line in the primary side. In this case the water increases the DH return temperature, decreasing the primary side ΔT .

A scheme of the high temperature DNet configuration is shown in Figure 8.3.

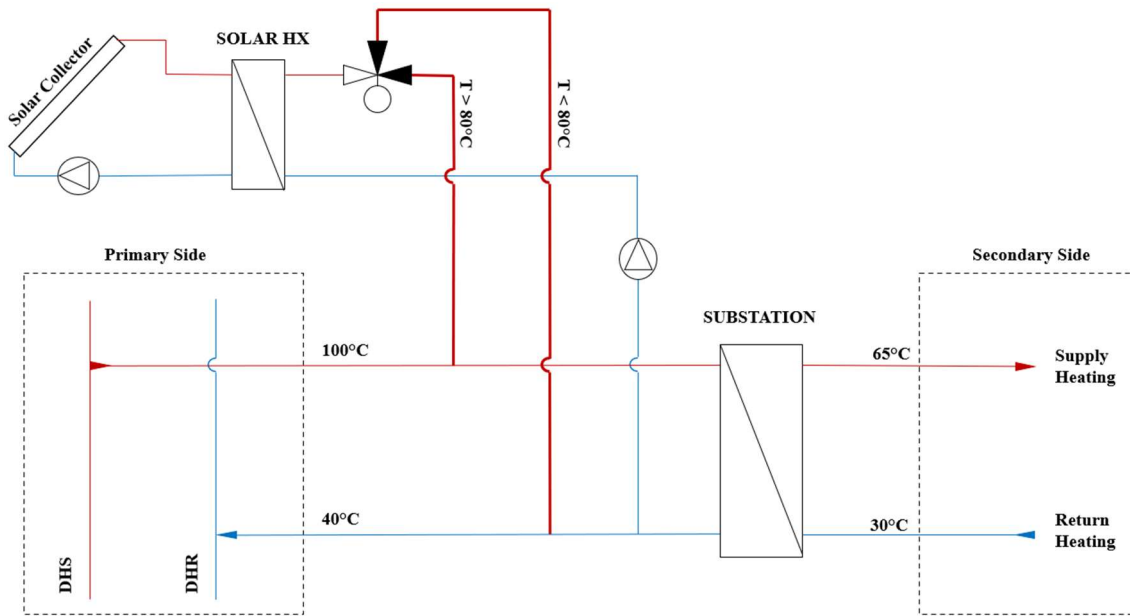


Figure 8.3 Generic scheme of a decentralised solar DH with HT configuration

The decentralised solar system is integrated to the primary side with a S/R as it is shown from the scheme above. The water is always withdrawn from the supply line and goes back to the return line.

After the decentralised solar district with HT configuration is studied the model will be created in TRNSYS to find the actual results. The simulation will be done, considering a constant mass flow rate for solar panels side equal to $30 \text{ kg/hm}^2 \cdot A_{\text{tot_coll}}$.

8.3.1 TRNSYS Model of Decentralised Solar System

The first simulation is run considering a constant mass flow rate on the solar panels side. It is assumed a panel mass flow rate equal to $30 \text{ kg/hm}^2 \cdot A_{\text{tot_coll}}$ according to the FPC model characteristics [38]. The scheme of TRNSYS model is shown below.

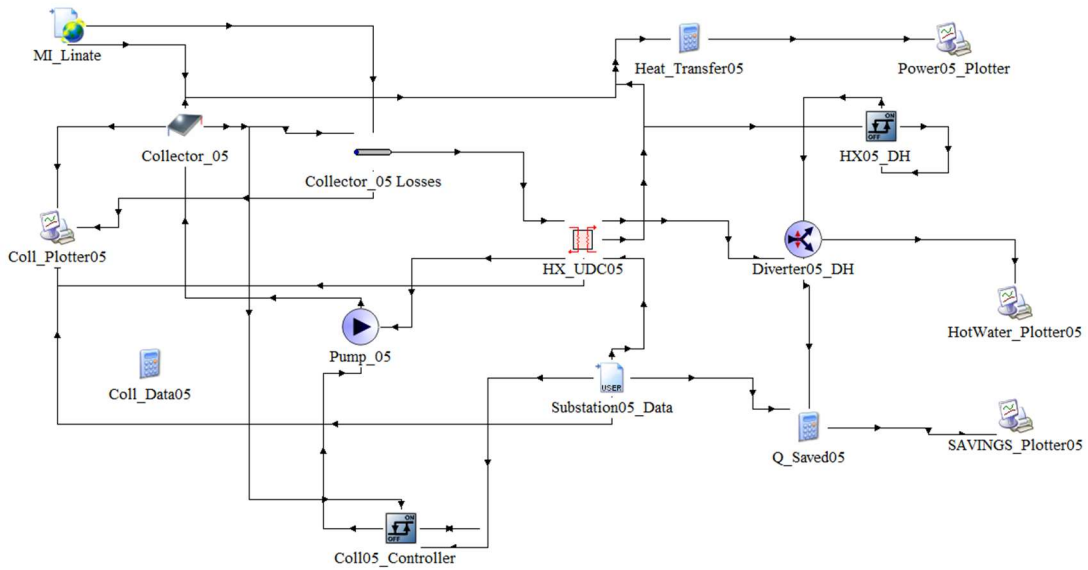


Figure 8.4 TRNSYS system model of decentralised solar thermal for UDC05

The main components of the system are: the solar collectors with their losses, the heat exchanger, the pump, the solar controller and the diverter valve with its controller for the feed-in system.

The new components with their types added in the simulation are reported in the following Table (Table 8.3). The fluid filled pipe is used to calculate the thermal losses of the solar collectors. All the other types not mentioned in the following Table are explained in the previous simulations.

Table 8.3 TRNSYS solar components

Component	TRNSYS Type
Solar Collector	Type 1b
Fluid Filled Pipe	Type 709
Pump	Type 3b
Controlled Flow Diverter	Type 11f

The solar collector receives weather information, such as solar radiation and environmental temperature, from the Type 109 (MI_Linate), representing the climate conditions of Merezzate. The solar field is connected to the hot side of the heat exchanger and the circulation pump, forming the primary loop or solar loop. While the UDC05 substations data, the cold side of the heat exchanger and UDC diverter compose the secondary loop.

The solar collector parameters are taken from the technical datasheet of the selected solar collector, as discussed in the Chapter 8.2. The solar controller is used for activating the panels when the environmental temperature is higher than DH return temperature + 10 °C and turning them off when T_{ext} is lower than DH return temperature + 2 °C (or the temperature exceeds 110°C).

The decentralised solar system is used as a renewable source for the Merezzate district heating, it withdraws the supply water from the primary side and heats it up after it is used by the substations as shown in the previous scheme (Figure 8.3). The UDC05 substation provided the data of mass flow rates and temperatures coming from the district heating during all the year in order to cover the multi-dwelling unit heating demand. The heated water from the solar field is distributed according to the control strategy represented in the following Table:

Table 8.4 HT control strategy model

$T < 80 \text{ }^\circ\text{C}$	Network
$T > 80 \text{ }^\circ\text{C}$	User

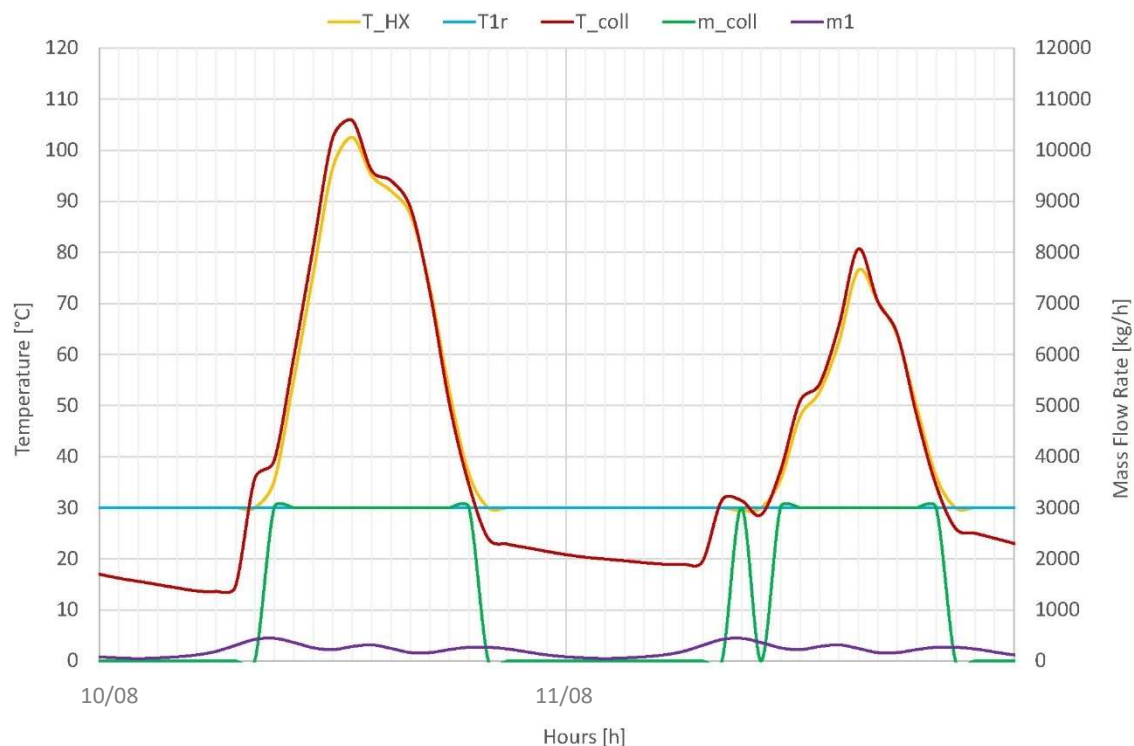
The simulations are also run with a timestep of 5 minutes in order to accurately the check stagnation hours and temperatures inside the collectors, considering all the peaks during the year.

The results obtained from the hight temperature network model are presented in the following Chapter.

8.3.2 Results of Decentralised Solar System HT

The first aim is to check the correct functioning of the solar panels. The temperature inside the collectors (T_{coll}), the temperature of the withdrawn water from the substation (T_{1r}) and the temperature of the heated water from the solar heat exchanger (T_{HX}) are analysed to understand the system behaviour. Moreover, the taken mass flow rate from the primary side (m_1) and the mass flow rate flowing in the solar system (m_{coll}) are also plotted in the following chart (Graph 8.1) to analyse the activation of the system and the consistency with the obtained temperatures.

The decentralised solar system is used during the whole year as a renewable source to cover the multi-dwelling unit heating demand. The annual hourly data is not very significant to understand the functioning of the solar panels, for this reason a short period is zoomed and analysed in the Graph 8.1.



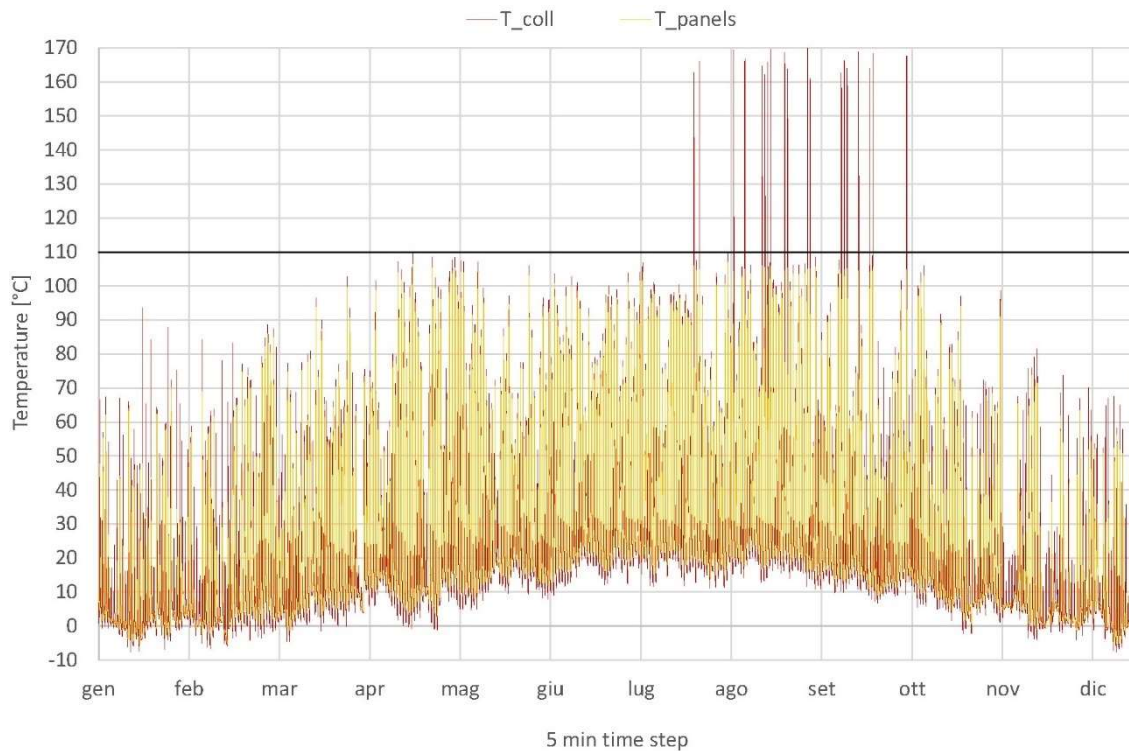
Graph 8.1 UDC05 solar panels temperatures & mass flow rates during August

48 hours during August are taken into account to study the solar panels trends within the day. The solar system is correctly working, according to the Graph in the previous page. The solar panels are activated during the day in order to exploit the solar gains and heat up the water coming from the return primary side. The system usually serves directly the network, but when temperatures exceed 80 °C it can be used by the substation providing heating to users. The temperatures of the heated water are higher than 80 °C during the 10th of August which means that the system will serve the multi-dwelling unit UDC05. The day after the temperatures never reach the 80 °C therefore, the solar source will be used from the return line of the primary side.

The mass flow rates are consistent with the solar field sizing. It is considered a solar field area about 100 m² and a mass flow rate of 30 kg/hm² for the panels. The result is exactly 3000 kg/h and the panels are activated when the external temperature is higher than temperature of the withdrawn water.

Another important result to check is the stagnation hours in order to analyse the system integrity. The next simulation is run with a timestep of 5 minutes in order to study also the peaks within the hours. The temperatures inside the collector (T_{coll}) and the working temperatures of the solar system (T_{panels}) are shown in the Graph 8.2. The temperature of the solar system demonstrate that the solar controller is working. There are no temperatures (T_{panels}) above 110 °C which means the system is correctly activated.

The temperature inside the collectors (T_{coll}) is shown to check the stagnation hours when the solar system is not working.

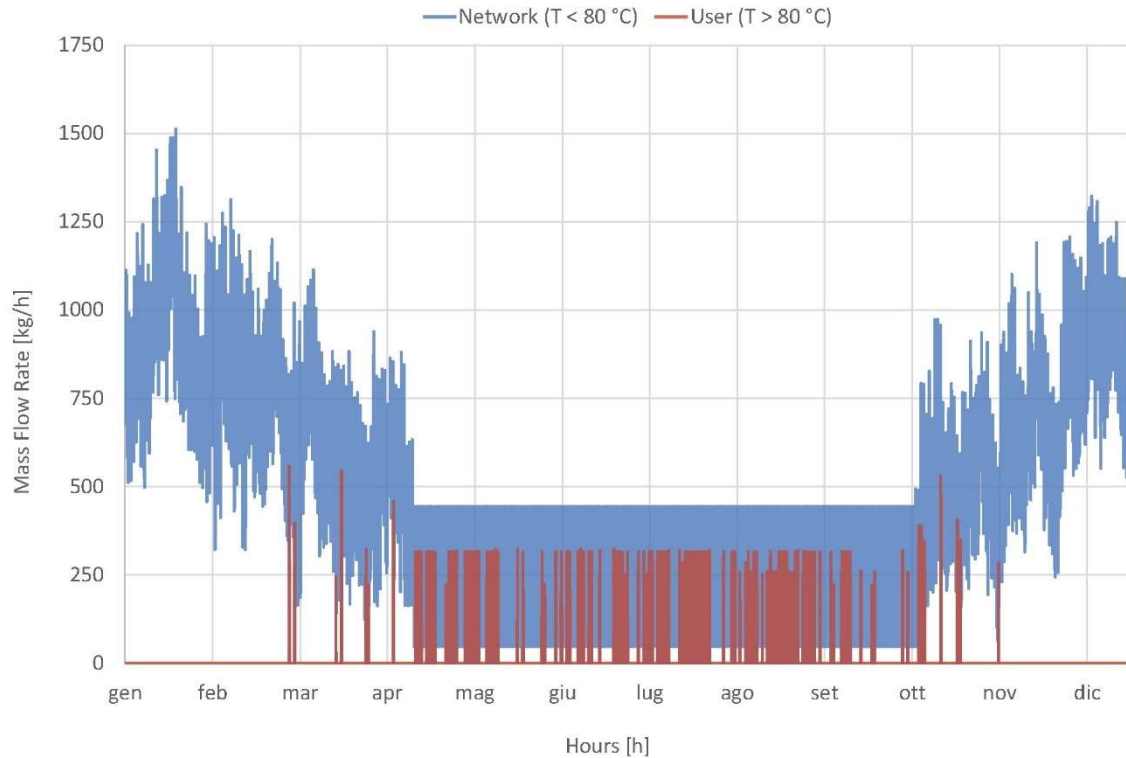


Graph 8.2 UDC05 solar collector temperatures with HT network

The temperature inside the collectors is never higher than 170 °C or lower than -10 °C which means the characteristics of the solar collector are respected according to the technical data sheet [38]. However, the stagnation hours resulted from the simulation are: 48 h << 50 h. The stagnation hours are lower than 50 but the value is a bit high. The number of stagnation hours should decrease to avoid any risk of damaging the system. It will be checked in next simulation at low temperature in order to understand the integrity of the solar field when the network temperatures decrease and the mass flow rate increases.

After the collectors are checked, the results from the distribution control strategy (Table 8.4) are analysed in the following Graph. The heated water from the solar field is shown in Graph 8.3. During the most part of the year the temperature is lower than 80 °C and the decentralised solar system serves the DH return network. When temperatures reach 80 °C the withdrawn water from the return line of the substation is used in the supply line by the multi-dwelling unit substation.

Decentralised Solar Thermal Model

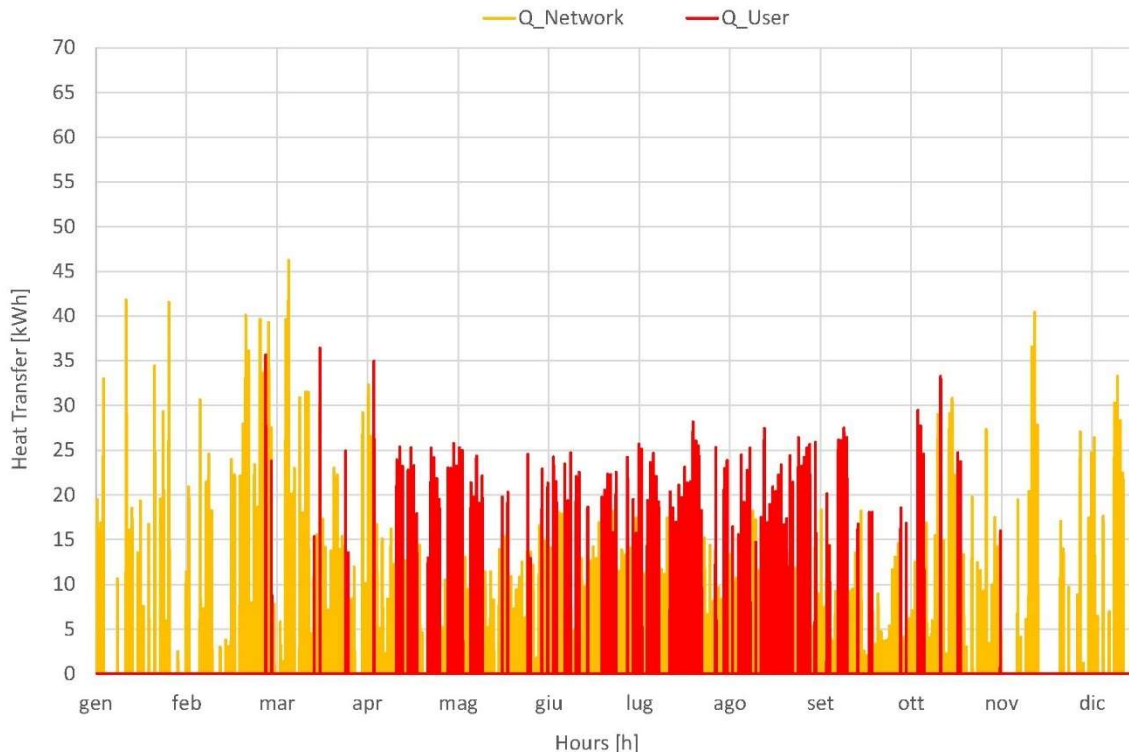


Graph 8.3 UDC05 heated water by solar system with HT network

The most part of the water does not reach the set-point of 80 °C therefore it goes back to the DH return line at higher temperature in order to be heated up by the thermal power plant of A2A. This configuration serves more the return line and it primarily works for the network. The solar thermal DH serves the users when the solar gains significantly increase. This configuration allows to exploit the hours with maximum solar contribution by the multi-dwelling unit. During summer in fact the temperature often reaches the 80 °C and the water goes to the supply line of the substation.

The energy saved by the network and the energy used by the users are shown in the following Graph. The energy used by users goes directly to the substation, allowing the thermal plant a lower heating production. The energy saved by network is calculated from the increase of the return temperature, heated by the solar system, compared to the design T_{1r}. A higher return temperature means a consequently decrease of the ΔT in the primary side. Therefore, the thermal plant will provide less heating to reach the supply temperature.

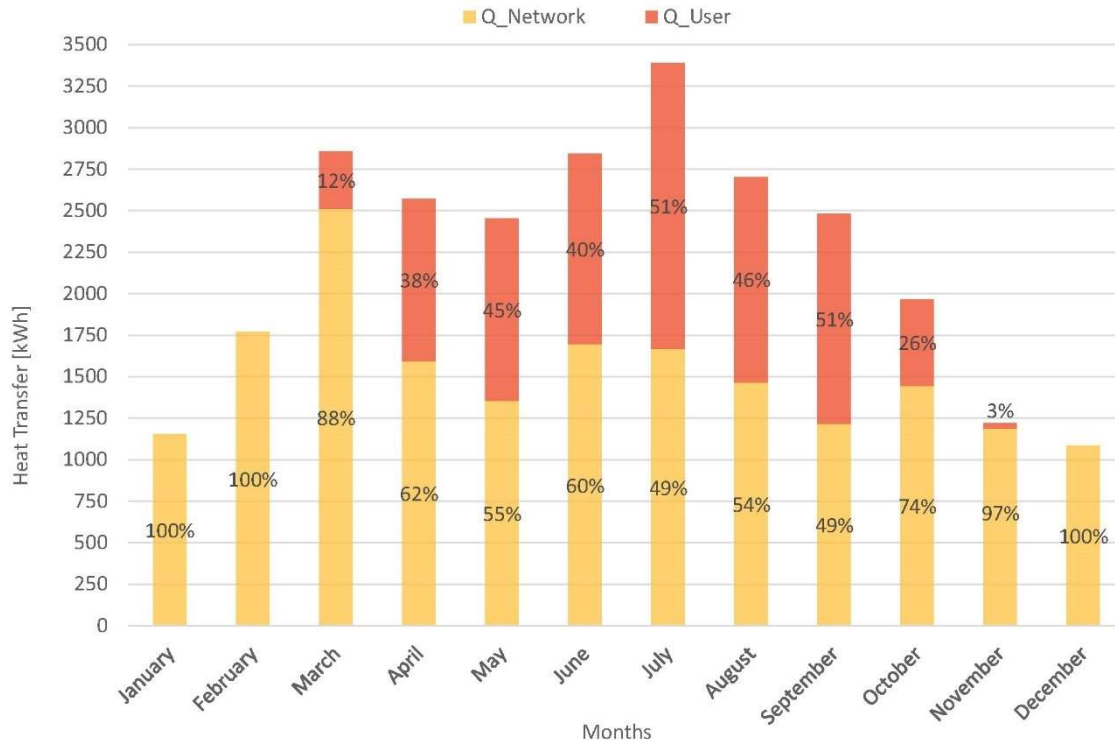
The hourly heat transfer is calculated by the mass flow rates (Network & User) reported in the Graph 8.3 and their relative ΔT .



Graph 8.4 UDC05 energy saved by solar system with HT network

The next step is to check the total monthly energy saved by the decentralised solar system and compare the energy saved by network and by user. The comparison is made in percentage to understand the solar gain exploitation by the two sides. The results obtained are shown in the Graph next page.

Decentralised Solar Thermal Model

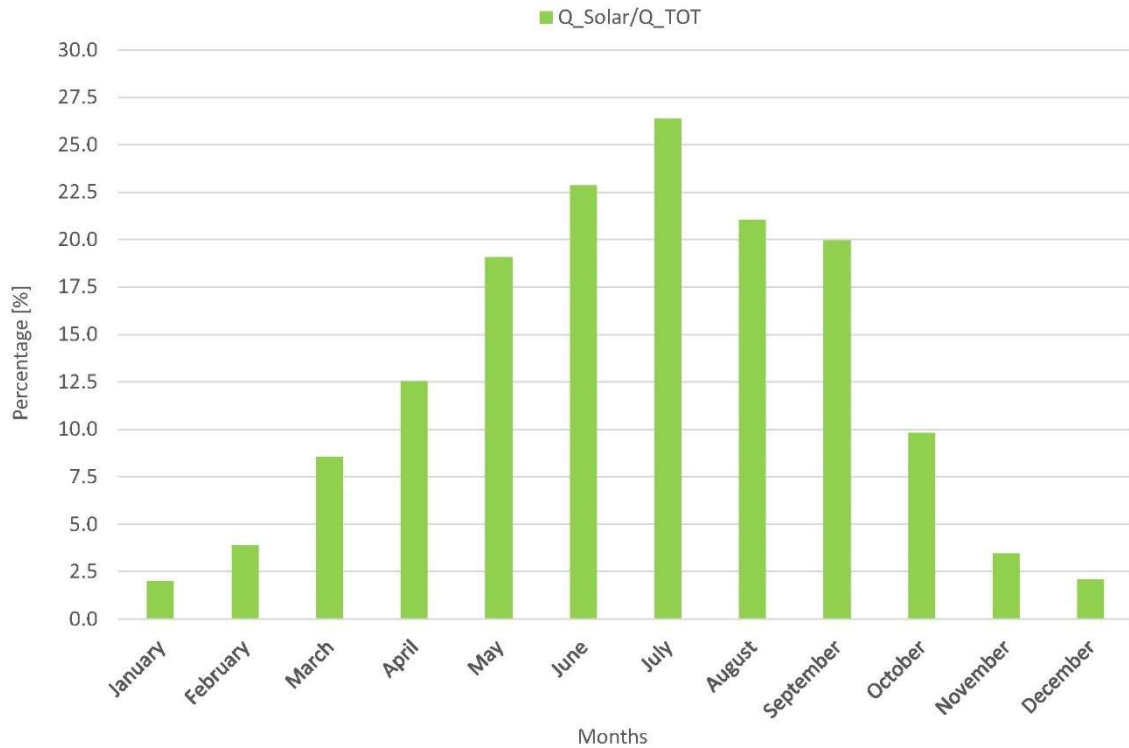


Graph 8.5 UDC05 monthly energy saved by solar field with HT network

The maximum solar contribution is more distributed among the network and the multi-dwelling unit, as it was expected from the previous chart. During the summer period around the 50 % of the energy is used by the UDC05 (Q_{User}), heating up the secondary side. The multi-dwelling unit UDC05 receives some benefits by the decentralised solar system from May to September. Instead, the district heating network exploit almost all solar energy produced during the rest of the year.

The total amount of heating energy produced by the decentralised solar system (Q_{Solar}) is analysed and compared to the total energy need of the multi-dwelling unit UDC05 (Q_{TOT}) in the following (Graph 8.11). The chart shows the monthly ratio between the two quantities.

Decentralised Solar Thermal Model



Graph 8.6 UDC05 monthly solar energy compared to energy need with HT network

The decentralised solar system can cover more than 20% by the total energy need of the multi-dwelling unit UDC05 during the summer period. Instead, it helps for less than the 5% during the winter season.

The decentralised solar system can cover until the 8.1% of the total annual energy needed by the multi-dwelling unit UDC05. This result will be studied and its limits will be understood in the last paragraph of this Chapter.

After the decentralised solar system is studied with today's high temperature network configuration, the next low temperature network is also analysed in the following Chapter to understand the future possible benefits of this solution.

8.4 Decentralised Solar District LT Configuration

The second analysis on the decentralised solar DH is made with the next low temperature configuration: 4th generation DH network. In this case the substations are removed but the solar integration does not change. The district network is now directly connected to the innovative flat stations analysed in Chapter 4.2.2. The solar thermal system is used also here as a sustainable energy source to cover the multi-dwelling unit heating demand. The return water (30 °C) coming from the flat stations is heated up by the solar heat exchanger connected to the solar collector and goes to the network in 2 different ways, as it is described in Figure 8.5:

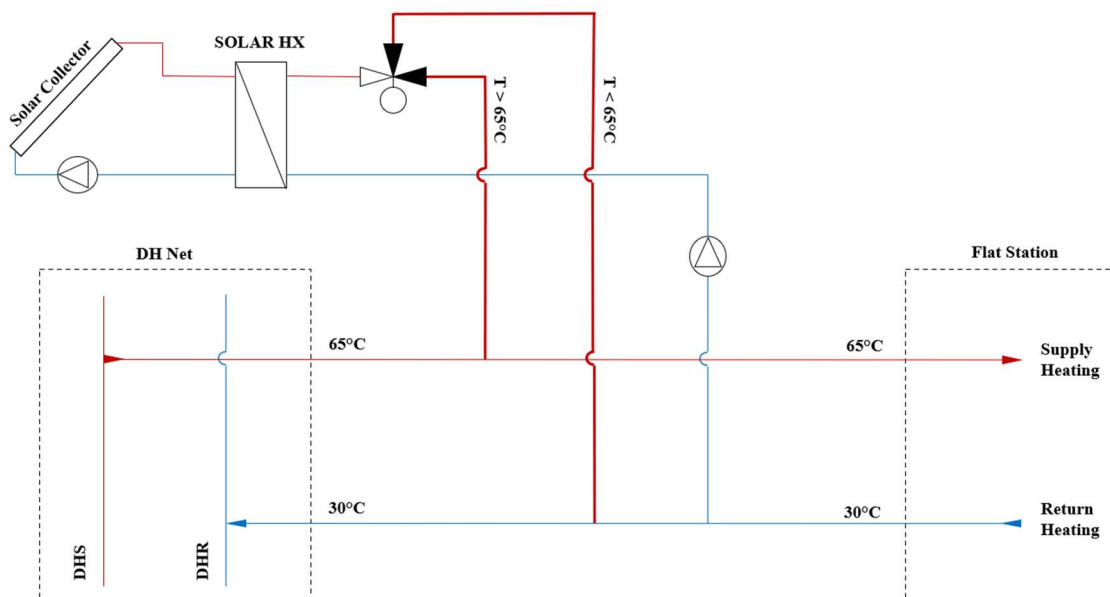


Figure 8.5 Generic scheme of a decentralised solar DH with LT configuration

- If $T < 65^\circ\text{C}$ it goes back in the network return line, increasing the district heating return temperature and decreasing the DNet ΔT .
- If $T > 65^\circ\text{C}$ it goes straight to the supply line in order to serve the flat stations and the water can be directly used by consumers.

The mass flow rate for solar panels side is consider equal to $30 \text{ kg/hm}^2 \cdot A_{\text{tot_coll}}$ also in this simulation and the solar controller for activating the panels are the same described in Chapter 8.3.1

The decentralised solar system is used as a renewable source for the next 4th generation district heating in Merezzate. It always withdraws the supply water from the DNet, according to the previous scheme (Figure 8.5) and it works as a S/R feed-in plant. It can serve the buildings of the UDC05 when the temperatures exceed 65°C or it work as a pre-heating plant when temperatures are lower.

The control strategy is represented in the following Table:

Table 8.5 LT control strategy model

$T > 65^\circ\text{C}$	User
$T < 65^\circ\text{C}$	Network

The simulation is also run with a timestep of 5 minutes in order to analyse the peaks within the hours. The panels are properly activated and the system correctly works, because it used the same TRNSYS model created in Figure 8.4. The solar field has the same dimensions of the previous case, but the withdrawn water mass flow rate and temperature change due to the new low temperature network.

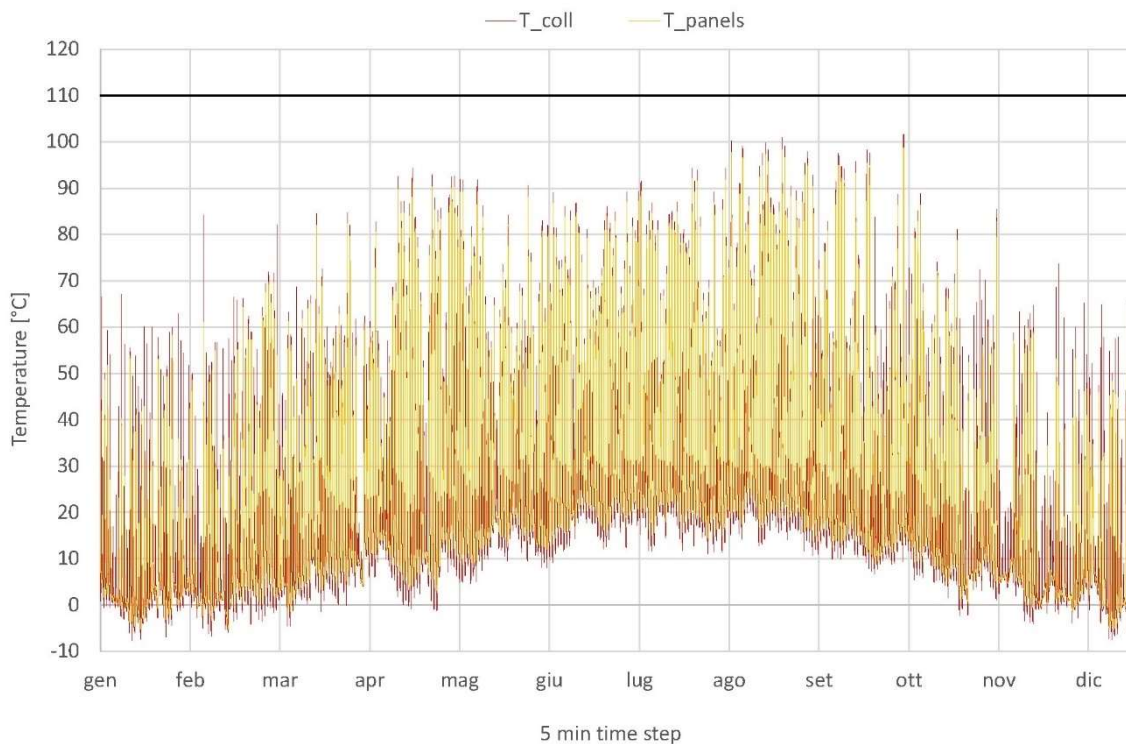
The results obtained from the low temperature network model are presented in the following paragraph.

8.4.1 Results of Decentralised Solar System LT

This configuration allows to the multi-dwelling unit to exploit the hours with maximum solar contribution. Solar gains are maximised during summer providing considerable benefits to the low temperature network. The lower temperatures allow to earn more

heating energy coming from the solar field. Moreover, there is only one circuit in the district and Merezzate and the heated water can be directly used by the flats when it reaches the set point of 65 °C without needing any substations.

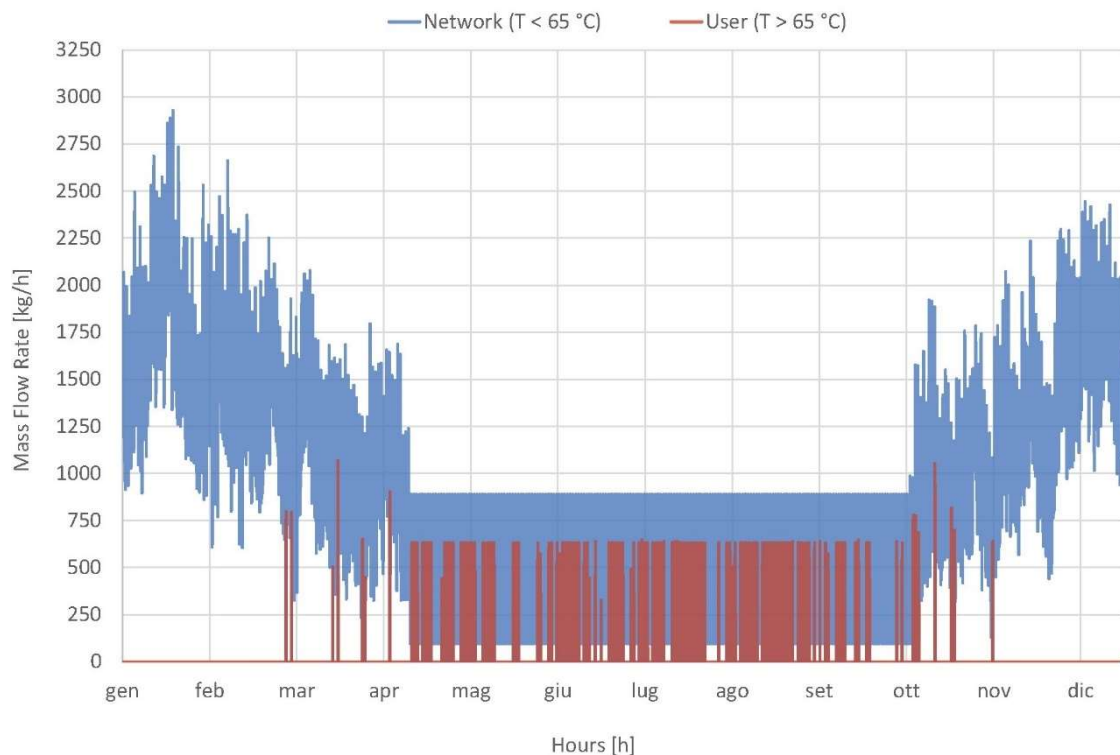
The withdrawn water mass flow rate and temperature are different from the HT network. Therefore, the stagnation hours will change in this case. In the following Graph the temperature of the collector (T_{coll}) and the working temperature of the system (T_{panels}) are also checked in the LT network configuration.



Graph 8.7 UDC05 solar collector temperatures with LT network

The stagnation hours resulted from the simulation are: 0 h << 50 h. Therefore, the solar system is working without risking any damage in this case. A higher mass flow rate and a lower temperature in the return line, allow a better exploitation of the solar energy provided by the collectors.

After the collectors are checked, the results from the distribution control strategy (Table 8.5) are analysed in the following Graph. The heated water from the solar field is shown in Graph 8.8. During the most part of the year the temperature is lower than 65 °C and the decentralised solar system serves the return line of the LT network. When temperatures reach 65 °C the withdrawn water is used directly by the users thanks to the flat stations of every apartment.

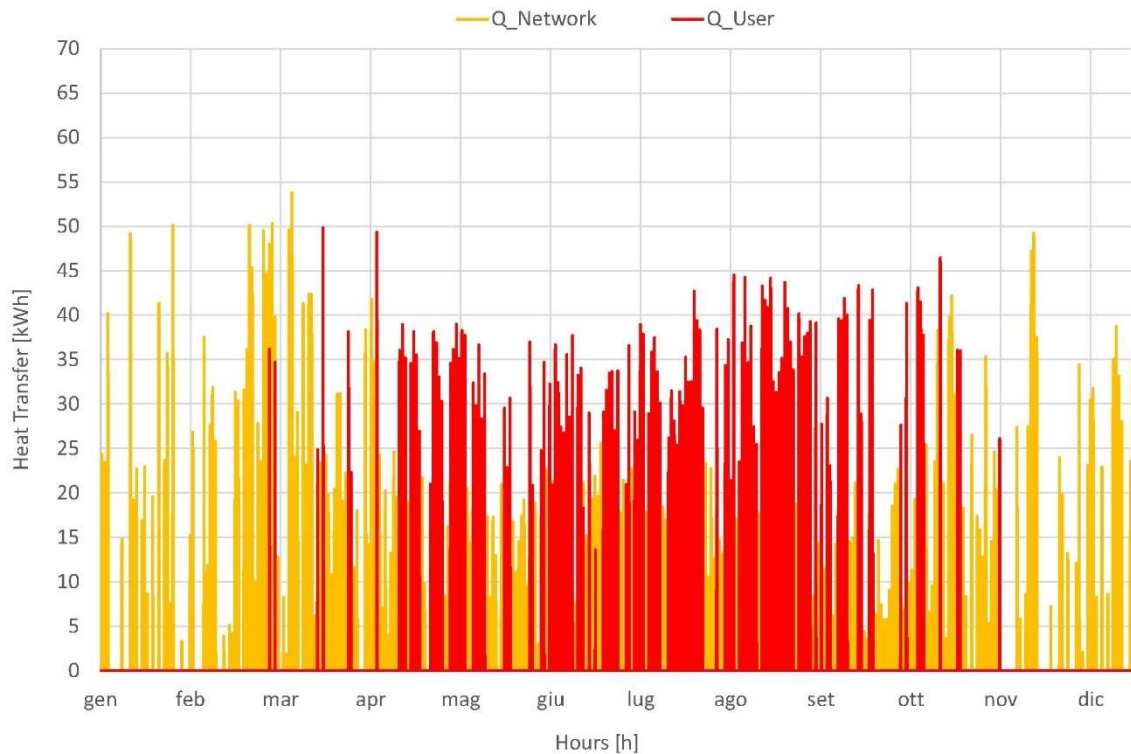


Graph 8.8 UDC05 heated water by solar system with LT network

The most part of the water does not reach the set-point of 65 °C therefore it goes back to the DH return line at higher temperature in order to be heated up by the thermal power plant of A2A. This configuration serves more the return line of the network, but it primarily works to supply heating to the flat station. In fact, this configuration allows to exploit the hours with maximum solar contribution by the users.

The energy saved by the network and by the users are shown in the following Graph. The energy saved by user can be directly exploited by the consumers thanks to the flat stations. The energy saved by network is calculated also here from the increase of the return temperature, heated by the solar system, compared to the design return temperature. A higher return temperature means a consequently decrease of the ΔT in the LT network. Therefore, the thermal plant will provide less heating to reach the supply temperature, which is also lower compared to the HT network (65 °C instead of 100 °C).

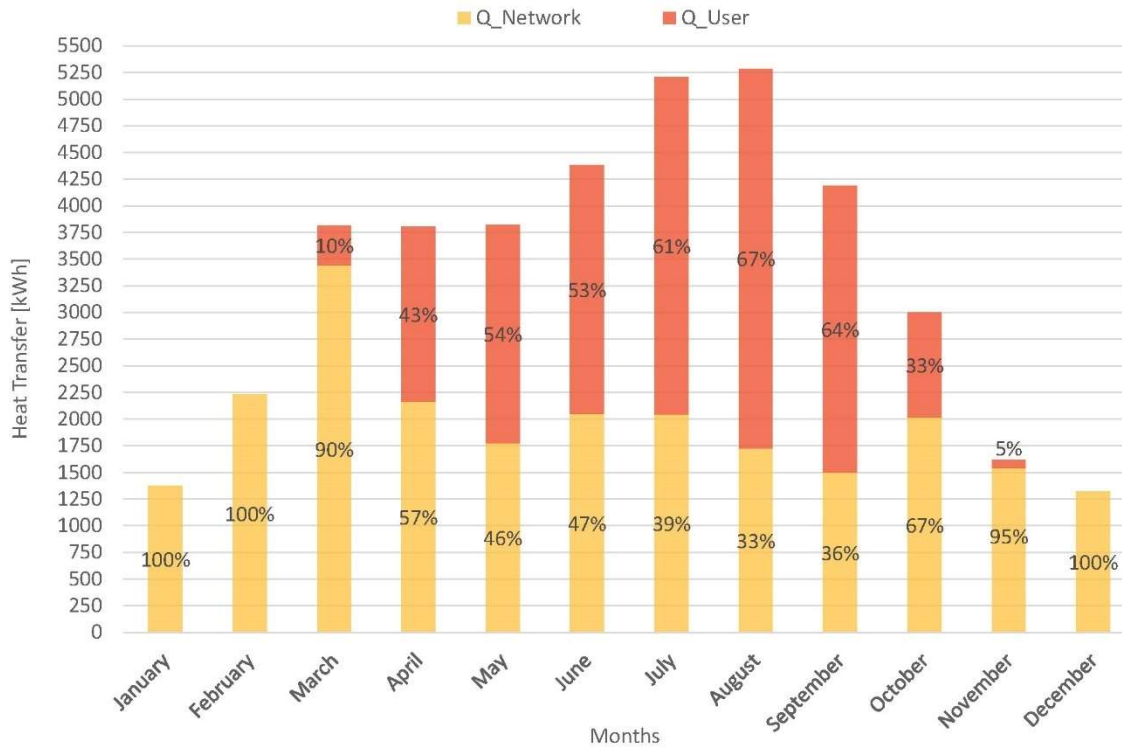
The hourly heat transfer is calculated by the mass flow rates (Network & User) reported in the Graph 8.8 and their relative ΔT .



Graph 8.9 UDC05 energy saved by solar system with LT network

The next step is to check the total monthly energy saved by the decentralised solar system and compare the energy saved by the network and by the user. The comparison is made

in percentage to understand the solar gain exploitation by each side. The results obtained are shown in the Graph below:

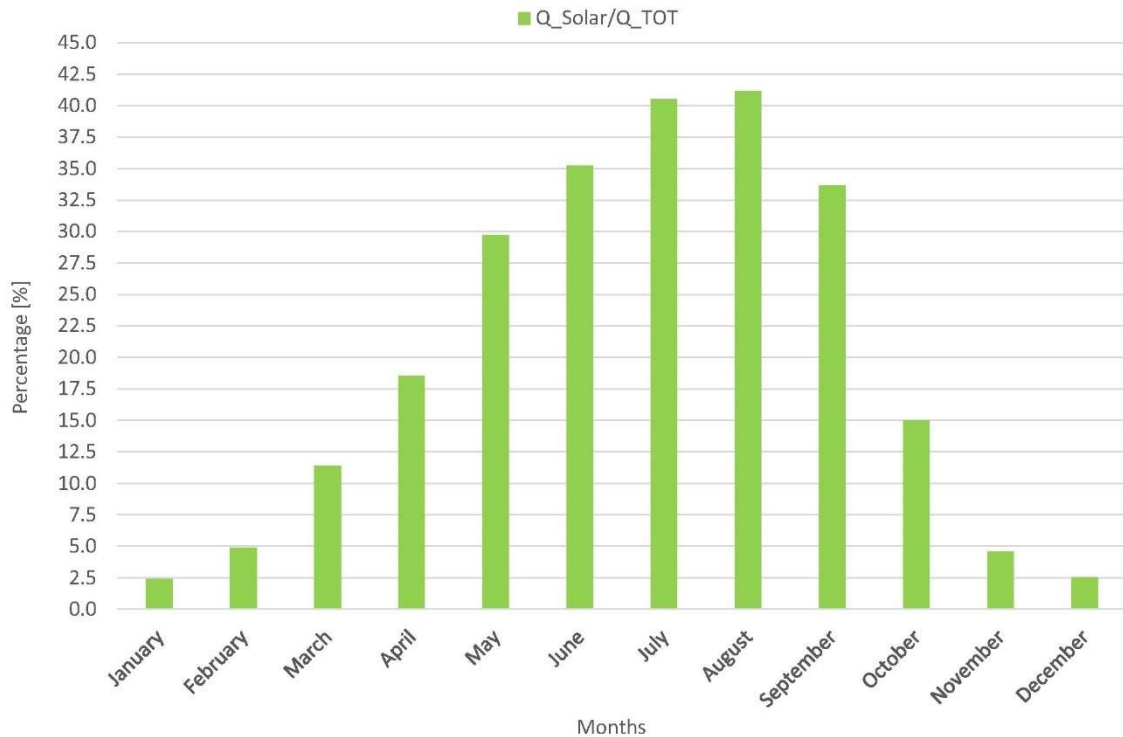


Graph 8.10 UDC05 monthly energy saved by solar field with LT network

The maximum solar contribution is more distributed to the apartments, as it was expected from the previous chart. More than 60 % of the energy goes to the flat stations, from July to September. The produced heat can be exploit by consumers of the multi-dwelling unit UDC05. Instead, the decentralised solar system benefits more the district heating LT network during the rest of the year.

The next step is to check the amount of solar energy provided by the LT model compared with the total energy need from the multi-dwelling unit. The total amount of heating energy produced by the decentralised solar system (Q_{Solar}) is analysed and compared to the total energy need of the multi-dwelling unit UDC05 (Q_{TOT}) in the following chart. The Graph 8.11 shows the monthly ratio between the two quantities.

Decentralised Solar Thermal Model



Graph 8.11 UDC05 monthly solar energy compared to energy need with LT network

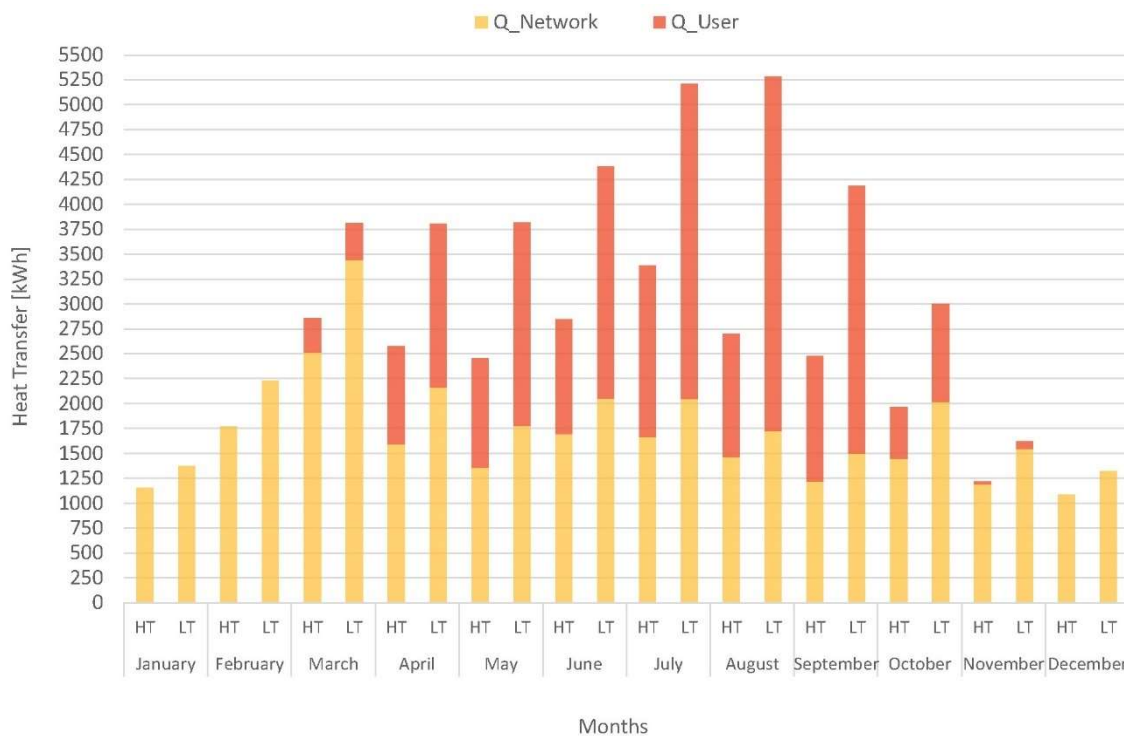
This configuration seems more performing compared to the HT network, because the solar source reaches more than 40% of the energy heating demand during July and August. The decentralised solar system covers more than 30 % of the total amount of heating energy needs from May to September, exploiting the solar gain to cover the multi-dwelling unit demand.

The decentralised solar system with LT network can cover until the 12.2% of the total annual energy needed by the multi-dwelling unit UDC05.

In the next paragraph the energy saved by the decentralised solar system of this case is compared with the results obtained by the high temperature network of the previous case, in order to understand better which are the benefits of having a low temperature district heating.

8.4.2 Comparison between HT & LT Network

In this paragraph the results from the high temperature network and low temperature network have compared each other. The monthly energy saved in both cases is shown in the following Graph. The contribute of the solar field to the user and the network is separately indicated for HT and LT network.



Graph 8.12 UDC05 monthly energy saved comparison between HT & LT

It is immediately clear that the low temperature network allows a better exploitation of the solar gains. The energy is more exploited by the users during the summer period. These performances are due to the low temperatures, in fact the district heating can absorb more heating energy from the solar field. The energy is usually exploited by the network in both cases during winter. Anyway, the LT configuration still cover a bigger amount of energy compared to the HT network. It is demonstrated that the total energy saved from the LT is higher than the one saved from the HT network for every month.

In the next paragraph an environmental and economic analysis will be performed to accurately study the implementation proposed within this Chapter.

8.5 Economic and Environmental Analysis

An economic and environmental analysis is made in this paragraph. Here, a total cost of the solar panels for all the district heating is evaluated. Moreover, the primary energy saved is calculated for the high temperature network and for the low temperature configuration.

The total cost for the decentralised solar system is calculated considering an average cost of €600/m² for panels area. The total collector area of the district heating has to be calculated to find the final cost. The collector area is calculated starting from the solar area of multi-dwelling unit UDC05. The stagnation hours are lower than the limit, therefore the system is properly working. The ratio between the collector area and the annual energy need of UDC05 is made to find the proportion: m²/kWh. This value is then multiplied for the design energy need of each multi-dwelling unit.

$$\text{Area_coll_UDC05} / \text{Q_annual_UDC05} = 0.00034 \text{ m}^2/\text{kWh} \quad (8.7)$$

The found ratio is multiplied for the annual energy need of each multi-dwelling unit. The total collector area is decreased a bit for every multi-dwelling unit in order to avoid the stagnation hours. The obtained value is then multiplied for an average cost of €600 per collector area. The results for the Merezzate district are shown in the following Table.

Table 8.6 Collector area for each multi-dwelling unit UDC

Residential Unit	Annual Heating Need [kWh]	Total Area Collector [m ²]	Cost [€]
UDC01	404689	135	81000
UDC03	309271	105	63000
UDC05	294486	100	60000
UDC06	277044	90	54000
UDC09	213597	70	42000
TOT	1499087	500	300000

The total area of the solar field for the Merezzate district is equal to 500 m². Therefore, the final cost of this solution is equal to €300'000, considering an average cost of €600/m².

The primary energy saved by the decentralised solar system is calculated within this section. The non-renewable primary energy coefficient (PE_nren) given by A2A is considered to calculate the non-renewable primary energy of the Merezzate district. The coefficient is equal to 1.07 kWh_{PE_nren} / kWh_t. Therefore, the total annual non-renewable primary energy for space heating and domestic hot water of the Merezzate district is equal to:

$$1.07 \text{ kWh}_{\text{PE}_{\text{nren}}} / \text{kWh}_{\text{t}} \cdot 1499087 \text{ kWh}_{\text{t}} = 16404023 \text{ kWh}_{\text{PE}_{\text{nren}}} \quad (8.8)$$

The energy saved by the decentralised solar system is calculated for today's configuration at high temperature and for the next low temperature network, considering the annual percentage of savings calculated from the multi-dwelling unit UDC05 in the Chapter 8.3.1 and Chapter 8.4.1. The same percentage of savings is considered for the total district because the same collector area per heating energy need is considered for each multi-dwelling unit, as it is calculated in the previous paragraph. Therefore, the heating energy needs request from the thermal power plant of A2A is calculated by removing the energy saved from the decentralised solar system as follows:

$$\text{Heating_Energy (with Solar)} = \text{Annual_Energy_Need} \cdot (1 - \% \text{ Solar_Savings}) \quad (8.9)$$

Where the percentage of solar savings is considered equal to 8 % for the high temperature network and 12 % for the low temperature network. The heating energy found from the equation 8.9 is then multiplied by the non-renewable primary energy coefficient, following the equation 8.8, in order to find the annual amount of non-renewable primary energy, considering a decentralised solar system. Finally, the difference between the annual non-renewable primary energy without the solar system and the annual non-

renewable primary energy with the decentralised solar system is calculated as primary energy saved, considering both configurations at HT and LT.

A Table of summary results is shown below:

Table 8.7 Non-renewable primary energy saved by the decentralised solar system

	Solar Energy [%]	Heating Energy with Solar [kWh]	Primary Energy with Solar [kWh_{PE_nren}]	Savings [kWh_{PE_nren}]
HT network	8.10%	1377661	1474097	129926
LT netowrk	12.20%	1316198	1408332	195691

The non-renewable primary energy saved by the decentralised solar district is equal to 129926 kWh_{PE_nren} for the high temperature district heating and 195691 kWh_{PE_nren} for the next low temperature district heating, considering a total solar area of 500 m² and a final cost of €300'000.

This solution allows to save up to 12 % of the annual primary energy with the next 4th generation of district heating. This analysis underlines the performances of the low temperatures network, highlighting a better integration with the solar thermal field. It can cover more than 40 % of the energy needs during July and August. The next 4th generation district heating has better performances due to the low temperature network, which allows to exploit more the renewable energy sources, decreasing the thermal losses and the risk of damaging the systems.

The last step is to understand the limits of this solution and the possible optimization for a decentralised solar system. The obtained results are discussed in the following paragraph to understand the margins of improvement.

8.6 Discussion of the Results

The energy saved from the decentralised solar system with a S/R feed-in is equal to 8 % for the high temperature network and 12 % for the next low temperature configuration. This solution is favourable from a construction point of view because it allows to maintain the same solar integration for HT and next LT network. Moreover, it has a simple control strategy and can be used as an over-heat protection system without an extra pipe (the 3rd pipe). Anyway, this configuration has some limits and some improvement margins.

The limit of this configuration is that it does not exploit the maximum potential of the decentralised solar integration. The percentage of savings probably would be higher if the solar field would exploit more the district heating network. In fact, the decentralised solar system could withdraw the water directly from the network with a 3rd pipe. This configuration allows a better exploitation of the solar field because it does not just cover the residential energy needs but it takes the most solar gains as possible and put the heated water in the district heating.

A solar integration which withdraws directly from the network can take a higher mass flow rate without going into stagnation. This means that the area of the collectors can be increased according to the withdrawn mass flow rate. Moreover, the decentralised solar system would also work when there is no heating demand from the multi-dwelling units and it would directly serve the entire district heating.

The solar district integration can be developed in the future steps without taking the return water from the substation but taking it directly from the district heating network, allowing a higher withdrawn mass flow rate and higher solar collector area. This configuration would exploit the maximum solar potential and it would cover more the total district energy demand, increasing the percentage of saved energy.

9. Conclusions

District heating is a consolidated technology with evident growing trend in Italy, as it has potential benefits in both environmental and economic terms. Its competitiveness arises from the good integration of centralized and distributed heat generation from renewable sources and optimized management. The need for models capable of carrying out operational optimization of district heating networks is clear from the success of the simulators on the market and by the rich literature on the topic.

A dynamic model in TRNSYS 18 is created in the thesis-work to propose a flexible simulator capable of describing significant quantities such as supply and return temperatures, mass flow rates and energies in all the components that make up the Merezzate network. The aim was to obtain a model that gives information both on the district heating side (primary side) and multi-dwelling unit side (secondary side), to evaluate the actual situation of the district network and simulate the future interventions.

A fundamental step is the validation of the model to understand the reliability of the obtained results. Once these values are consistent with reality the created model opens doors to many monitoring and implementation opportunities. The validated model together with detailed description of the network allow some investigations on distributed interventions for integrating renewable sources.

One of the aims of this thesis-work was to implement the Merezzate district through a decentralised solar thermal system which exploit the district heating network as a storage tank for the multi-dwelling units. The solar district optimisation and the flexibility of the simulation, together with a validated thermodynamic model, allow to integrate the future intervention for renovating the Merezzate district into the first 4th generation district heating in Italy.

The system is analysed with HT configuration and with the next LT network to understand the benefits of having a 4th generation district heating. The low temperatures of the network reduce the thermal losses and allow to enhance the exploitation of solar gains, avoiding the risk of damaging the solar system. The energy saved in both cases is

equal to the 8% of the annual district heating demand for a HT configuration and 12% for the next LT network.

From the results, the low temperature district heating performs better than the HT both for its higher efficiency and for the lower non-renewable primary energy used. However, the obtained results have some limitation and margins of improvements. Some more analysis can be assessed in order to better exploit the integration with the next 4th generation of district heating.

A logical next step of this thesis work could be the analysis of different integration of the decentralised solar system, in order to further exploit the solar gains and cover the largest value of the district energy needs. The different feed-in connections allow to analyse the different types of configuration with relative benefits to understand the most suitable integration for Merezzate district. Another route to explore could be a different management of the solar panels, considering a variable mass flow rate in order to match the multi-dwelling unit heating demand.

This thesis-work lays the foundations for more extensive implementation of all future projects in Merezzate area, providing a dynamic network model and a deep insight for possible integration of renewable energy sources.

Conclusions

List of Figures

Figure 2.1 Scheme of the delivery of heat in DH networks [6].....	17
Figure 4.1 Merezzate Plus district area [22].....	27
Figure 4.2 Merezzate Plus plan [24].....	29
Figure 4.3 Scheme of a generic multi-dwelling unit substation.....	32
Figure 4.4 Simplified scheme of innovative flat station.....	33
Figure 4.5 Image of the flat station [26].....	34
Figure 4.6 Scheme of the next 4 th generation DH at low temperatures.....	35
Figure 6.1 Plant type of building E06 [23].....	49
Figure 6.2 Geometric modelling scheme of flat n°25 and flat n°30 [28].....	51
Figure 6.3 TRNSYS system model representation [28].....	53
Figure 6.4 Structure of the thermo active construction element system [30].....	57
Figure 6.5 Heat flow in a cross section of a thermo active construction element [30] .	57
Figure 6.6 Network of resistances with triangular arrangement [30].....	59
Figure 6.7 Network of resistances with star arrangement [30].....	60
Figure 6.8 Merezzate district heating network.....	70
Figure 6.9 Multi-dwelling unit substation modelling scheme.....	71
Figure 6.10 Scheme of the substation heat exchanger.....	74
Figure 6.11 TRNSYS Merezzate district network model.....	76
Figure 6.12 Pipes of Merezzate Network.....	79
Figure 7.1 TRNSYS network model with monitoring heat transfers.....	85
Figure 7.2 Secondary side scheme with recirculation.....	87
Figure 7.3 Scheme of validation of the network model.....	93
Figure 8.1 Generic scheme of the four different feed-in connections [17].....	101

List of Figures

Figure 8.2 Efficiency trend complies to T_m referred to absorber area [38] 104

Figure 8.3 Generic scheme of a decentralised solar DH with HT configuration 107

Figure 8.4 TRNSYS system model of decentralised solar thermal for UDC05 108

Figure 8.5 Generic scheme of a decentralised solar DH with LT configuration 117

List of Tables

Table 4.1 Merezzate heat generation plants by AIRU [25]	31
Table 5.1 UDC 1 pre-sizing data	36
Table 5.2 UDC 3 pre-sizing data	36
Table 5.3 UDC 5 pre-sizing data	37
Table 5.4 UDC 6 pre-sizing data	37
Table 5.5 UDC 9 pre-sizing data	37
Table 5.6 Merezzate district total pre-sizing data	37
Table 6.1 Transmittances of the apartment's layers [28].....	50
Table 6.2 Building E06 TRNSYS components for energy needs.....	53
Table 6.3 Annual energy needs comparison	55
Table 6.4 Resistance in x-direction & criteria [30].....	62
Table 6.5 TRNSYS controller component.....	63
Table 6.6 Annual heating comparison of different set-point for flat n°25	67
Table 6.7 Merezzate district TRNSYS components	77
Table 6.8 Used pipes dimensions	78
Table 6.9 Pipe materials thermal conductivity	80
Table 6.10 Pipes global coefficient of thermal exchange	80
Table 7.1 Average difference between recirculation results and monitoring data	92
Table 7.2 Percentage difference between recirculation results and monitoring data	92
Table 7.3 Average difference between simulated results and monitoring data	95
Table 7.4 Percentage difference between simulated results and monitoring data	98
Table 8.1 Main characteristics of the four different feed-in connections [37]	102
Table 8.2 Characteristic of the selected model of FPC [38].....	103

List of Tables

Table 8.3 TRNSYS solar components	108
Table 8.4 HT control strategy model	109
Table 8.5 LT control strategy model.....	118
Table 8.6 Collector area for each multi-dwelling unit UDC	125
Table 8.7 Non-renewable primary energy saved by the decentralised solar system ...	127

List of Graphs

Graph 5.1 UDC01 space heating obtained by applying the BIN method	40
Graph 5.2 UDC03 space heating obtained by applying the BIN method	40
Graph 5.3 UDC05 space heating obtained by applying the BIN method	41
Graph 5.4 UDC06 space heating obtained by applying the BIN method	41
Graph 5.5 UDC09 space heating obtained by applying the BIN method	42
Graph 5.6 Residential daily profile for DHW	44
Graph 5.7 UDC space heating & DHW monthly energy needs.....	45
Graph 5.8 Annual energy needs compared with pre-sizing data.....	46
Graph 6.1 Monthly energy needs of flat n°25 [29]	54
Graph 6.2 Monthly energy balance of flat n°25 [29]	55
Graph 6.3 Radiant panels outlet temperature & heat transfer for flat n°25	64
Graph 6.4 Radiant panels data analysed in a short period for flat n°25.....	65
Graph 6.5 Radiant panel outlet temperatures and heat transfers during the day.....	66
Graph 6.6 Monthly heating comparison of different set-point for flat n°25	68
Graph 6.7 Merezzate network primary side results.....	81
Graph 7.1 UDC01 model results compared with monitoring data.....	84
Graph 7.2 UDC01 results from actual energy compared with monitoring data	86
Graph 7.3 UDC01 recirculation results compared to the monitoring data.....	88
Graph 7.4 UDC01 recirculation results compared to monitoring data during November	89
Graph 7.5 UDC03 recirculation results compared to the monitoring data.....	90
Graph 7.6 UDC05 results with recirculation compared to the monitoring data	90
Graph 7.7 UDC06 recirculation results compared to the monitoring data.....	91

List of Graphs

Graph 7.8 UDC09 recirculation results compared to the monitoring data.....	91
Graph 7.9 UDC01 primary side validation	94
Graph 7.10 UDC01 primary side validation in November	95
Graph 7.11 UDC03 primary side validation	96
Graph 7.12 UDC05 primary side validation	96
Graph 7.13 UDC06 primary side validation	97
Graph 7.14 UDC09 primary side validation	97
Graph 8.1 UDC05 solar panels temperatures & mass flow rates during August.....	110
Graph 8.2 UDC05 solar collector temperatures with HT network	112
Graph 8.3 UDC05 heated water by solar system with HT network.....	113
Graph 8.4 UDC05 energy saved by solar system with HT network	114
Graph 8.5 UDC05 monthly energy saved by solar field with HT network	115
Graph 8.6 UDC05 monthly solar energy compared to energy need with HT network	116
Graph 8.7 UDC05 solar collector temperatures with LT network.....	119
Graph 8.8 UDC05 heated water by solar system with LT network.....	120
Graph 8.9 UDC05 energy saved by solar system with LT network	121
Graph 8.10 UDC05 monthly energy saved by solar field with LT network.....	122
Graph 8.11 UDC05 monthly solar energy compared to energy need with LT network	123
Graph 8.12 UDC05 monthly energy saved comparison between HT & LT	124

Nomenclature

ΔT	Temperature Difference	K
A	Area	m ²
a1	Slope Coefficient	W/m ² K
a2	Curvature Coefficient	W/m ² K ²
G	Solar Irradiance	W/m ²
C	Heat Capacity	kW/K
D	Diameter	m
dx	Pipe Spacing	m
K	Global Coefficient of Thermal Exchange	W/mK
P	Power	W
R	Resistance	mK/W
Q	Heat Transfer Rate	kWh
NTU	Number of Transfer Unit	-
T	Temperature	°C
UA	Global Heat Transfer Coefficient	kW/K
cp	Specific Heat	kJ/kgK
t	Thickness	m
m	Mass Flow Rate	kg/h

Greek Letters

ε	Effectiveness	-
η	Efficiency	-
γ	Azimuth Angle	°
β	Slope of Collector	°
λ	Conductivity	W/mK
θ	Incidence Angle	°
η_0	Intercept Efficiency	-
ρ	Density	kg/m ³
δ	Pipe Diameter	m

Subscripts

01,03,05,06,09	Number of Multi-Dwelling Units
1,2	Primary or Secondary Side
amb	Ambient

Nomenclature

c	Cold
coll	Collector
dehum	Dehumidification
e	Electric
ext	External
h	Hot
H	High
in	Inlet
inf	Infiltration
int	Internal Gains
L	Low
m	Mean
max	Maximum
min	Minimum
monit	Monitoring
nren	Non-Renewable
out	Outlet
p	People
r	Ratio
rec	Recirculation
sf	Solar Field
sens	Sensible
sol	Solar
sim	Simulation
t	Thermal
tot	Total
trans	Transferred
vent	Ventilation
w	Water

Abbreviations

DH	District Heating
DHW	Domestic Hot Water
DNet	Distribution Network
E	Building
EU	European Union
FC	Flow Controlled
FPC	Flat Plate collector
h	Hur
HT	Hight Temperature
HX	Heat Exchanger
IAM	Incidence Angle Modifier
LT	Low Temperature
NZEB	Nearly Zero Energy Building

Nomenclature

PE	Primary Energy
PLR	Partial Load Ratio
R	Return
RES	Renewable Energy Source
S	Supply
SCR	Selective Catalytic Reduction
SH	Space Heating
TC	Temperature Controlled
UDC	Multi-Dwelling Unit

Nomenclature

Bibliography

- [1] Di Leo S, Salvia M. Local strategies and action plans towards resource efficiency in South East Europe. *Renewable and Sustainable Energy Reviews*. 2017; 68, pp. 286-305.
- [2] Nagy K, Körmendi K. Use of renewable energy sources in light of the “New Energy Strategy for Europe 2011–2020”. *Appl.Energy*. 2012; 96, pp. 393-399.
- [3] Merezzate+ - Poliedra [Internet]. Polimi.it. 2018 [cited 10 January 2021]. Available from: <http://www.poliedra.polimi.it/project/merezzate-plus/>
- [4] e-Media Resources. Welcome [Internet]. Trnsys.com. 2021 [cited 10 January 2021]. Available from: <http://www.trnsys.com/>
- [5] Werner S, Frederiksen S. *District Heating and Cooling*, Lund: Studentlitteratur AB. 2013.
- [6] Scoccia R, Motta M, Dénarié A. Deliverable Task: Report on the district heating system flexibility exploitation, Merezzate + Climate-KIC. 2018.
- [7] Fahl U, Dobbins A. District Heating in Europe: Opportunities for Energy Savings, Business, and Jobs, in Welsch, M. et al. (eds), *Europe's Energy Transition "Insights for Policy Making"*. Academic Press. 2017; pp. 249-259.
- [8] EUROPEAN COMMISSION. Public Consultation Roadmap for a low-carbon economy by 2050. AGFW – Statement; Frankfurt; 8.12.2010.
- [9] Colmenar-Santos A, Rosales-Asensio E, Borge-Diez D, Blanes-Peiró JJ. District heating and cogeneration in the EU-28: Current situation, potential and proposed energy strategy for its generalisation. *Renewable and Sustainable Energy Reviews*. 2016; 62, pp. 621-639.
- [10] Haoran L, Nord N. Transition to the 4th generation district heating - possibilities, bottlenecks, and challenges. *Energy Procedia*. 2018; 149, pp. 483-498.

- [11] Lund H, Werner S, Wiltshire R, Svendsen S, Thorsen J.E, Hvelplund F, et al. 4th Generation District Heating (4GDH) Integrating smart thermal grids into future sustainable energy systems, *Energy*. 2014; 68, pp. 1-11.
- [12] Rosa AD, Li H, Svendsen S, Werner S, Persson U, Ruehling K, et al. Towards 4th Generation DH Experiences with and Potential of Low Temperature DH, *Annex X Final report*. 2014.
- [13] Fisch MN, Guigas M, Dalenbäck JO, A review of large-scale solar heating systems in Europe, *Sol. Energy*. 1998; 63, pp. 355–366.
- [14] Heller A. 15 Years of R&D in central solar heating in Denmark, *Sol. Energy*. 2000; 69, pp. 437–447.
- [15] Bauer D, Marx R, Nußbicker-Lux J, Ochs F, Heidemann W, Müller-Steinhagen H. German central solar heating plants with seasonal heat storage, *Sol. Energy*. 2010; 84, pp. 612–623.
- [16] Perez-Mora N, Bava F, Andersen M, Bales C, Lennermo G, Nielsen C, et al. Solar district heating and cooling: a review. *Int. J. Energy Res*. 2018; 42, pp. 1419–1441.
- [17] Lennermo G, Lauenburg P, Werner S. Control of decentralised solar district heating, *Sol. Energy*. 2019; 179, pp. 307–315.
- [18] Yadav P, Davies PJ, Sarkodie SA. The prospects of decentralised solar energy home systems in rural communities: User experience, determinants, and impact of free solar power on the energy poverty cycle. *Energy Strat. Rev*. 2019; 26, (100424).
- [19] Calore e servizi [Internet]. A2a.eu. 2021 [cited 15 January 2021]. Available from: <https://www.a2a.eu/it/servizi/calore-e-servizi>
- [20] UNI/TS 11300-4: Prestazioni energetiche degli edifici. *CTI - Impianti di riscaldamento - Progettazione, fabbisogni di energia e sicurezza*. 2016

- [21] Volume 01: Getting Started. *Manual TRNSYS 18 a TRaNsient SYstem Simulation program*. 2019.
- [22] THE PROJECT – Development [Internet]. Merezzateplus.it. 2021 [cited 2 February 2021]. Available from: <https://www.merezzateplus.it/the-project>
- [23] Redomilano - Progetto [Internet]. Redomilano.it. 2021 [cited 2 February 2021]. Available from: <https://www.redomilano.it/progetto>
- [24] PII via Merezzate, Milano - Studio di Architettura Corsi Milano [Internet]. Studiocorsimilano.it. 2021 [cited 2 February 2021]. Available from: <https://www.studiocorsimilano.it/lavori/pii-via-merezzate-milano>
- [25] AIRU Riscaldamento Urbano – *Annuario 2019*; pp. 162-163.
- [26] Flat stations [Internet]. Danfoss.com. [cited 8 February 2021]. Available from: <https://www.danfoss.com/en/products/dhs/stations-and-domestic-hot-water/flat-stations/>
- [27] Weather Data by Location [Internet]. Energyplus.net. [cited 12 February 2021]. Available from: https://energyplus.net/weather-location/europe_wmo_region_6/ITA//ITA_Milano-Linate.160800_IGDG
- [28] Scoccia R, Colombo P, Filippini G. Descrizione Building Model. 2019.
- [29] Scoccia R, Colombo P, Filippini G. MEREZZATE+ Energy needs: analysis UDC1, E06, APT25+30. 2019.
- [30] Volume 05: Multizone Building modeling with Type56 and TRNBuild. *Manual TRNSYS 18 a TRaNsient SYstem Simulation program*. 2019.
- [31] Volume 04: Mathematical References. *Manual TRNSYS 18 a TRaNsient SYstem Simulation program*. 2019.
- [32] Ayompe L, Duffy A, Mc Keever M, Conlon M, McCormack S. Comparative field performance study of flat plate and heat pipe evacuated tube collectors (ETCs)

- for domestic water heating systems in a temperate climate, *Energy*. 2011; 36 (5), pp.3370-3378.
- [33] Reuss M. Solar District Heating in Germany. *Bavarian Centre for Applied Energy Research*. 2012.
- [34] Han T, Zheng Y, Gong G. Exergy analysis of building thermal load and related energy flows in buildings. *Indoor and Built Environment*. 2015; 26 (9), pp. 1257-1273.
- [35] Mazarrón FR, Porras-Prieto CJ, García JL, Benavente RM. Feasibility of active solar water heating systems with evacuated tube collector at different operational water temperatures, *Energy Conversion and Management*. 2016; 113, pp. 16-26.
- [36] Wang D, Orehounig K, Carmeliet J. A Study of District Heating Systems with Solar Thermal Based Prosumers. *16th International Symposium on District Heating and Cooling*. 2018 DHC2018, 9–12 September 2018, Hamburg, Germany.
- [37] Lennermo G, Lauenburg P. Feed-in from Distributed Solar Thermal Plants in District Heating Systems. *Environmental Science*. 2016.
- [38] Solar Collector Factsheet. Riello CSAL 25 RS. 2019.
- [39] Kovacs P. A guide to the standard EN 12975. *Technical Research Institute*. 2012

Bibliography

Acknowledgments

Ci tengo a ringraziare tutti quelli che mi hanno supportato e motivato per la stesura di questo lavoro, che segna la fine di un percorso durato cinque anni. In particolare, vorrei ringraziare la mia correlatrice Alice Dénarié per essere sempre stata disponibile e avermi dato gli spunti giusti per analizzare a fondo le tematiche trattate e il professor Rossano Scoccia per avermi dato la possibilità di partecipare ad un progetto così innovativo, aprendomi le porte ad interessanti sbocchi professionali.

Un ringraziamento particolare va alla mia famiglia e a Sofia che mi sono sempre state vicino nonostante le distanze e non hanno smesso un secondo di credere in me e nel mio percorso. Ringrazio il mio coinquilino Pietro, nonché amico di una vita che mi ha dato un sostegno costante in questi ultimi cinque anni come neanche un fratello saprebbe fare.

Un ringraziamento speciale va anche ad Emanuele ed Etien che sono stati fondamentali per superare i periodi difficili durante questi anni, lasciandomi sempre aperta la porta di casa loro, in qualsiasi momento o circostanza. Infine, ci tengo a ringraziare tutte le persone meravigliose, nuove e vecchie conoscenze, con cui ho instaurato un rapporto di amicizia e fiducia reciproca durante questo percorso.

Per ultimo ma non meno importante voglio dire GRAZIE al Politecnico di Milano per avermi dato un'opportunità unica di formazione e crescita personale che mi ha portato ad essere la persona che sono oggi.

È stata una bella avventura!

Acknowledgments